AAiT
ADDIS ABABA INSTITUTE OF TECHNOLOGY
አዲስ አበባ ቴክኖሎጂ ኢንስቲትዩት
ADDIS ABABA UNIVERSITY
አዲስ አበባ ዩኒቨርሲቲ

School of Mechanical and Industrial Engineering (SMIE)
Department of Mechanical Engineering
Mechanical Design Stream

Numerical Simulation for High Cycle Fatigue Life Prediction of Pre-tightened Bolts of Connecting Rod: TOYOTA D4D Dolphin Case

By:

Bikila Debela Gemeda

[GSR/5751/12]

A Thesis Submitted to School of Graduate Studies of Addis Ababa University in Partial Fulfillment of the Requirements for Degree of Masters of Science in Mechanical Engineering (Mechanical Design)

Advisor: Samuel Tesfaye (Ph.D)
Ph.D. in Material Engineering
Addis Ababa Institute of Technology

March, 2022

Addis Ababa, Ethiopia

Declaration

I hereby declare that the work which is being presented in this thesis entitled "Numerical Simulation for High Cycle Fatigue Life Prediction of Pre-tightened Bolts of Connecting Rod: TOYOTA D4D Dolphin Case" is original work of my own, has not been presented for a degree of any other university and all the resource of materials used for this thesis have been duly acknowledged.

Bikila Debela Gemeda

Signature: _____ Date: _____

This thesis has been submitted for examination and signed by:

Advisor: **Samuel Tesfaye (Ph.D)** Signature_____Date_____

Addis Ababa University
Institute of Technology (AAiT)
School of Mechanical and Industrial Engineering

M.Sc. Final Thesis Approval

Submitted By:

Bikila Debela	_____	_____
Student Name	Signature	Date

Recommended By:

Samuel Tesfaye (PhD)	_____	_____
Advisor	Signature	Date

Examined By:

Mulugeta Habtemariam (PhD)	_____	_____
Internal Examiner	Signature	Date
Tolossa Debrie (PhD Candidate)	_____	_____
External Examiner	Signature	Date

Approved By:

Araya Abera (PhD)	_____	_____
Chair	Signature	Date

Endorsed by:

Yilma Tadesse (PhD)	_____	_____
Dean	Signature	Date
Ermiyas Tesfaye (PhD)	_____	_____
Associate Director,	Signature	Date
Post graduate program		

Acknowledgment

First of all, I would like to thank the almighty **God** for reaching me with such a fruitful success. Then, I would like to express my heartfelt thanks to my advisor **Dr. Samuel Tesfaye** for his excellent advice and time consumed with me during this thesis work. I would also thank **Henok Tsige Garage Center** mechanics and workers for their significant help in my data collection. Last but not least, I would like to express my appreciation to **all staff members** of the School of Mechanical and Industrial Engineering, **my friends,** and **my families,** those who helped me directly or indirectly during the progress in my thesis work.

Abstract

The connecting rod (Conrod) bolts are integral components of the engine that are used to connect the piston with the crankshaft through the connecting rod. If the conrod bolts pretension reliability is insufficient or excessive, deformation and fatigue failure will occur, resulting in component breakage and engine failure. At local maintenance shops, they are using different replacement materials than the initial material of the new automobile. The use of improper material is also the problem of engine failure. The focus of this thesis is to estimate the fatigue life of TOYOTA D4D Dolphin connecting rod bolts at high cycle using Finite Element Modeling with the help of software—ANSYS 2020 R_2 and MATLAB tools. The high cycle fatigue life was analyzed at different pretension forces to examine the effect of bolt pretensions and determine the appropriate bolt pretension value. The prediction of high cycle fatigue life was estimated using the Stress-Life approach. Additionally, the total deformation at insufficient and excessive bolt pretension was analyzed. Then the proper bolt pretension has been selected based on the analysis. Again, the existing in-use material for conrod bolts was compared with those the materials used by local automotive maintenance shops as a replacement. Their safety factor was identified to suggest which material is suitable for connecting rod bolts. The study results from the numerical simulation show that the value of bolt pretension has a more significant effect on the fatigue life and total deformation of connecting rod bolts, especially at higher cycles. When bolt pretension changed from 22KN to 30KN, the number of cycles of the materials reduced. The Insufficient values (<22KN)(i.e., 20KN to 0KN) of bolt pretension were applied to the model, and the total deformation increased from 0.16494mm to 0.26291mm, respectively. Again, the excessive values (>22KN) (i.e., 23KN to 50KN) of bolt pretension were applied to the model, and the total deformation increased from 0.16451mm to 0.21111mm, respectively. At the value of 22KN bolt pretension, the total deformation showed the lowest number (0.16449mm), which is the appropriate point to apply the clamping torque. In addition, the applied 22KN to 30KN pretension loads on the existing material (ARP2000), ARP625+, and ARP3.5 resulted in the fatigue life of $498.93*10^6$ to $489.13*10^6$, $409.71*10^6$ to $399.4*10^6$, and $407.59*10^6$ to $397.29*10^6$, respectively. For checking the safety factor of the materials, ARP2000 has a good safety factor. The ARP2000 has a greater number of life cycles than the replacement materials. To avoid early failure, therefore, tightening of the bolt needs to be controlled, and a replacement materials selection requires scientific methods of selection.

Keywords: High cycle fatigue, number of cycles, pre-tightened connecting rod bolts, Total deformation, Fatigue life prediction, Bolt pretension torque, Numerical simulation

Table of Contents

List of Figures

List of Tables

List of Abbreviations and Acronyms

P.E	Pin end
B.E	Big end
Conrod	Connecting rod
ARP	Advanced Racing Parts
C to C	Center to Center
UHL	Under Head Length
TDC	Top Dead Center
BDC	Bottom Dead Center
UNJF	Unified National Fine thread series with an external thread-controlled root radius
QTY.	Quantity
MATLAB	MATrix LABoratory
FEA	Finite Element Analysis
IC	Internal Combustion
ARP	Automotive Racing Products
ANSYS	Advanced Numerical System
M8x1	Nominal diameter 8mm with 1mm pitch
S-N	Stress-Life
AMS	Aerospace Material Standards
AISI	American Iron and Steel Institute
ANSYS	Analysis System

Terms

Clamp load: This is the same as preload and is the force exerted by a tightened bolt.

Fatigue: The process by which a material fails after several repetitions of loads that are less than its ultimate strength.

Preload: When a bolt is placed with a torque greater than hand tight, it is called preload. The less-than-accurate "turn-of-the-nut" method or measuring torque or bolt strain can be used to determine preload.

Reciprocating Load: The acceleration force placed on a connecting rod as a result of the piston's up and down motion and its accompanying mass.

Pretension: It is the term used in ANSYS workbench, when a nut and a bolt work together to keep two parts together, tension is created.

CHAPTER ONE

INTRODUCTION

1.1. Background of the Study

The automotive vehicle has become a basic necessity of today. In the recent development of high-speed and high-power lightweight engines, the harsh fatigue failure of the conrod bolt is frequently caused by the overload load due to some without unrecommended bolts pretension. Selection of the torque value to tighten the connecting rod bolts for high speed and great execution of automotive engine at high cycle is difficult. The value of bolt pretension utilized within the connecting rod bolts should be chosen shrewdly because, during the engine operation, it has got to experience different tensile loadings and subsequent which is exceptionally critical for fatigue life and for the parts total deformation. The common form of the connecting rod in the internal combustion engine is, comprised of a long shank, small end, and a big end. The cross-section of the shank may be rectangular, circular, tubular, H-section, or I-section is favoured for high-speed motors. The length of the I-beam connecting rod depends on the proportion of I/r, where r represents the radius of the crank. For any automotive vehicle, human comfort, durability, and safety are considered significant criteria. Reducing fatigue failure and deformation of small parts and ensuring unexpected cost, the safety of the vehicle, and the pleasure of the owners (customers) and passengers is the paramount consideration in the design of an automotive engine [1]. The bolt pretension while tightening the individual parts plays a significant role in the generation of noise and vibration and in the lifetime of the components during the operation of the engine. The costive parts may fail and may also require repetitive technician maintenance due to inappropriate bolts pretension. So, the bolt pretension in relation to fatigue life of the engine parts must be studied to eradicate unnecessary short lifetimes and failure while the vehicle is no longer serviced and to sound the entire engine reliable and durable.

Unquestionably the most important fasteners in any engine are the connecting rod bolts, as they hold the key to the entire rotating assembly. A broken bolt will lead to catastrophic engine failure. As it can be imagined, the most critical joint is where the connecting rod halves mate. The rod bolts must support the primary tension loads caused by each crankshaft's rotation (or cycle). With alternating tension loads of the bolts, installing fasteners that can exert a clamping force greater

than the load imposed upon the joint (tension) is very important. In addition to utilizing a rod bolt with sufficient strength to withstand the tremendous cyclical strains placed upon it, the bolts must be tightened appropriately. Moreover, by subsequently checking the rod bolt's length at tear-downs, it is possible to determine if it has been stressed beyond safe limits and must be replaced. This checking is practically done at the initial point when pre-tightening. This paper examined a bolted joint currently in service in one of the world's most successful automotive engine lines. Numerous experiments and finite element analyses are necessary to find the appropriate bolt pretension of the geometries and material life cycle that ensure the integrity of the component for the whole product life. Hence, there is a demand for reliable computational methods that allow the calculation lifetime of the components and optimize the components via computer simulations. Bolted joints are one of the most common joints in the industry and assemble most machine elements and segments. The majority of structures are affected by fluctuating forces; therefore, there is the risk of failures that causes countless damages; thus, finite element analysis of bolted joints has always been critical. With the rapid development of the automotive industry, connecting rod bolts have been widely used in automotive engine structures because of their simple and easy-to-assemble and dis-assemble behaviour during maintenance and some other lubrication and inspections. However, inappropriate bolt pretension is becoming the core origin of connecting rod bolts failure. If the bolt tightening axial force that determines the tightening strength is insufficient, the outer force of the bolt increases as the fastening surface is separated; it can be damaged by fatigue. Conversely, if the bolt tightening axial force is greater (excessive), the bolt will have a large average axial force. Small elastic strains generate high cycle fatigue, which occurs over a large number of load cycles before breakdown. A combination of mean and alternating stresses causes the stress. Because HCF is driven by elastic deformation, stress is a more practical metric to utilize as a failure criterion than strain. A stress–life curve is commonly used to describe the component's HCF life. Parts certified for use on automotive engines were first analyzed in the late 1970s and early 1980s using finite element codes that were emerging for commercial use. Many of the components in use today are based on previous designs verified primarily with field experience, engine tests, and hand calculations [2]. It has only been in recent years that finite element analysis (FEA) has been useful in understanding the behaviour of early, fielded engine components [2].

Engine components are generally subjected to many repeated run-stop cyclic loadings. So that the bolt used for the assembly of engine parts also faces the action of loadings from the run-stop condition of automotive engine components. Here, the bolt-nut used for this study analysis is connecting rod bolts. According to the current research of the static analysis for threaded connections, it can be seen that many researchers have studied the finite element behaviors of bolts through various theoretical and experimental methods. However, a limited kind of literature was dedicated to studying the pre-tightened connecting rod bolts for specific functional working load through numerical simulation. Motivated by this aspect, this paper was examined the numerical simulation of pre-tightened connecting rod bolts.

Figure 1.1: Connecting rod bolts failure (a & b) [3] [4] and observations from Henok Garage Center (C, D and E) image by Bikila

This thesis has looked at examining the proper bolt pretension suitable for the clamping of automotive engine connecting rod bolts. It was also concerned with identifying the impact of taking different bolt pretensions on the parameters like total deformation, equivalent stress, alternating stress, and fatigue life. Additionally, it simulated interchangeably used materials and analyzed them by the varying value of bolt pretension with common external tensile loading. The materials were examined to discover the best material appropriate for the high cycle fatigue life of the connecting rod bolts using numerical analysis technique. Solid works software was used to

model the functional part and is saved using .step204 format for simulating on ANSYS workbench 2020 R_2. Regarding whether the numerical analysis is accurate, the thesis provides numerical simulation for comparing results from the existing functional connecting rod bolts to validate the static model analysis. The main fact for applying these approaches is to make the parts in an integral manner and to achieve the highest productivity with reduced cost [5].

1.2. Statement of the Problem

Bolted joints are broadly utilized in different mechanical designs because of their boss securing properties. However, bolt pretensions, fluctuating loads, and the type of material selected for bolts are likely to cause the failure of bolted joints, mostly in automotive engines. Many engine parts are subjected to varying loads during start-up and shutdown, leading to non-uniform and non-stable operation. The connecting rods are subjected to fatigue due to alternating loads[1] and over-revving inside the engine. Their failure is one of the most common causes of catastrophic engine failure, mainly from the deformation and fatigue of connecting rod bolts that come from improper bolt-nut tightening. Thus, today, connecting rod bolts are facing different failure types—high cycle fatigue and deformation. High cycle fatigue occurs on the components having a high number of cycles and low stresses value which causes deformation; thus, in the engine connecting rod, it is causing the bolts failure to operate. Deformed bolt nut connections can cause the entire operation of a car engine to stop working and standstill, thereby leading to crushing and damaging the whole of the vehicle [6].

According to the Henok Tsige Garage Center visit in Addis Ababa, Ethiopia, the case of two TOYOTA D4D Dolphin had the same type of bolts that deformed inside their engine 3RZ-FE 2.7L model [6]. The cars faced the problem at the connecting rod bolts, failure to clamp the connecting rods with the crankshafts. The garage maintenance men replaced the existing bolt of ARP2000, usually either ARP 3.5 or ARP625+ materials. The replacement is done without identifying why the existing material was failed. The maintenance men use non-recommended clamping force to tighten the bolts by simply turning the nuts until they are beyond their applied force. Also, regarding the TOYOTA company, in the case of bolts torque recommendation, they did not specify the value, but torque recommendation range 32N.m to 43N.m [7] [8]. When the conrod bolt is damaged, the entire engine is failed; since the damage results in safety are critical, it is very

important to prevent it before the failure by the correct evaluation. But the problem is that the case of deformation at the connecting rod bolt is not only due to fatigue. The type of material used for the parts has a critical issue with the durability of the connecting rod bolts.

This work presented the high cycle fatigue and deformation case observed at the existing on-use I-beam shape connecting rod (2006 Model-TOYOTA D4D Dolphin) produced from AISI 4340 and its connecting bolts from the existing (ARP2000) and replacement (ARP625+ and ARP3.5) materials. The purpose of this thesis work is to carry out a numerical investigation on fatigue life of engine pre-tightened connecting rod bolts at different variable bolt pretensions applied at the existing and different replacement materials used by the local automotive garage. So, the research fascinated to examine the effect of bolts pretension on the total deformation, stresses, and high cycle fatigue life of the connecting rod bolts and checking an appropriate material selection of connecting rod bolts to obtain a high number of cycles by correcting a proper bolt pretension.

1.3. Objectives

1.3.1. General Objective

The main objective of this thesis is the numerical investigation for high cycle fatigue life prediction of pre-tightened connecting rod bolts, the case for the 2006 Model-TOYOTA D4D Dolphin.

1.3.2. Specific Objectives

- ✓ To analyze the effect of insufficient, appropriate, and excessive bolt pretension on the total deformation of the connecting rod bolts;
- ✓ To analyze the effect of bolt pretension on equivalent stress and alternating stress;
- ✓ To predict and compare the high cycle fatigue life of connecting rod bolts of different materials at different values of bolt pretension using MATLAB;
- ✓ To analyze the effect of bolt pretension on fatigue life parameters like life and damage using ANSYS workbench 2020 R_2;
- ✓ To compare the safety factor for the connecting rod bolts materials at different bolt pretension; and;

1.4. Research question

A research question is a specific question to which the research aims to respond. It is at the heart of systematic investigation and aids in the clear definition of a research route. As a result, the following question must be answered in order to handle the stated problem.

1. What is the cause for the failure of connecting rod bolts at high cycle?
2. What is the effect of bolt pretension on the high cycle fatigue life of the connecting rod bolts?
3. What is the effect of bolt pretension values on the total deformation of connecting rod bolts?
4. What is the effect of bolt pretension values on the stresses employed inside the connecting rod bolts?
5. Which bolt pretension is proper (or recommended) for the component to protect deformation and for the high life cycle of TOYOTA D4D Dolphin connecting rod bolts?
6. The effect of bolt pretension on materials interchangeably used at high cycle fatigue life and their safety factor?

1.5. Aim of the Study

The work aims to create a three-dimensional model of the existing connecting rod with its pre-tightening bolts, suggest the suitable bolt pretension for connecting rod bolts, and examine the parameters that affect the fatigue life of connecting rod bolts.

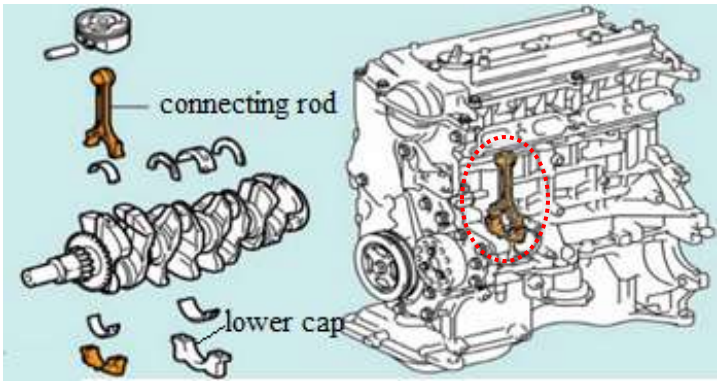

Figure 1.2: Aim of the study [4]

1.6. Scope

The scope of this thesis work is listed as follows:

- Literature study on high cycle fatigue life of pre-tightened connecting rod bolts for various parameters like bolt pretension and materials
- Determining the fatigue life at high cycle and behaviour of pre-tightened connecting rod bolts under different values of bolt pretension using Basquin formula, ANSYS Workbench 2020 R_2, and MATLAB
- Numerical simulation of connecting rod bolt and nut assembly inside the engine car that subjected to different tensile loading fluctuation using ANSYS Workbench 2020 R_2 and MATLAB
- Comparing the results of numerical simulation with each other selecting the best result, and recommending for putting into practice

1.7. Limitation

The thing that will not significantly skew the result of this research is that while working with simulation on ANSYS workbench and MATLAB, the manual data taken from the garage center and literature used as a reference in this work did not provide all the necessary data, especially for dynamic analysis. Ordinarily, the static analysis has to be carried out at all examinations of revolution. In any case, this is often time expending and requires lots of computational time, so the investigation is restricted to a particular position of connecting rod angles. Therefore, this work only focused on high cycle fatigue life prediction at Top Dead Center.

1.8. Significance

The significance of this thesis work will be:

- ❖ Many of the joining components are based on previous designs verified by field experience, engine tests, and hand calculations. On the other hand, this thesis will benefit from simplified modelling capability, minimized time consumption, and reduced budget when analyzing the high cycle fatigue life prediction of the engine's pre-tightened connecting bolts using the Finite Element Method software packages (ANSYS and MATLAB).

- This thesis also helps the owners of cars not to spend their money at the garage center due to the failure of a small part (bolt-nut), causing further failure to operate the whole engine system.
- This newly best-selected bolt pretension for engine connecting rod bolts motivates the researchers to examine the other effects of bolt pretension to conduct further efficiency of pre-tightened connecting rod bolts within the same methodological analysis or using another methodology.

1.9. Expected Outcomes

Due to the results from the study of higher model accuracy, solutions obtained for the analysis of connecting rod bolts were achieved so that the output results are taken from the ANSYS workbench, and MATLAB can be applied to the practical operating engine system in the future. The automotive engine connecting rod bolts analysis using FEM for the different values of bolt pretension and materials under typical connecting rod loading introduced at the end of this research. The response of bolt pretension and the material due to uniaxial tension load established. The simulation ensured that the designers, the researchers, and the concerned person will study the behaviours for different values of bolt pretension based on the analyzed results.

1.10. Geometrical Concept of the study

The geometrical concept of the study is required to get the idea of the analysis without any complexity. It is used to understand better how the modelled part will be examined, simulated, and analyzed. In this research, the concept of the work conducted was simplified in figure 1.3.

Figure 1.3: Concept of the study using geometry

1.11. The research methodology

In this work, TOYOTA's specifications for the 2006 Model-TOYOTA D4D Dolphin with 3RZ-FE 2.7L engine connecting rod and connecting rod bolts have been observed from Henok Tsige

Garage Center to examine, analyze and compare the effect of bolt pretension for connecting rod bolts high cycle fatigue and deformation.

FEM methodology is advantageous to reduce the cost of the component to know its actual behaviour before production and implementation. This type of analysis (numerical simulation) technique only needs physical property and parametric geometry with load conditions, making fast evaluation time. The mathematical approach of non-linear interpolation is useful for predicting data points, which contributes to decreasing the time for conducting experiments. The numerical simulation was performed under the action of uniaxial tensile loading with the same loads and varying values of bolt pretension to identify which value of bolt pretension can withstand fluctuating load occurring inside the automotive engine and which material is also recommended at that bolt pretension. The followings are the methodologies waged:

Literature Review: From the literature review, many theories and data have been supported and pivoted in order to ensure methodology and get important information about the analysis of the pre-tightened connecting rod bolts, digging different materials. In addition to the secondary data (works of literature), also additional available data is used from Henok Garage Center, various books, the internet, and journals.

Data Collection: The data was gathered before the analysis work, and all the essential data regarding connecting rod bolts were taken from the Henok Tsige Garage Center and the internet. The connecting rod model is prepared based on the available standard according to the bench (experimental) tests and literature for conducting the numerical simulation. The pre-tightened bolt's geometrical specifications and loading conditions data are collected from Henok Garage Center, the earlier works of literature and automotive manual catalogues.

Modelling and Simulation of Connecting rod bolts: The modelling of the functional part is done by using Solid Works 2021 and imported to ANSYS workbench to simulate and analyze their fatigue life prediction at various bolt pretension. The first step (Simulation 1) was simulated to obtain the alternating stress to determine the number of cycles using the Basquin formula by MATLAB software. In this step, the alternating stress was used as an input for the second step (Simulation 2) to obtain the life, the damage, and safety factor of connecting rod bolts. In the third

step (Simulation 3), the existing material and the materials used as replacement was analyzed and compared with each other.

Results and Discussion, Conclusion, Recommendation and Future work: Results are taken from the simulated model from the ANSYS workbench 2020 R_2 and MATLAB. Discussion and conclusion are written depending on the finite element analysis results. The recommendation is drawn out from the results conducted. Finally, future work has put the points for further study of the paper. Generally, the methodology of this thesis work is:

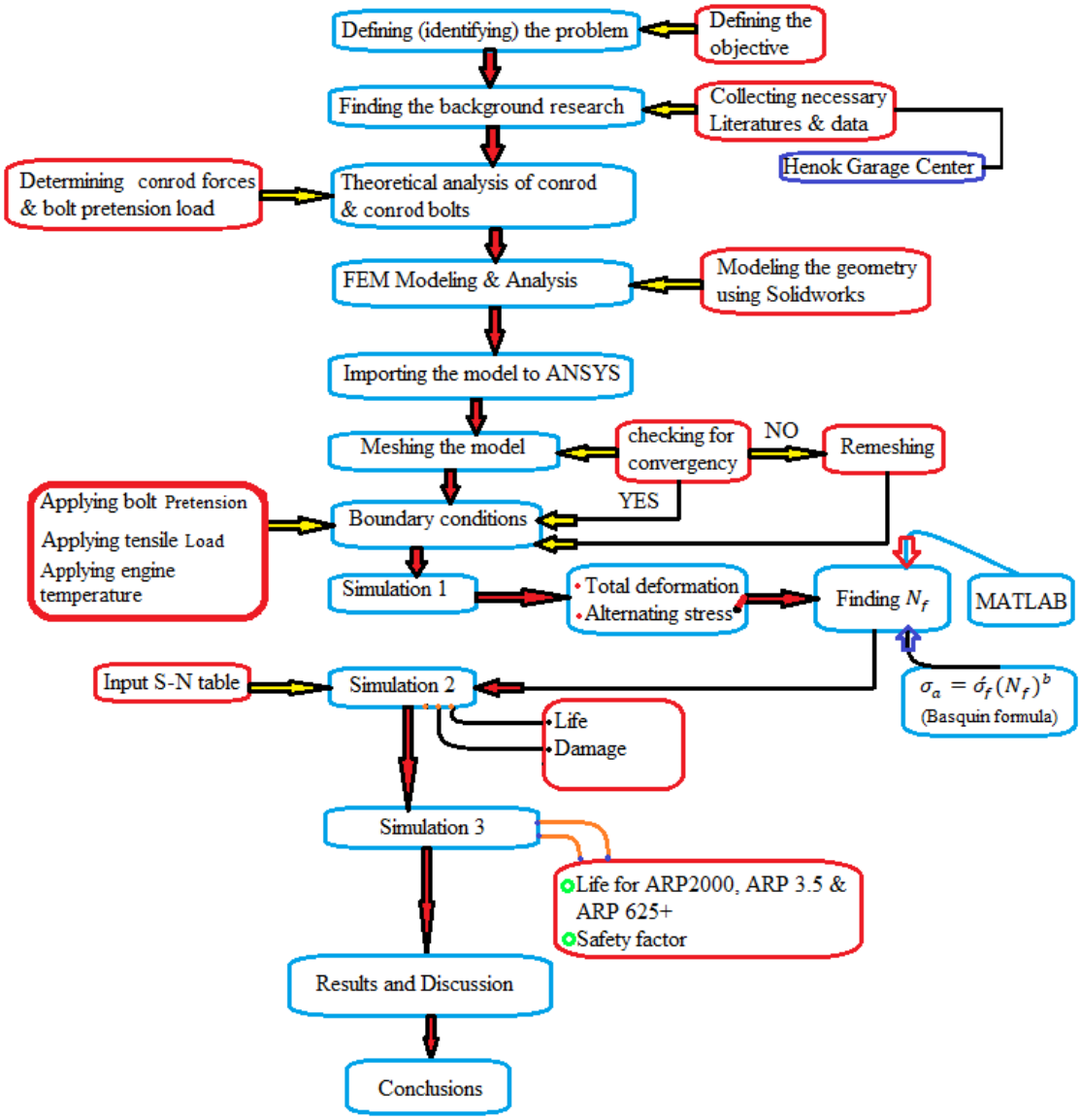

Figure 1.4: Methodology of the research

1.12. Organization of the study

This study is organized into five chapters. Chapter one deals with the introductory part, which consists of the background, problem statement, objective (general and specific objectives), scope, limitation, significance, expected outcome, geometrical concept, and organization of the study. The second chapter states the review of related literature. Chapter three presents the theoretical research analysis of connecting rod and connecting rod bolts. Chapter four deals with Finite Element Modelling and Analysis, chapter five states research results and discussion, conclusion, and recommendation.

CHAPTER TWO

LITERATURE REVIEW

2.1. Introduction

Engine fastening, which uses bolt nuts, is the common method of joining structural parts due to their relative ease of assembling and disassembling during maintenance, lubrication, and replacement of engine parts. The appropriate instruction-based installation and materials with high fatigue strength at operation are needed in automotive engine components. Cylinder head, piston, engine oil pan, and gears are some of the examples of high-speed operating automotive engine components. Failure to reach an appropriate bolt pretension for automotive engine connecting rod bolts may cause fatigue, misalignment and deformation in the engine, leading to reduced expected life parts, fracture of the whole system, and causing a catastrophic accident. Consequentially, to improve automotive connecting rod bolts' failure/deformation and high cycle fatigue life, the research areas have an essential role in fulfilling improved and accurate connecting rod bolts.

2.2. The fatigue life of the materials

The total number of stress cycles necessary to cause failure is known as fatigue life (N_f). Researchers have utilized the stress-life approach, strain-life, and linear-elastic fracture mechanics methods to determine a material's fatigue life. Fatigue is a type of surface failure. Because faults are inside, this surface can be both internal and external. Fatigue is caused by the application of repetitive loads, according to material science. Fatigue causes the material to deteriorate. When a material is subjected to cyclic loading, it develops gradual and localized structural deformation. The nominal maximum stress that causes this type of damage in a material is usually substantially lower than the material's strength, often known as the ultimate tensile stress limit or yield stress limit. When a material is subjected to repetitive loading and unloading circumstances, fatigue develops. Microscopic cracks will occur at stress concentrators such as the surface, persistent slip bands (PSBs), and grain interfaces if these loads exceed a particular threshold. A crack will eventually reach a critical size, at which point it will abruptly propagate, culminating in fracture [9].

2.3. Fatigue life S-N curve for high tensile steel

Fatigue curve, named S-N curve, is defined as the regression of stress range with increasing fatigue lifetime. In the middle 1800s, fatigue failures increased because of the industrial revolution; Wohler initially developed the S-N curve; therefore, in honour of him, the S-N curve was also called the Wohler curve since 1936. Incidentally, his experimental results were expressed in the form of tables at that time, and only his successor Spangenberg plotted them as curves in the unusual form of linear abscissa and ordinate. Not until 1910 did Basquin represent them in the form of logarithm ordinate and abscissa and found the simple linear formula such that [10].

$$log\sigma_a = log\acute{\sigma}_f + blog(N_f) \quad [2.1]$$

Where, σ is stress amplitude (alternating stress), $\acute{\sigma}_f$ is the fatigue strength coefficient (for metal material, the $\acute{\sigma}_f$ value is the true fracture strength of the material), N_f is the number of cycles to failure, and b is the fatigue strength exponent on a log-log plot and also named as Basquin exponent [10]. The fatigue life, N_f, is defined by the American Society for Testing and Materials (ASTM) as the number of stress cycles of a specific type that a specimen may withstand before failing of a stated nature. Cyclic stresses, residual stresses, material characteristics, internal flaws, grain size, temperature, design geometry, surface quality, oxidation, corrosion, and other factors all affect fatigue life. There is a theoretical threshold for stress amplitude for some materials, notably steel and titanium, below which the material will not fail for any number of cycles, known as a fatigue limit, endurance limit, or fatigue strength [11].

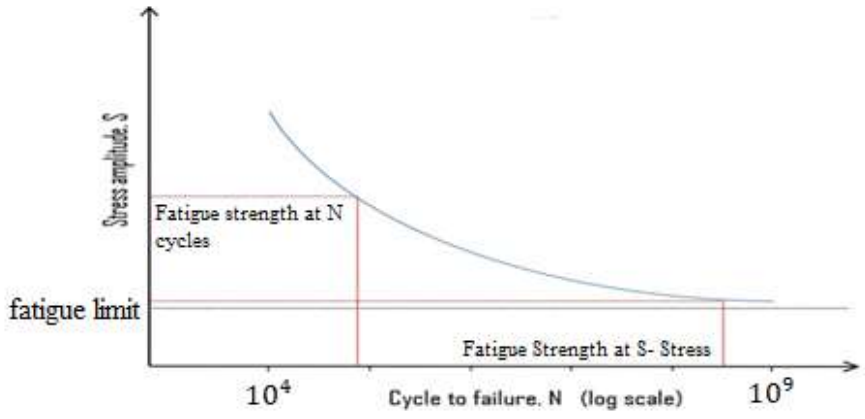

Figure 2.1: S-N curve [11]

The stress-life approach, which is often characterized by an S-N curve, also known as a Wohler curve, is one of the most useful. This procedure is depicted in the diagram. It shows applied stress (S) versus component life or the number of failure cycles (N). Component life grows slowly at first and then rather rapidly as stress drops from a high value. Because fatigue, such as brittle fracture, is so varied, the data required to plot the curve will be statistically treated. The results are skewed due to fatigue sensitivity to a number of test and material parameters that are difficult to control exactly [11] [12].

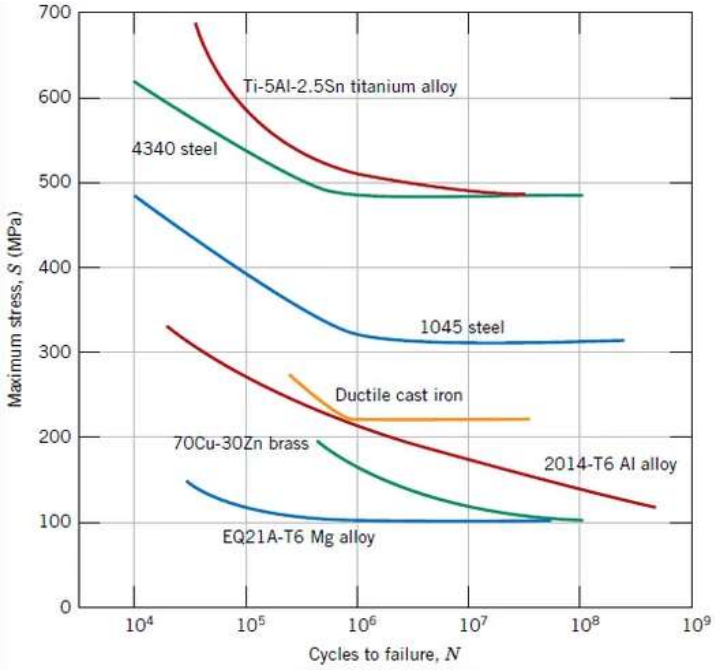

Figure 2.2: S-N curve for different materials [11] [13]

The below figure 2.3 illustrates the experimental S-N curve for AISI 4130 steel tensile specimens under fully reverse loading (R = -1). The specimens were prepared under ASTM guidelines. The study by Singh et al. contains more information [9] [14].

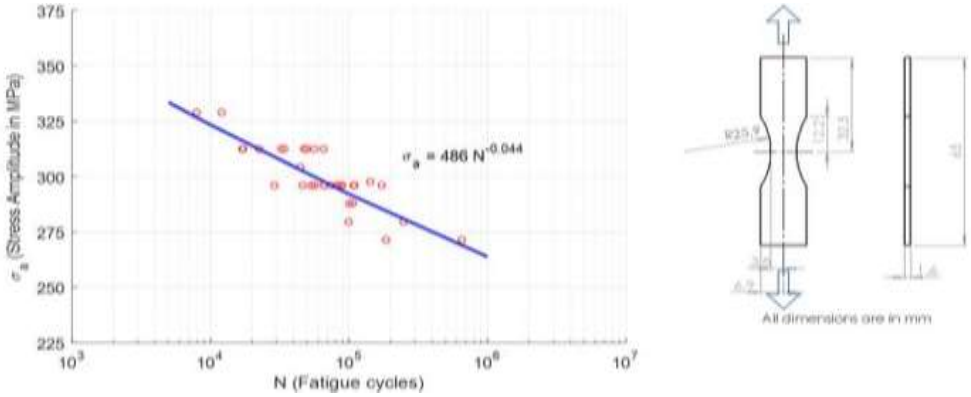

Figure 2.3: Experimental S-N curve for AISI 4130 tensile specimen-fully reversed loading [9]

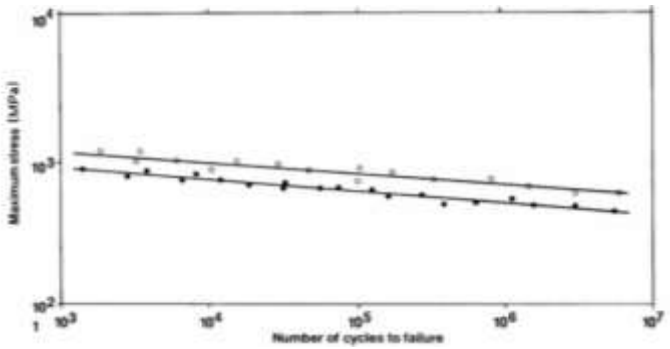

Figure 2.4: S-N curve for AISI steels [9]

2.4. Low and high cycle fatigue life

There are two types of fatigue: high cycle and low cycle fatigue lifes. The number of cycles to failure is the main distinction between high and low cycle fatigue. The stress level, i.e. the transition between plastic and elastic deformations, determines the transition between LCF and HCF [9]. High cycle fatigue requires more than 104 cycles to failure when the load is minimal and predominantly elastic. Low cycle fatigue is defined by recurrent plastic deformation (i.e., within each cycle), resulting in a low number of cycles to failure. Small variations in tension can cause substantial changes in strain in the plastic region. Low cycle fatigue has been linked to crack growth in experiments. The effect of cold expansion, interference fit, clamping force, bolt types on the S-N curve for high cycle fatigue test joints is shown in figure 2.5.

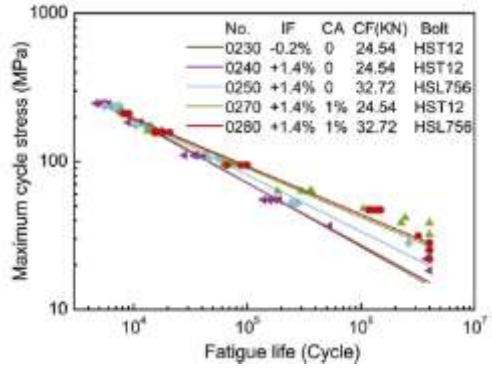

Figure 2.5: S-N curve for high cycle fatigue life [15]

2.5. Failure of jointed bolts

Several reasons may lead to the failure of bolted joints, and the majority of them are related to the clamping force. The five most common issues are [16]:

- Insufficient clamping force
- Shear failure

- Excessive clamping force
- Fatigue failure
- Thread stripping

2.6. Related works

The following section is a literature survey presenting previous research findings on the fatigue life prediction of pre-tightened bolts.

(Oh et al., 2020)[17] analyzed the failure of connecting rod bolts in a diesel engine that operates for military tracked vehicles. The authors conducted the engine's failure mechanism in this study based on hardness test, overhaul test, and fracture surface analysis. The result from the overhaul test shows bolt separation from connecting rod. The result from the fracture surface shows the type of fracture found to bolt was a ductile fracture. Depending on these results, they concluded that fracture to a diesel engine was due to loosening of connecting rod bolts. The question comes to mind as the gap is, "what is the reason behind the loosening of connecting rod bolts?".

(Zhu et al., 2017)[18] published the study on the analysis of failed connecting rod caps and connecting rod bolts for a reciprocating compressor device. The work focused on the 48.67 cycles per second in service connecting rod cap and connecting rod bolts failure cause. Material characterization and numerical analysis are performed on connecting rod cap and connecting rod bolts to know the failure mechanism and which component was broken first. The authors analyzed the macro and micro structures of connecting rod cap and connecting rod bolts using Scanning Electron Microscope (SEM) and optical microscope technique. The results show that high cycle fatigue fracture and initial crack location are the reason for the failure of both components, and connecting rod cap was broken before connecting rod bolts. This study has a gap for software analysis for the failed connecting rod caps and connecting rod bolts to optimize and compare with the failed parts.

(Q. Yu et al., 2018)[19] reported the experimental research on high-temperature low cycle fatigue life of pre-tightened bolts. According to this study, the experimental test is conducted on M8*1 pre-tightened bolt to analyze its fatigue life at the temperatures of 550℃ and 650℃ and validate the accuracy of the new proposed low cycle fatigue theoretical model from Socie model and Morrow model based on the von Mises equivalent stress/strain criterion. The research provided

the theoretical basis. The study didn't validate the experimental test results in comparison with numerical simulation and did not predict the damage, biaxiality indication, safety factor, and fatigue damage sensitivity of pre-tightened bolts. Finally, it concluded that the fatigue failure occurs at the first engaged thread of the bolt and nut interface, using inserting the stress and strain results taken from ANSYS into the newly proposed models.

(Habibi & Amoorezayi, 2019)[20] estimated fatigue life and simulated 3D model of the bolted joint using critical distance technique. In this paper, the experimental results of the fatigue life test were correlated with the bolted joint that predicted using critical distance technique by considering helix angle for threads. The 3D dimensional bolted joint is simulated in ABAQUS software. In the end, the study concluded that the stress versus the number of cycles to the failure curve (S-N curve) was in good agreement with the experimental result.

(Q. M. Yu et al., 2018)[21] studied the relationship between preload of threaded connections using experimental. The work in this paper examined Nickel-based super alloy bolts and nuts of M8*1, M10*1.25, and M10*1.5 to carry out the pre-tightening test at room temperature. The influence of surface lubrication and toughness on the nut factor was analyzed. The result shows that the lubrication of contact surfaces has a significant effect on the nut factor. But the study did not validate the results using the finite element method.

(Seifert, 2008)[22] predicted the fatigue life of high-temperature components in combustion engines and exhaust systems using computational methods. The study predicted the fatigue life based on the law for micro crack growth. Sheet metal and Cast-Iron exhaust manifolds are proposed to determine the model parameters experimentally and numerically to predict their fatigue life. In both cases, failure locations and the number of cycles to failures were well agreed with results obtained from experimental tests. On the other hand, the paper did not cover the proposed model's bolt and nut fatigue analysis.

(Saranik et al., 2013)[23] implemented the experimental and numerical study to predict the low cycle fatigue life of the bolted connection. In this work, the experimental test is carried out by specimens of cantilever beams fixed at one end by a bolted joint and a free end at the other side with tip mass. The numerical study is conducted to conduct the experimental model's error and

predict the lifetime of bolted connection. The Monte Carlo simulation has been used to identify the influence of the uncertainties. Finally, the Monte Carlo simulations were compared with the experimental results. Concluded that due to repeated excitation, a loosening phenomenon can reduce the clamping force of the bolts, and then the cyclic loading causes sliding in the assembled elements, which change the stress distribution and gradually produce fatigue damage in the bolted connection.

(Liu et al., 2018)[15] reported the experimental and numerical investigations on fatigue behaviour of Aluminum alloy 7050-T7451 single lap four joints. The main contribution of this study is the Aluminum alloy 7050-T7451 single lap four bolted joints was investigated by high-frequency fatigue test and finite element (FE) methods to obtain fatigue behaviour of the joints. The fatigue test results showed a better enhancement of fatigue life achieved for the joints with high-locked bolts by employing the combinations of cold expansion, interference fit, and clamping force. FE models were used to obtain the stress variation in the joint plates at the hole edge to help explain the trends observed in the experimentally obtained fatigue data. The evaluation of residual stress conducted by FE methods confirmed fatigue crack initiation's experimental results and locations.

(Sapieta & Sulka, 2019)[24] analyzed the fatigue damage of bolted joints for two types of models. The first type of model is a screw without thread and the second type is a screw with thread. The study is conducted using numerical simulation by the Finite Element Method (FEM). Finally, the paper compared the results of the two models and concluded that the model which has been considered with thread on the screw is more accurate because the value of the damage is greater.

(Series & Science, 2018)[25] experimentally studied the influence of thread bottom radii and slight pitch difference of bolt-nut joint specimens on fatigue life and fatigue limit, and also crack propagation path by slight pitch difference. The result showed that increasing the bolt's thread radius and introducing the pitch difference can improve the fatigue life of the bolt-nut joint. The experimentally conducted tests are compared and discussed regarding stress analysis using FEM.

(Zheng et al., 2013)[26] analyzed the stress distribution and fatigue life of a lightweight engine connecting rod using commercial ANSYS software. According to this study, the connecting rod material is selected as 40Cr steel and the analysis considered the big end, shank, and small end

only. The big end of the connecting rod is simplified, and connecting rod bolts are ignored from the analysis. The result shows that the connecting rod's maximum stress distribution and deformation are 190.23 MPa and 0.0507mm, respectively. The safety factor is 1.584.

2.7. TOYOTA Engines

2.7.1. TOYOTA

Toyota Motor Corporation, based in Japan, is one of the world's leading automobile manufacturers. Toyota is the largest Japanese automobile manufacturer, with numerous subsidiaries operating in a variety of fields (financial services, for example). Toyota owns Lexus and Scion automobile brands, as well as a majority ownership in the Daihatsu automotive industry. In terms of design and technical components, Toyota, Lexus, and Scion vehicles are remarkably similar, with just minor changes. This is also true with engines. Toyota engines come in a variety of gasoline and diesel configurations, with the majority being four-cylinder and V-shaped six-cylinder engines. Toyota also makes hybrid engines. The Toyota Prius is the most well-known hybrid vehicle. Toyota primarily produces huge and strong V8 engines for big pickup trucks and Sports Utility Vehicle (SUV) in North America. Toyota engines are known for their durability and dependability. Toyota engines employ cutting-edge technology while relying on tried-and-true technical improvements. Engines are highly efficient and environmentally friendly [27].

2.7.2. Types of Models of TOYOTA engines and their application area

The selected model of engine for this study is encircled by red colour [27], and it was briefly explained in the next section. The reason for selecting 3RZ-FE 2.7L Engine is that the damage is frequently happening on this model as described in the problem of statement, and this model is abandont in Ethiopia.

1AR-FE 2.7L Engine	1GR-FE 4.0 V6 Engine	1MZ-FE 3.0L Engine
Highlander, Venza	4Runner, Tundra, Tacoma	Camry, Avalon, Solara
1AZ-FE/FSE 2.0L Engine	1JZ-GTE/GE/FSE Engine	1NZ-FE/FXE 1.5L Engine
Camry, RAV4	Supra, Mark II	Auris, Prius, Corolla
1GD-FTV 2.8D Engine	1KD-FTV 3.0 D-4D Engine	1UR-FE 4.6L Engine
LC Prado, Hilux	Prado 120/150, Hilux	

Tundra, Lexus LS 460, GS 460

1UZ-FE 4.0L Engine

Lexus LS 400, Toyota Crown

1VD-FTV 4.5L V8 D Engine

Land Cruiser 200, LX450D

1ZZ-FE 1.8L Engine

MR2, Corolla, Celica

2AR-FE 2.5L Engine

Camry, Scion tC

2AZ-FE 2.4L Engine

Camry, Scion tC

2GR-FE/FSE/FKS 3.5 V6 Engine

Camry, Highlander, Lexus GS/IS/ES 350

2JZ GE/GTE/FSE Engine

Supra, IS300

2KD-FTV Engine (2.5 D-4D)

Hilux, Fortuner

2NZ-FE 1.3L Engine

Yaris, Corolla

2TR-FE 2.7L Engine

4Runner, Tacoma, LC Prado

2UZ-FE 4.7L Engine

Tundra, Land Cruiser, Lexus LX 470

2ZR-FE/FAE/FXE 1.8L Engine

Corolla, Prius, Yaris

3MZ-FE 3.3L Engine

Highlander, Lexus RX 330/400h

3RZ-FE 2.7L Engine

Tacoma, 4Runner, **Toyota HiAce**, Toyota HiAce Regius, Toyota Land Cruiser Prado, Toyota Touring Hiace

3S-GE 2.0L Engine

Celica, Altezza

3S-GTE 2.0T Engine

Celica, MR2

3UR-FE 5.7L Engine

Toyota Tundra, Land Cruiser 200, Lexus LX 570

3UZ-FE 4.3L Engine

Crown Majesta, Lexus GS 430, LS 430

3VZ-FE 3.0L Engine

4Runner, Camry

3ZR-FE/FAE 2.0L Engine

Corolla, Rav4, C-HR

5VZ-FE 3.4L Engine

4Runner, Tacoma

8AR-FTS 2.0T Engine

Lexus NX 200t, IS 200t

8NR-FTS 1.2T Engine

C-HR, Auris

A25A-FKS 2.5 D-4S Engine

Camry 70, Rav4

M20A-FKS 2.0L Engine

Corolla, Rav4

V35A-FTS 3.5L Twin Turbo Engine

LS 500

2.7.3. TOYOTA 3RZ-FE 2.7L Engine

Toyota's 3RZ-FE engine is a 2.7-liter inline four-cylinder gasoline engine. It was mostly utilized in commercial trucks and four-wheel-drive vehicles. A deep-skirt cast iron cylinder block is used in the 3RZ engine. Both the bore and stroke are 95.0 mm (square engine). A forged crankshaft with eight counterweights and a torsional damper pulley is used in the engine. Carbon steel connecting rods are shot-peened and forged. Oil jets are inserted inside the cylinder block to spray oil on the bottom of the pistons for further cooling. Two gear-driven balancing shafts are installed

in the engine's crankcase. An aluminium cylinder head with two overhead camshafts sits atop the engine block (DOHC layout). It has two intakes and two exhaust valves per cylinder, with a 19-degree, included valve angle between them. The intake valve is 37.5 mm in diameter, while the exhaust valve is 30.5 mm in diameter. There are no hydraulic buckets or lifters. A shim over bucket design provides valve adjustment (preferably every 25-30k miles). The timing chain of the 3RZ FE engine only operates the intake camshaft. A scissors gear connects the intake and exhaust camshafts. Intake duration is 230 degrees, and exhaust duration is 224 degrees, according to the camshaft specifications. A hydraulic timing chain tensioner and an oil jet lube the chain on the engine. Aluminium alloy is used to make the intake manifold. Each cylinder has two intake runners that are uniquely engineered to maximize torque. The engine received an electronically controlled multiport fuel injection system as well as Toyota's Electronic Spark Advance (ESA) ignition, which allowed the Electronic Control Module (ECM) to determine ignition timing based on sensor inputs. Instead of a coil pack, early engines used a single ignition coil and a basic distributor [28].

Figure 2.6: Toyota 3RZ-FE 2.7L Engine [28]

2.8. Bolts materials

It's critical to choose the best material for a particular fastening application. That's why high-performance fastener producers use a diverse range of materials, from common stainless steel and 8740 chrome moly to exotic alloys created specifically for land and space transportation. It should also be informed that different alloys have different grades. 8740, for example, comes in four grades: SDF (Guaranteed Seamless and Defect-Free), CHQ (Cold Head Quality), Aircraft, and Commercial. Even though they cost more than twice as much as "Aircraft" quality, only the first two (SDF and CHQ) are used to make high-quality car fasteners [29].

Stainless Steel: Because stainless steel is heat resistant and almost impenetrable to rust and corrosion, it is ideal for many automotive and marine applications [29].

Figure 2.7: Stainless steel

8740 Chrome Moly: Chrome-moly was often regarded as a high-strength material until the development of today's new alloys. 8740 chrome moly is still considered good strong steel with appropriate fatigue qualities for most racing applications, but only if the threads are rolled after heat treatment. When heat-treated, chrome-moly is often classed as a quench and temper steel with tensile strengths ranging from 180,000 to 210,000 psi [29].

ARP2000: This hybrid-alloy was created exclusively for fastener business ARP to provide enhanced strength and fatigue qualities. While the 8740 and ARP2000 have comparable properties, the ARP2000 has a 215,000-220,000 psi clamp load range. ARP2000 is a popular upgrade from 8740 chrome moly in both steel and aluminum rods in short track and drag racing. Stress corrosion and hydrogen embrittlement are usually not a concern if proper installation precautions are adopted[29] [30].

ARP3.5 (AMS5844): These super-alloys, which are similar to Inconel 718, are used in a variety of jet engine and aerospace applications where heat and stress shorten the life of key components. This alloy's high cobalt concentration, while costly, results in a material with better fatigue properties and tensile strengths in the 270,000 psi range. The resistance of these materials to hydrogen embrittlement and corrosion is an important design consideration. These materials are typically employed in connecting rods for Formula 1, Winston Cup, and CART applications, where exceptionally high loads, high RPM, and endurance are critical [29].

Figure 2.8: ARP3.5 (AMS5844)

Custom Age 625+ (ARP625+): This newly created super-alloy has better fatigue cycle life, tensile strength, and toughness, as well as total resistance to corrosion and oxidation in the atmosphere. Best of all, it's less expensive, and it's predicted to overtake MP-35 as the material of choice in the high-strength, super-alloy industry in the near future. The typical tensile strength is 260,000 pounds per square inch [29].

Inconel 718: Inconel 718 is a nickel-based superalloy that is used in high-temperature applications but is also suited for lower-temperature applications. This material has tensile strengths of up to 220,000 pounds per square inch and better fatigue characteristics. Above all, Inconel 718 is unaffected by hydrogen embrittlement or corrosion.

L19: This is high-quality steel that has been treated to provide exceptional strength and fatigue resistance. When compared to 8740 and ARP2000, L19 has much higher strength and can deliver clamp stresses in the 230,000-260,000 psi range. It's generally employed in short track and drag racing applications where inertia loads are greater than ARP2000's clamping capacity. L19, like most high-strength, quench-and-tempered steels, necessitates extra caution during production to minimize hydrogen embrittlement. This material is prone to contamination and stress corrosion. It must be well-oiled and kept away from dampness [29].

AISI 4340 Steel, oil quenched 855°C (1570°F), 230°C (450°F) temper for 4 hrs: AISI 4340 has a favourable response to heat treatment (usually oil quenching followed by tempering) and exhibits a good combination of ductility and strength when treated thusly. Uses include piston pins, bearings, ordnance, gears, dies, and pressure vessels [31].

CHAPTER THREE

THEORETICAL ANALYSIS OF CONNECTING ROD AND CONNECTING ROD BOLTS

3.1. Introduction

Nowadays, the automotive vehicle has gotten to be an essential and a basic necessity. For any car vehicle, human consolation is considered a significant measure. The most thought within the plan of a vehicle engine is decreasing fatigue, deformation, and guaranteeing the safety of the vehicle. Additionally, the delight and consolation of the travellers are also the primary concern of an automotive engine. The force transmitting through the parts of the automotive vehicle like connecting rod, connecting rod bolts, crankshaft, valve trains, and camshaft is mainly producing the high cycle fatigue and the deformation. The high cycle fatigue and deformation come from due to the parameters like flactuating loads, and pretension of bolts and nuts of the moving parts. Thus, fluctuating loads, and pretension of bolts and nuts of the moving parts must be investigated to trim down the problem of fatigue life of connecting rod bolts during the operation of the engine. In order to withstand the low life of bolts and their deformation as well as catastrophic fracture of the entire engine, these parts should be studied, investigated, and analyzed carefully to secure and make sure that the engine is in a real condition and have better durability. In an automobile engine connecting rod and connecting rod bolts are a critical part having high-volume production. The connecting rod bolts connect the upper cap of the reciprocating piston with the lower part of connecting rod to hold the crankshaft as well as to rotate and transmit the pushing force of the piston to the crankshaft. In fact, every vehicle with an internal combustion engine needs the minimum single connecting rod based upon the number of cylinders inside the engine.

3.2. Engine Connecting rod

The connecting rod is the connection between the piston and the crankshaft. It joins the piston pin with the crankpin; the small end of the connecting rod is connected to the piston and the big end to the crank pin. The function of the connecting rod is to convert the linear motion of the piston into the rotary motion of the crankshaft.

The connecting rod carries the power thrust from the piston to the crankpin, and hence it must be very strong, rigid, and also as light as possible. Connecting rods are subjected to fatigue due to alternating loads. In the case of four-stroke engines, during compression and power strokes, the connecting rod is subjected to compressive loads and, during the last part of the exhaust and the beginning of the suction strokes, to tensile loads. In double-acting steam engines, during the forward stroke, the connecting rod is subjected to compressive load and, during the return stroke, to tensile load. Connecting rod materials should have good fatigue at high cycle and deformation resistance. Connecting rods for automotive applications are typically manufactured by forging from different materials. They could also be cast. However, castings could have blown-holes which are detrimental from durability and fatigue points of view. The fact that forgings produce blown-hole-free and better rods gives them an advantage over cast rods. Between the forging processes, powder forged or drop forged, each process has its own advantage and disadvantage. Powder metal manufactured blanks have the advantage of being near net shape, reducing material waste [32]. Engine connecting rod (conrod) consists of a bearing cap and a pair of bearings. During engine driving, the dynamic load generated by the high-speed reciprocating as it functions as an external force to separate the large part result, the conrod large should be assembled properly with bolts. A connecting rod comprises six main parts: piston pin end, shank section, upper cap, connecting rod shell, lower cap (crankpin end), connecting bolts, as shown in figure 3.1, and its exploded view was shown in Appendix II. The upper part of the pin end is fixed in order to distribute the force that comes from the piston head to the rod bolt and nut. The connecting rod shape has been selected from catalogue specifications based on the shape of the section which has the highest fatigue life according to [5] comparison analysis of different sections of connecting rod shapes. In this research, the material used for the connecting rod is AISI 4340 and ARP200/ARP3.5/ARP625+ for connecting rod bolts.

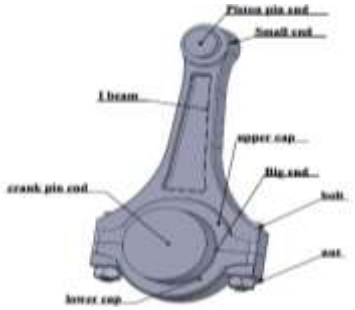

Figure 3.1: Parts of Connecting rod: The image is taken from Solidworks and ANSYS

3.3. Connecting rod bolts

The stresses within the connecting rod bolt are set up by a combination of loads, a few due to outside forces such as inertia, gas pressure, and a few due to inertia of the connecting rod bolt itself. These stresses are due to the action of direct tensile (figure 3.2) loads that come from the head of the cylinder and the crankshaft resulting from the oscillating parts of the connecting rod. For the conduct of structural analysis of the connecting rod bolt, the above-defined axial loads are taken into account. The structural analysis is carried out with the help of ANSYS Workbench 2020 R2.

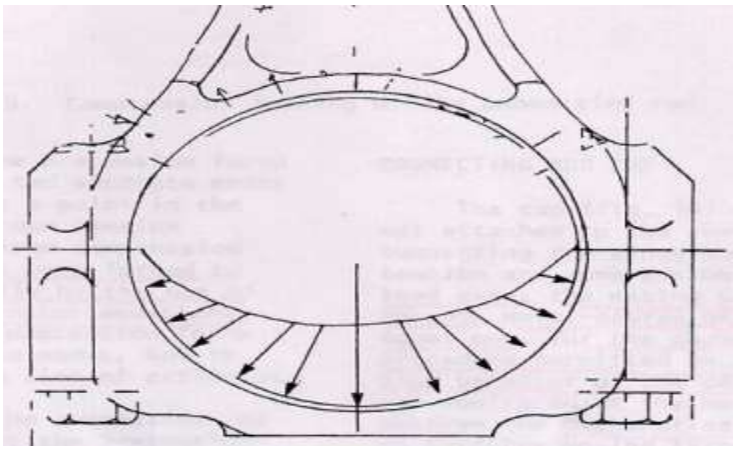

Figure 3.2: Tensile load at the lower cap [33]

3.4. Static Analysis

The static analysis determines the influences of stable loading conditions on the connecting rod bolt. The loads that vary by change in time, like inertia loads, are considered as static equivalent loads, and their influences can also be determined using this analysis. Due to the fact that static analysis is utilized to evaluate stresses, strains, fatigue life, displacements, and forces on the structures, the type of loading that can be applied in a static analysis incorporate remotely applied forces and gas pressures, steady inertial forces, which include like rotational velocity, displacement, and temperatures [1]. The static analysis of the connecting rod bolt is conducted with known values of applied loads calculated from the standard given torque of the automotive engine model catalog and from the properties of the different materials collected from the Garage Center and the published research, respectively. The effects of other parameters like lubrication,

dynamic motion, and bending forces were ignored. The listed below parameters are thoroughly investigated from the numerical model simulation:

- ✓ The bolt pretension effect on the high cycle fatigue life of connecting rod bolts
- ✓ The material best fit for the operation of connecting rod bolts
- ✓ The Stresses produced inside the connecting rod bolts
- ✓ The life of connecting rod bolts
- ✓ The damage on the connecting rod bolts
- ✓ The influence of bolt pretension on the material used for connecting rod bolts

These observations from the Finite Element Method (FEM) will give enough(abundant) information to characterize them capable of withstanding the failure of bolted automotive engine connecting rods.

Figure 3.3: Connecting rod bolts inside combustion chamber[33]

3.5. Numerical determination of maximum loading of the Connecting Rod

Determination of forces acting on connecting rod: To determine the forces acting on connecting rod, we should have the functional specifications of connecting rod. Ordinarily, the static analysis has to be carried out at all examinations of revolution. In any case, this is often time expending and requires lots of computational time, so the investigation is restricted to a particular position of connecting rod angles. In this analysis, the connecting rod position is placed at the top dead center (TDC), and the connecting rod is perpendicular to the crankshaft. In fact, the pressure in the cylinder is the maximum at TDC [34]. The following forces are acting on the connecting rod:

- ✓ Force applied into the piston due to the action of gas pressure
- ✓ Force used into the connecting rod due to the inertia and the reciprocating mass
- ✓ Force generated due to friction of piston contacts

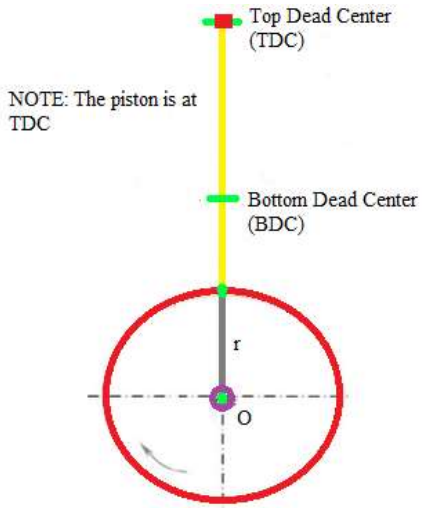

Figure 3.4: Forces acting on connecting rod

Table 3.1: Tabular specification of functional conrod engine from Toyota [6] [28] [35]

Properties List	**Specifications**
Fuel type	Gasoline
Fuel system	Multi-point fuel injection
Configuration	Inline
Number of cylinders	4
Valves per cylinder	4
Valve train layout	DOHC
Bore (mm), d	95
Stroke (mm), s	95
Displacement (cc)	2693
Type of IC engine	Four strokes, naturally aspirated
Compression ratio	9.5: 1
Power (hp)	150hp/4800rpm
Torque (N.m)	240/4000rpm
Torque ($\boldsymbol{\tau}$)	240Nm/4000 rpm
Connecting rod length ($\boldsymbol{l}$)	141mm
Cylinder Diameter (d)	74mm
Maximum Speed (W_{max})	4800rpm
Engine weight	173kg
Firing order	1-3-4-2
Engine oil weight	SAE 5W-30
Weight (g)	426
Mass of Piston (g)	200

Petrol engine constants: The constants are taken from [36], [37].

The density of petrol (C_8H_{18}) (ρ) at temperature 15°(288.85K) (60F) = $770x10^{-3}\ {}^{kg}/_{m^3}$

The molecular weight of petrol (M) $= 114.228\ {}^{g}/_{mol}$

Ideal gas constant (R) $=$ 8.3143 J/mol. k

Evaluating mass:

$$m = \rho.v = \rho * [\pi \left(\frac{d}{2}\right)^2 * s] \quad \text{[3.1]}$$

Determining $R_{Specific}$:

$$R_{Specific} = \frac{Ideal\ gas\ constant}{molecular\ weight\ of\ petrol} = \frac{R}{M} \quad \text{[3.2]}$$

To obtain the gas pressure applied inside the engine cylinder, use the formula of Ideal gas equation:

$$P_g v = m * R_{Specific} * T \quad \text{[3.3]}$$

Then, pressure on connecting rod can be determined by rearranging equation 3.3, the gas pressure P_g can be obtained as follows:

$$P_g = \frac{m * R_{Specific} * T}{v}$$

Calculations of forces acting on connecting rod are as follows:

A) Gas pressure force

The force due to gas pressure or combustion pressure during the time of firing/explosion in the internal combustion engine can be determined by the following formula:

$$F_{gas} = \frac{\pi d^2}{4} P_g \quad \text{[3.4]}$$

Where,

P_g is cylinder manometer pressure and, d is the diameter of cylinder.

B) Inertia force due to reciprocating mass

Connecting rod comprises of big end/upper cap, connecting rod shank, upper cap, bolt and nut. The mass of the reciprocating connecting rod is produced from these parts. Therefore, the force applied due to the inertia of connecting rod consists of reciprocating inertia force on the small end and inertia force on the big end due to its rotation.

The inertia force due to reciprocating mass is calculated using the following formula [38] [39]:

$F_{inertia} = Mw^2r(\cos\Theta + \frac{r\cos\Theta}{L})$ ……..……...……... [3.5]

$\theta = 0°$ since the analysis in this paper is considering the connecting rod at the top dead center.

Where: M =Masses of piston and rings plus Piston pin plus, one third ($\frac{1}{3}$) of connecting rod, w= angular speed, rad/s, r = crank radius, mm, L= length of connecting rod, mm

First, determining the mass of AISI 4340 material:

- Mass of I-beam connecting rod = 0.426kg
- Mass of piston = 0.2kg

$$m = mass\ of\ piston + \frac{1}{3}rd\ of\ connecting\ rod$$

The angular speed at maximum is calculated by:

$$W_{max} = \frac{2\pi w_{max}}{60} = 565.49 rad/s$$

The crank radius:

$$r = \frac{stroke}{2} = 47.5 * 10^{-3} m$$

This work taken that the connecting rod position is at the top dead center of the stroke. Inertia force at maximum angular speed using the equation [3.5]:

$$(F_{inertia})_{max} = MW_{max}{}^2 r(\cos\Theta + \frac{r\cos\Theta}{L})$$

During the high speed of the piston connecting rod, the stretching or tension of connecting rod is due to inertia force from the external.

C) Frictional force

The greatest sum of the contact force that a surface can apply upon an object can be effortlessly calculated with the use of the given formula:

$F_{fric} = \mu * F_{normal}$……... [3.6]

To find the normal force, simply use the following formula:

$F_{normal} = mgcos\beta$……..…… [3.7]

But from this study case, the angle between the top dead center and the cylinder head guide is zero (i.e., $cos0° = 1$). Therefore, we use:

$F_{normal} = mg$……..……...……...… [3.8]

From the table of data specifications, use the weight of connecting rod equal to 426 gram (table 3.1). The coefficient of friction (μ) for AISI 4340 is 0.05 [40].

D) Force acting on the piston

The force acting on the piston is determined by the formula of the summation of force due to gas pressure and inertia force minus frictional force.

Taking the weight of reciprocating parts into consideration:

$W_{reci} = m_{reci} * g$……..…... [3.9]

Generally, the force acting on connecting rod is [5] [39]:

$F_{con\,rod} = \frac{F}{cos\beta}$……..……..... [3.10]

The position of connecting rod at the top dead center is considered for this study, and the angle β is equal to zero.

Therefore, the maximum force applied on the connecting rod [38] is:

$(F_{conrod})_{max} = F_{gas} + (F_{inertia})_{max} + W_{reci} - F_{friction}$……..……. [3.11]

$$(F_{conrod})_{max} = 19.6KN \cong 20KN$$

Therefore, the maximum external load acting on connecting rod is $20KN$. In the above calculation, the coefficient of the friction force is subtracted from the forces acting on connecting rod when the position of the piston head is at the top dead center. The reason is that when the tensile load is acting on the connecting rod at the position, the contact between the assemblies is not frictional, and there is no frictional contact between the contacting regions. Based on the specifications and data from the TOYOTA connecting rod engine and rod geometry, the maximum force acting on the connecting rod is 20KN. This value is used as a force applied on connecting rod for the static analysis in ANSYS Workbench 2020 R_2.

3.6. Fatigue life Equations

When parts are subjected to fluctuating stresses, they are likely to fail at stress levels that are much less than yielding or ultimate strengths if subjected to large numbers of stress cycles. In this research, the fatigue prediction for connecting rod bolts is estimated using the Stress-life method. For high-cycle fatigue analysis, the stress method has been widely adopted [41].

From the ARP2000 property of material, yield tensile strength and ultimate tensile strength (σ_{ult}) is 1241MPa and 1516MPa, respectively. From the SAE (Society of Automotive Engineers) data handbook for fatigue, the fatigue strength coefficient $\acute{\sigma_f}$ (in MPa) for steels can be approximated by the following formula when Brinell hardness is less than 500HB, which is in the case of ARP2000 is 242HB [10]:

$$\acute{\sigma_f} = \sigma_{ult} + 345 \quad \text{[3.12]}$$

The endurance limit can be obtained based on the standard experiment, and the knee can be obtained, which clearly identifies the endurance limit or fatigue limit. The knee does not exist in S-N curves for all materials of engineering importance. The materials which exhibit the knee are low-strength carbon and alloy steels, some stainless steels, irons, titanium alloys, and molybdenum alloys. There are some other materials such as aluminum, copper, nickel alloy, high strength carbon and alloy steel, and some stainless Steel do not exhibit knee. For such materials, fatigue strength at 5×10^8 cycle is taken as fatigue limits. Sometimes we even do not have the experimental fatigue data; in such case following relations are used for calculation purposes [42]:

$$S'_e = 0.5S_{ut}\ for\ S_{ut} < 1400MPa$$

$$S'_e = 700\text{MPa}\ for\ S_{ut} \geq 1400MPa$$

$$S'_{se} = (0.5 \text{ to } 0.6)S'_e$$

In this study, materials selected ARP2000/ARP3.5/ARP625+ for connecting rod bolts has greater than 1400MPa ultimate strength. So, it can be possible to take the theoretical endurance limit as 700MPa. To find fatigue strength exponent, b, use an infinite number of cycles $N_f = 10^6$:

$$b = \frac{\log\left(\frac{\acute{\sigma_f}}{\acute{S_e}}\right)}{\log(N_f)} \quad \text{[3.13]}$$

There is still a relationship between fatigue strength and the number of cycles at the high cycle region. Within the fatigue analysis under the action of stress control conditions, the link between fluctuating stress and fatigue life can be expressed by the author [43] [38]:

$\sigma_a = \acute{\sigma_f}(N_f)^b$ ..... [3.14]

Within operating connecting rod force for TOYOTA D4D Dolphin, which is 20KN (the one calculated according to the specifications), generated the alternating stresses of 754.76MPa (with bolt pretension only) to 976.87MPa (bolt pretension + conrod force), the values which are obtained from the real device model using ANSYS software. The alternating stress applied varies from the minimum to maximum which is $754.76MPa \leq \sigma_a \leq 976.87MPa$. So, using equation 3.14, we have the following equation:

$\sigma_a = 1816MPa(N_f)^{-0.069}$ ..... [3.15]

There are two alternatively proposed materials to compare with the existing materials for connecting rod bolts. These are ARP 3.5 and ARP 625+. Basically, the existing and the materials used as a replacement are high tensile steel with different strengths. The range of variation of alternating stress at different values of pretension is tabulated in the following table 3.2.

Table 3.2: The alternating stress values with varying bolt pretension using ANSYS workbench

Bolt pretension (KN)	Alternating stresses range (MPa)		
	ARP2000	ARP 625+	ARP 3.5
14	$415.5 \leq \sigma_a \leq 813$	$415.5 \leq \sigma_a \leq 813$	$415.5 \leq \sigma_a \leq 813$
16	$547.85 \leq \sigma_a \leq 854.85$	$547.85 \leq \sigma_a \leq 854.85$	$547.85 \leq \sigma_a \leq 854.85$
18	$617.23 \leq \sigma_a \leq 893.62$	$617.23 \leq \sigma_a \leq 893.62$	$617.23 \leq \sigma_a \leq 893.62$
20	$686.45 \leq \sigma_a \leq 934.63$	$686.45 \leq \sigma_a \leq 934.63$	$686.45 \leq \sigma_a \leq 934.63$
22	$754.76 \leq \sigma_a \leq 976.87$	$754.76 \leq \sigma_a \leq 976.87$	$754.76 \leq \sigma_a \leq 976.87$
24	$823.51 \leq \sigma_a \leq 1021.93$	$823.51 \leq \sigma_a \leq 1021.93$	$823.51 \leq \sigma_a \leq 1021.93$
26	$893.94 \leq \sigma_a \leq 1069.42$	$893.94 \leq \sigma_a \leq 1069.42$	$893.94 \leq \sigma_a \leq 1069.42$
28	$962.86 \leq \sigma_a \leq 1119.38$	$962.86 \leq \sigma_a \leq 1119.38$	$962.86 \leq \sigma_a \leq 1119.38$
30	$1032.95 \leq \sigma_a \leq 1171$	$1032.95 \leq \sigma_a \leq 1171$	$1032.95 \leq \sigma_a \leq 1171$

For **ARP 3.5** and **ARP 625+,** the materials have the ultimate strength (σ_{ult}) of 1816MPa and 1792MPa, repectively.

$\acute{\sigma_f} = \sigma_{ult} + 345$ ..... [3.16]

$S'_e = 700\text{MPa}\ for\ S_{ut} \geq 1400MPa$, (1816MPa, 1792MPa) > 1400MPa

$b = -\frac{\log(\frac{\acute{\sigma_f}}{\acute{\varepsilon_e}})}{\log(N_f)}$ .....[3.17]

Equations of existing and proposed materials

ARP2000: $\sigma_a = 1816MPa(N_f)^{-0.069}$

ARP 3.5: $\sigma_a = 2161MPa(N_f)^{-0.0816}$

ARP 625+: $\sigma_a = 2137MPa(N_f)^{-0.0808}$

Taking the values of alternating stress for the materials that simulated from ANSYS workbench 2020 R2, the number of cycles was evaluated using MATLAB software. The comparison was made between the existing and the replacement materials at the same value of bolt pretension with constant connecting rod force to obtain the enhanced fatigue life. Another comparison was made between the given (existing) bolt pretension and other values beyond the proper bolt pretension to ensure that the bolt pretension torque/preload greatly affects the modelled real device.

3.7. TOYOTA's company torque and preload recommendation for the conrod bolts

Pre-tightening of connecting rod bolt is important and it should be pre-tightened before analyzing the model. In order to get the preload that should be applied on M8x1 connecting rod bolts to tighten bolt and nut together for the purpose of clamping the piston pin end to bearing end, there should be a torque specification since it is necessary to have the value of torque to obtain the rod bolts preload. The amount of preload (F_P) required that is applied to achieve desired torque (T) can be taken from the analytical formula and calculated as:

$T = F_P(k * D)$ [19]..... [3.18]

Rearranging,

$F_P = \frac{T}{k*D}$..... [3.19]

Where T is input torque, F_P is preload, k is non-dimensional nut factor which can vary from 0.09 to 0.62 [44] (also called torque coefficient), and D is the nominal diameter of the thread. The value

of torque used to tighten the connecting rod bolts depends on the material yield strength taken from general torque recommendations for the TOYOTA data table [7]. For the existing connecting rod bolts, the material ARP2000 has a tensile yield strength of $1241x10^6$ Pa, the maximum tensile strength of $1516x10^6$ Pa, and as well as at medium or mean tensile strength, its tensile strength is $1379x10^6$ Pa. According to the TOYOTA engine connecting rod specification, three torque specifications have different tensile strengths.

Table 3.3: Bolts recommended torque to achieve optimum preload [7] [8]

Fastener Diameter	Fastener tensile strength					
	170,000/180,000Psi (1172/1241N/mm^2)		190,000/200,000Psi (1310/1379N/mm^2)		220,000Psi (1516N/mm^2)	
	Torque (ft.lb)	Preload (lbs)	Torque (ft.lb)	Preload (lbs)	Torque (ft.lb)	Preload (lbs)
1/4"	12	3492	14	3967	16	4442
5/16"	24	5806	28	6588	32	7371
3/8"	45	8622	50	9782	55	10942
7/16"	70	11880	80	13470	90	15060
1/2"	110	16391	125	18515	140	20639
9/16"	160	21220	180	23944	200	26668
5/8"	210	26372	240	29756	270	33140
6mm	11	3359	13	3814	15	4269
8mm	24	5801	28	6581	32	7361
10mm	54	9970	62	11305	70	12640
11mm	72	12184	82	13961	92	15738
12mm	98	14472	112	16949	125	19425
14mm	N/A	N/A	184	22771	205	25730

Conversion of Units: Preload and torque are in lbs. and ft.lb, respectively. There should be a conversion of the units into Newton (N) and Newton-meter (N.m), as shown in the table below.

Table 3.4: Unit Conversions

Bolt nominal diameter, D	Bolt material tensile strength					
	1172/1241N/mm^2		1310/1379N/mm^2		1516N/mm^2	
8mm	Torque, T (N.m)	Preload (N)	Torque, T (N.m)	Preload (N)	Torque, T (N.m)	Preload (N)
	32	21471	37.96	28584.34	43	32740

From the reference [7] for TOYOTA, the torque of connecting rod bolts with nominal diameter 8mm and pitch size 1mm, should not exceed 43N.m. The value of torque coefficient (k) can be

obtained from the Finite Element Method and Motosh equation from [44]. Therefore, the value of torque coefficient, k of the bolts that were used in the fatigue test is 0.183 for a bolt with a nominal diameter of 8mm and pitch 1mm [19] [21]. The recommended value of preload (F_P) according to TOYOTA company manual is $F_P = T/k.D$, from which the minimum bolt pretension is 21.47 KN and the maximum is 32.74 KN. Thus, according to TOYOTA, the maximum recommended preload to tighten Toyota M8x1 connecting rod bolts is 32.74KN and the minimum value of $21.471KN$. These values were used in the analysis of connecting rod bolts in ANSYS Workbench.

CHAPTER FOUR

FINITE ELEMENT MODELLING AND ANALYSIS

4.1. Introduction

The Finite Element Method (FEM) is very important for predicting different static and dynamic structural responses. For instance, large automotive industry companies use FEM to estimate fatigue parameters, deformations, stress-strain curves, safety factors, and failure of many other different types of parts and components. FEA reduces the need for costly experiments and allows engineers to optimize parts before they are built and implemented. A fundamental understanding of modelling will allow engineers to design automotive engine parts that match or exceed the performance of the parts. The Finite Element Analysis (FEA) can be used as a good alternative to slow, time-consuming experimental work for fatigue life predictions. The steps to be followed for the Finite Element Method are as follows:

- Modelling the geometry of the model to be analyzed
- Saving the model using appropriate format and importing the model to another software where simulation is done
- Defining the type of element
- Defining the properties of the material (s) to be used
- Defining the size of meshing and meshing the model
- Applying the boundary conditions to the geometry (Degree of Freedom (DOF) constrains, forces are to be applied on the model)
- Inserting and applying load
- Solving, results and analyzing model

4.2. Finite Element Modelling

After substantial simulations of the model were conducted, usually the researchers will perform the actual experiment. Studies that use the FEM could help the researchers to predict, characterize, and to know the working life cycle of the pre-tightened bolt before performing a bench experiment.

In this paper, all the dimensions of models of the connecting rod and connecting rod bolts were taken from the real existing device, and they are almost the same.

4.3. Connecting rod bolt

The geometry of the modelled part depends on ISO standard metric fine bolt thread profile [45].

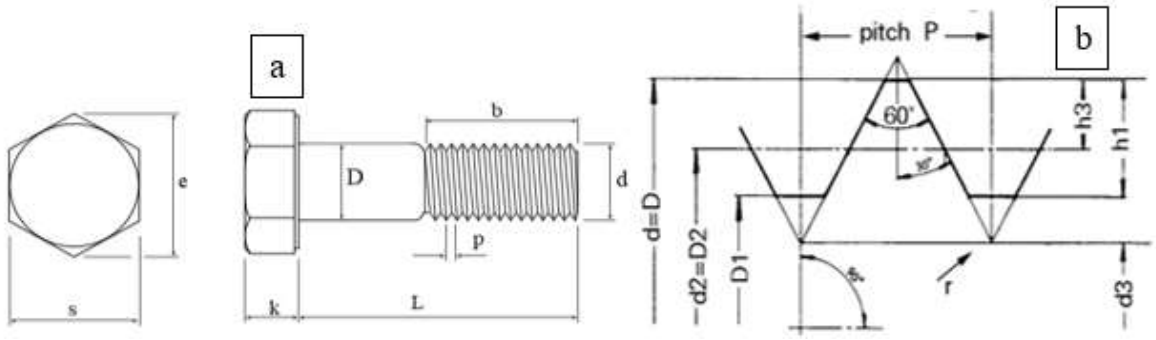

Figure 4.1: Basic mathematical model: a) Bolt geometry b) 60° Metric thread profile

Where, P= 1mm, D=minimum 7.78mm and maximum 8mm, S= minimum 12.73mm and maximum 13mm, L= as required, b= minimum 22mm for less than 125mm and minimum 28mm for 125mm to 200mm of length L, k= minimum 5.10mm and maximum 5.54mm

Table 4.1: M8x1 thread profile specification [45] [46]

THREAD DATA CHART: Metric Thread-Fine Pitch										
Nominal Size ISO MF	Thread Form Type	Major Diameter mm d=D	Pitch mm p	Root Radius mm r	Pitch Diameter mm d2=D2	Minor Diameter Male Thd. d3	Minor Diameter Female Thd. D1	Thread Height Male Thd. h3	Thread Height Female Thd. H1	Tap Drill Diameter mm
6x0.75	M	6.00	0.75	0.108	5.513	5.080	5.188	0.460	0.406	5.20
7x0.75	M	7.00	0.75	0.108	6.513	6.080	6.188	0.460	0.406	6.20
8x0.75	M	8.00	0.75	0.108	7.513	7.080	7.188	0.460	0.406	7.20
8x1.0	**M**	**8.00**	**1.00**	**0.144**	**7.350**	**6.773**	**6.917**	**0.613**	**0.541**	**7.00**
9x 1	M	9.00	1.00	0.144	8.350	7.773	7.917	0.613	0.541	8.00

The above table 4.1 which is bolded by bright green colour indicates the M8x1 bolt thread profile data table taken from [46].

4.4. Hexagonal Bolt dimensions and Specifications

There are several bolts design and model standards, such as the International Organization for Standardization (ISO), Society of Automotive Engineers (SAE), German Institute for Standardization (DIN), Industrial Fasteners Institute (IFI), and American Society of Mechanical Engineers (ASME). According to this paper, the bolt dimensions and input model specifications were taken from DIN 931 /DIN EN ISO 4014/DIN EN 24014 standards. They all have the same standard [47].

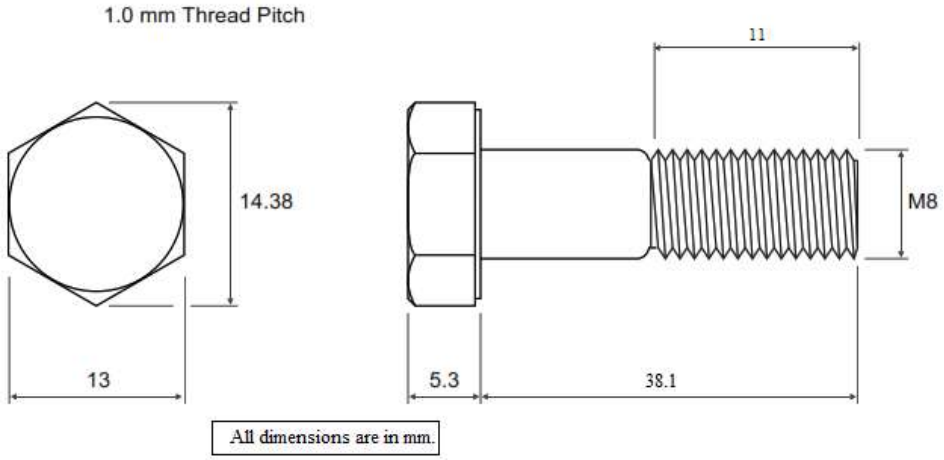

Figure 4.2: M8x1 Bolt design model

4.5. M8x1 thread profile dimensions

The thread profile dimension is based on the ISO Metric thread bolt profile standard formula and is calculated depending on the length of the pitch [48]. The values obtained below is exactly the same as the one which is selected from the thread data chart from above table 4.1. For the M8 bolt, the fine threaded pitch used was is 1mm. The thread profile calculated in this section was the model used for creating each thread using Solidworks 2021.

Pitch, P= 1mm

Vertical depth, $D_V = 0.866P = 0.866mm$ $\quad \frac{D_V}{6} = \frac{0.866}{6} = 0.14433\ mm$

Thread depth, $D_t = 0.614P = 0.614mm$ $\quad \frac{D_V}{8} = \frac{0.866}{8} = 0.10825\ mm$

Thread angle, $\theta = 60°$

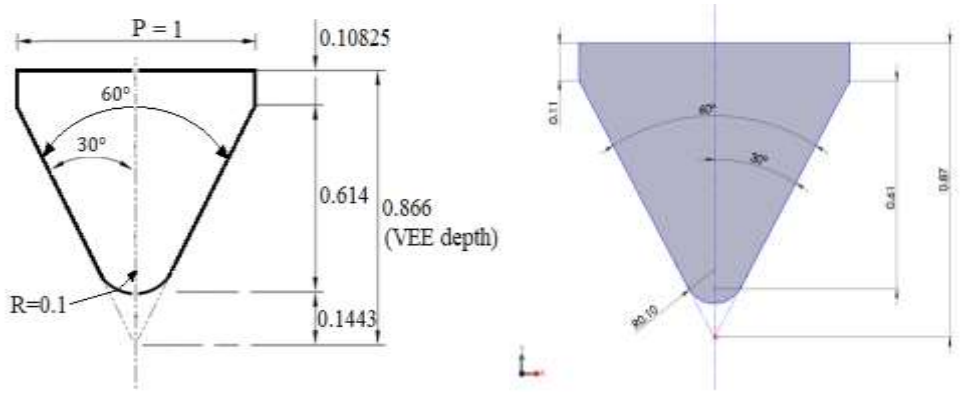

Figure 4.3: Single thread profile (Left), Thread profile model in SOLIDWORKS 2021 (Right)

4.6. Nut dimensions

The dimension selected for nut modelling was according to DIN 934, which has the same specification as ISO 4032. The value of M, e, m, and S are listed in the table below, which is dragged by red colour, and it was directly used in modelling the Nut geometry [49].

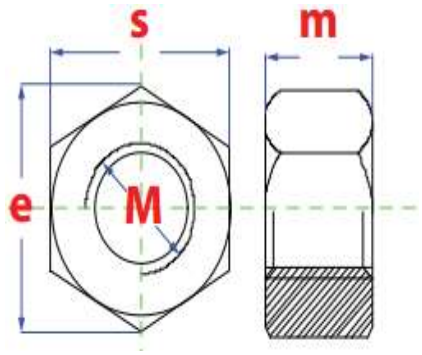

Figure 4.4: Nut dimension and specification data [49]

M	*e*	*m*	*s*
M4	7.66	32	7
M5	8.79	4	8
M6	11.05	5	10
M8	14.38	6.5	13
M10	18.9	8	17
M12	21.1	10	19
M14	24.49	11	22

4.7. The bolt model with thread Profile

Because Solidworks does not have operating standard parts to be selected for the analysis, all the threads were created manually. In this paper, the thread of the bolt profile was defined by height and pitch, which are 11mm and 1mm, respectively. The hexagonal bolt was used with 15 revolutions of threads, 8mm shank diameter, and 11mm thread length. In the case of nut, in order to get the perfect fit of bolt and nut, the Combining method command is adapted to create the thread of the Nut. The connecting rod bolt is modelled with the option of sweep cut command in Solidworks 2021 with the help of the above-discussed thread profile. The modelled threaded bolt has been shown in Appendix II.

4.8. The connecting rod geometry data

In this paper, the model (geometry) of the connecting rod was taken from Henok Garage Center [6]; the data has all necessary information belonging to the geometry of the TOYOTA connecting rod. The major specifications required for the analysis and dimensions were measured using vernier caliper for the connecting rod with its bolts from the real in-use engine were taken in tabular form, as shown in table 4.2. The other dimensions are shown in the modelled geometry shown in Appendix II. The hole for lubrication is ignored from the model since the lubrication effect is not covered in this study. For the evidence of the data, all the pictures and problems captured are checked and stamped by the Garage Center owner and director which was shown in Appendix I.

Table 4.2: The connecting rod Specification for the study [6]

Data collected from Henok Garage Center	
2006 Model-TOYOTA D4D Dolphin	
Category	Connecting Rods
Engine make	TOYOTA
Model	3RZ-FE 2.7L
Shape	I-Beam
Length (mm)	130.5
Pin Diam. (mm)	18
Housing Bore (mm)	46
B.E width (mm)	20.85
Weight (g)	426
Bolt size (mm)	8
Material	ARP2000/ARP625+/ARP 3.5
Minimum torque (N.m)	32N.m
Maximum torque (N.m)	43N.m
Minimum Preload (N)	21471
Maximum Preload (N)	32740

4.9. Material properties and necessary input data for ANSYS analysis

4.9.1. Necessary inputs

For static analysis of connecting rod bolts, inputs like force acting on the connecting rod, preload required to tighten the bolts (bolts pretension), the values of frictional coefficients between contact regions, and the material properties should be defined first. The input for bolts preload and force

acting on connecting rod is obtained from analytical calculations in chapter three. The following are ANSYS workbench static analysis input data for existing connecting rod and connecting rod bolts for Toyota 3RZ-FE 2.7L engine.

Table 4.3: Input data for Static analysis in ANSYS Workbench

Connecting rod material	AISI 4340
Connecting rod bolts materials	ARP2000(in-use), Custom Age 625+ (ARP 625+), ARP 3.5
Connecting rod bolts pretension load	$21.471KN \leq F_{conrod\ bolts} \leq 32.74KN$ (Form analytical calculation)
Force acting on connecting rod	$20KN$(From the analytical calculation)
Frictional coefficient between contact regions	0.15 and 0.1 (for bolts)

4.9.2. Engineering Materials Property input for ANSYS

In order to get a good working behaviour, the products should be manufactured using a correct fitting material. In this study, four materials were used. AISI 4340 and ARP2000 are the existing materials, and ARP 3.5 and ARP625+ are the replacement materials whose properties are taken from the TOYOTA manual connecting rod and connecting rod bolts [7] [50]. In this thesis work, static analysis was performed on clamped bolts of connecting rod in assemble with the whole connecting rod. The existing connecting rod is made of American Iron and Steel Institute-AISI 4340 (TOYOTA company standard), and pre-tightening bolts are made from ARP 2000 (high tensile steel) and ARP 625+ and ARP 3.5 as a replacement, figure 4.5. Selecting the ideal material for utilization in a given fastener application is of vital significance. Mechanical properties for connecting rod and connecting rod bolts materials are shown in Figures 4.6, 4.7, 4.8, and 4.9.

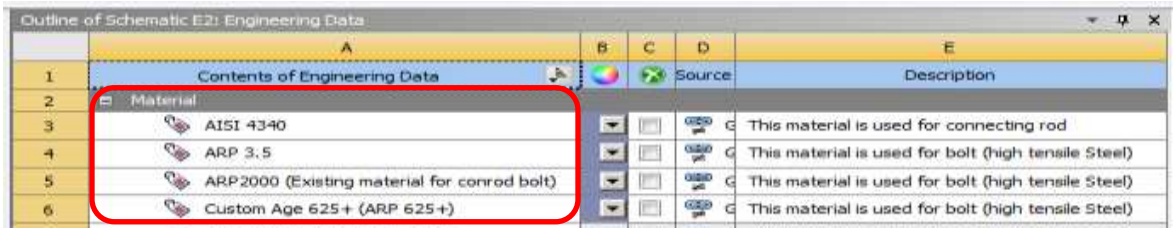

Figure 4.5: List of Engineering Materials used

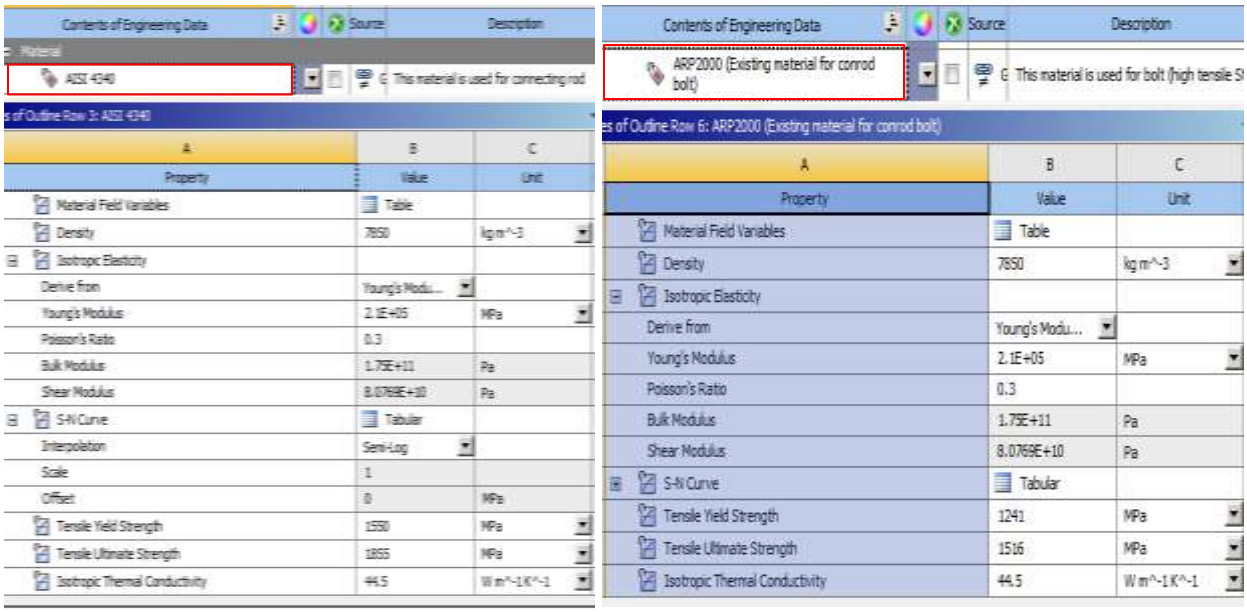

Figure 4.6: AISI 4340 and ARP2000 mechanical property [50], [7]

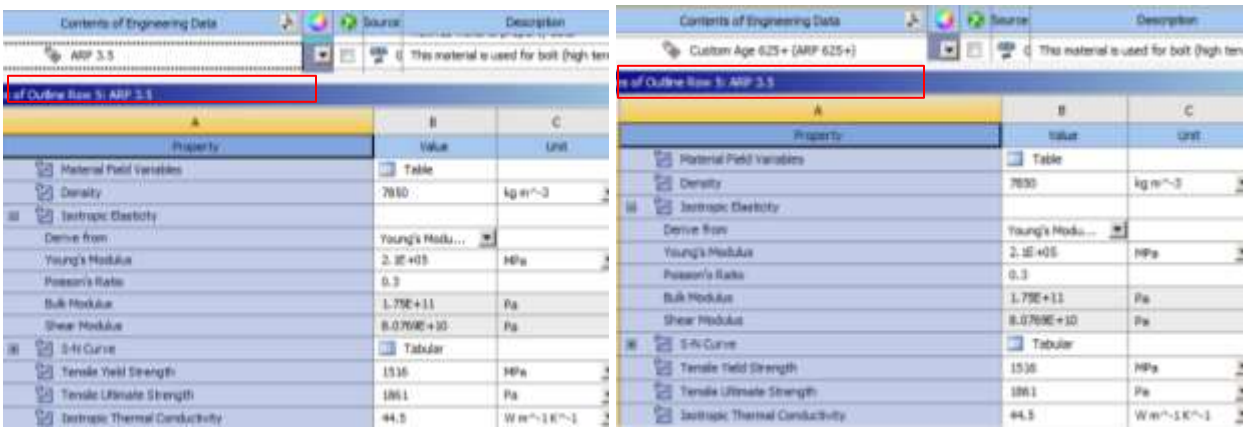

Figure 4.7: ARP 3.5 and ARP625+ mechanical property [7]

4.10. Existing connecting rod bolts torque recommendation and preload

According to the existing connecting rod recommended value of bolt pretension, as calculated from the formula, $T = F * k * D$, depending on the given data specification of torque and the selected nominal diameter of the bolt, from the taken value of nut factor, the bolt pretension ranges minimum 21471N and maximum 32740N as tabulated in table 4.4.

Table 4.4: Torque datasheet for 8mm connecting rod bolt diameter

Bolt	**Torque**		**Bolt pretension (Preload)**	
Diameter	Min.	Max.	Min.	Max.
8mm	32N.m	43N.m	21471N	32740N

4.11. The Coordinate System for the imported model in ANSYS

The modelled geometry generally has three coordinate systems. The one is the global coordinate system for the entire geometry of the assembled device, and two local coordinate systems for the bolt pretension to clamp using preload and lock the bolt at the first step. The local coordinate system created is because, as it is clearly explained in other sections, there are two-step loading. The loadings are different and should be considered with the different coordinate systems.

4.12. Boundary Conditions and Loading

A very attentional concern task to be taken into account before numerical analysis is the correct definition of the boundary conditions. Boundary conditions are applied to the model in order to obtain results that answer the objective of the work. The movement of the geometry perpendicular to its symmetry plane is constrained for the face on the symmetry plane of the model. The stress and strain are the most serious when the explosive pressure of the fuel gas achieves maximum when the piston is at TDC. The maximum pressure is calculated using the numerical calculation for the given engine parameters. The force is maximum when the piston is at TDC, and the same force is transferred to the connecting rod [34]. The smaller pin restrictions for the rod are let to be in a static condition. In tensile axial load, the lower half is constrained. Force to be applied to connecting rod was evaluated analytically. Figure 4.10 describes the boundary conditions for static FEA under tensile load [5]. X and Y directions are fixed, and connecting rod force in -Z direction (uniaxial tensile loading).

Due to the additional forces acting on the connecting rod, the tightening load is applied on pre-tightened connecting rod bolts. The bolt was prescribed preload to the bolt model volume, calculated according to the analytical formula. The maximum preload (clamping force) value is 32.74KN, and the minimum value of 21471KN (or) torque value of 32N.m and 43N.m. In the simulation, two steps of load were used; the first step was used for loading bolt-nut with preload force. Then in the second step, a load of preload force in the bolt was locked, and the next external force on the lower cap was considered. Therefore, the maximum connecting rod load 20KN was prescribed on connecting rod lower cap, it is shown of red colour, figure 4.10 [C] and on the opposite side of the lower side of connecting rod was prescribed fixed support shown with blue colour on figure 4.10 [D].

Necessary Condition: In uniaxial in static connecting rod tensile load, the small end of the connecting rod is fixed at the half part from its center, and the other side of connecting rod, the big end, has the external force at half part from its center. This necessary boundary condition is adopted in this study to distribute the stresses that occurred into connecting rod to both sides of connecting rod bolts. The boundary condition was explained geometrically in figure 4.10.

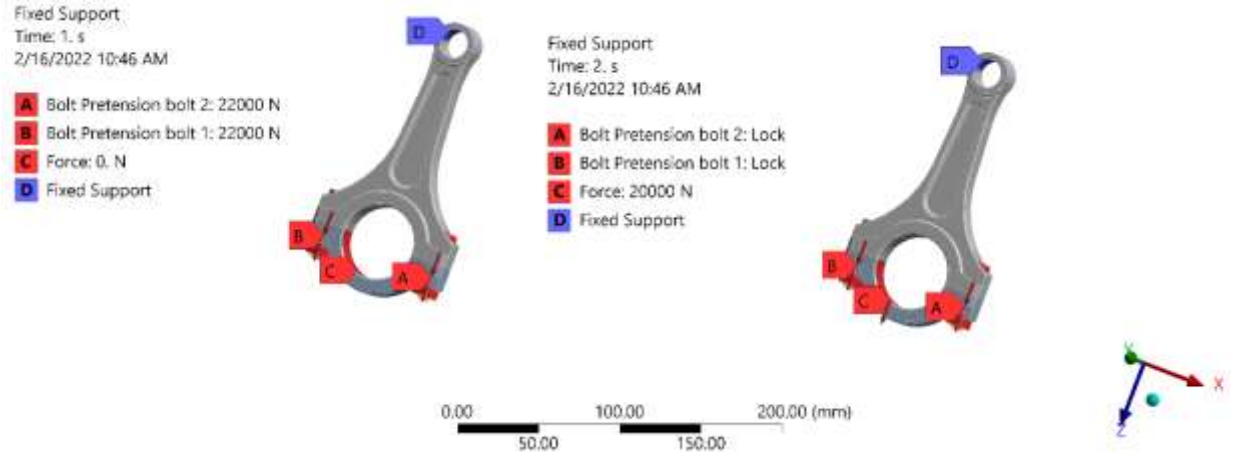

Figure 4.8: Boundary condition and loading

One loading scenario was investigated with a 20KN load applied at the crank end, varying the values bolt pretension at both sides of connecting rod and limited at the piston pin end.

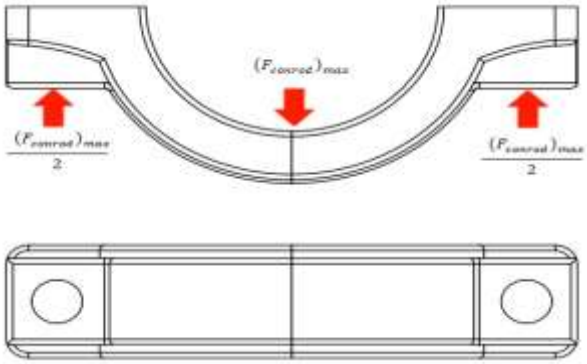

Figure 4.9: Tensile loading condition on the bolts (Reaction forces at bolts)

4.13. Thermal State of the connecting rod

The effect of temperature on connecting rod bolts is shallow and did not consider in this analysis because the maximum entire engine temperature is about 150℃ [51]. This is due to the temperature not affecting the high cycle fatigue of connecting rod and bolts material, but the fluctuating loading. For metals, the minimum temperature required for creep deformation is 30-

40% of the melting point, while for ceramics, it is 40-50% of the melting point [52], [53]. But in this study, the melting point of connecting rod material and connecting rod bolts are more than 850℃ [54], [55]. So, the criterion to consider the creep analysis failed from these fact. The thermal conductivity of thematerials is considered to obtain the optimized results and to make the analysis in a real operating condition. Therefore, the maximum operating temeperature of the engines is 90℃ – 150℃ [51]. In this study the maximum temperature has been taken (i.e., 150℃) as shown in the figure 4.12.

Figure 4.10: Thermal State of the connecting rod

4.14. Uniaxial tensile loading simulation using ANSYS workbench

Uniaxial tensile loading is the one-directional application of loading to the real or modelled devices to investigate/identify/make sure that the modelled device assembly's material, geometry, and definition are good enough to accomplish the desired results purpose without any risk. To simulate pre-tightened connecting rod bolts, all the boundary conditions and loads are applied on the prepared model, with common functional loading and varying bolt pretension values to identify which bolt pretension gives reduced total deformation and life than the given and existing and in-use material. The existing connecting rod bolts are also analyzed to compare them with other used materials interchangeably. The simulation using ANSYS workbench 2020 R_2 includes setting up the contact between the detail parts and additional external loading to the rod bolts. The different simulations were conducted by varying the values of bolt pretension (preload) and inputting

common external loading to the connecting rod. The different analysis is conducted for different values of bolt pretension, as shown in figure 4.13.

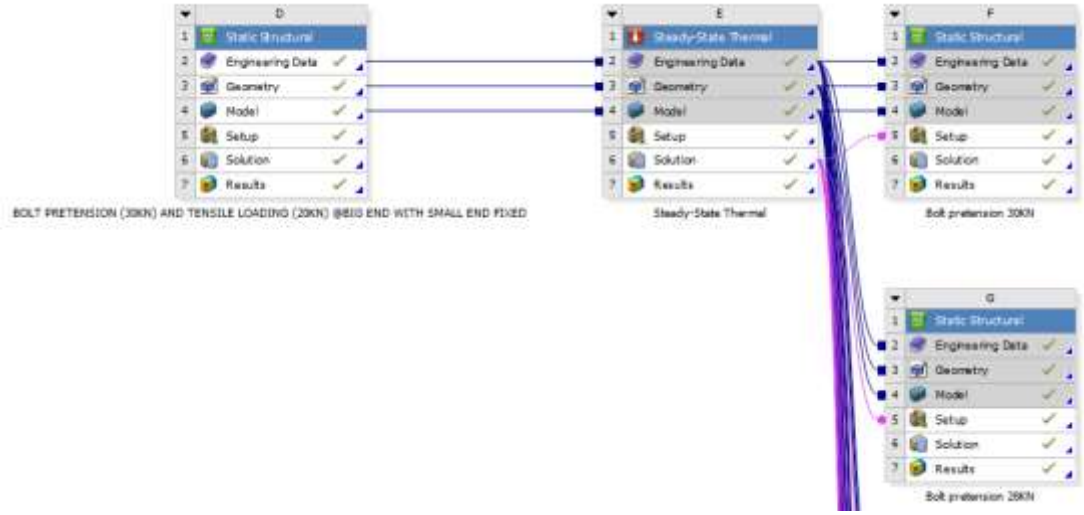

Figure 4.11: Tensile loading at big end with small end fixed simulation layout

4.15. Modelling, Defining, and Meshing the geometry

The finite Element Modeling software (Solidworks 2021) was used to model and assemble the bolt and connecting rod after finishing the dimensional data from the garages and the engine manuals. The connecting rod has a big end thickness of 20.85mm and 46mm crankshaft diameter and a center-to-center length of 130.5mm. All dimensions are put in Appendix X. First, each of the parts needed for analysis is modelled in the parts command. After the detailed parts of the con rod were created, they were assembled in the Assembly command option. The geometry assembled in Solidworks is saved into the document using .step204 file format to import the geometry into ANSYS workbench for definition and analysis. The meshing, boundary conditions, and numerical analysis were done using ANSYS software to analyze the relationship between the tightening force, the external operation loads, and the stress magnitude resulting in the bolt. The material of each part is assigned differently according to the common existing real device. The geometry has meshed in a good manner in order to obtain a good result for the analysis. The meshed connecting rod has 127134 nodes and 82763 elements.. The mesh convergence was checked for the equivalent stress, as shown in the meshing convergency section.

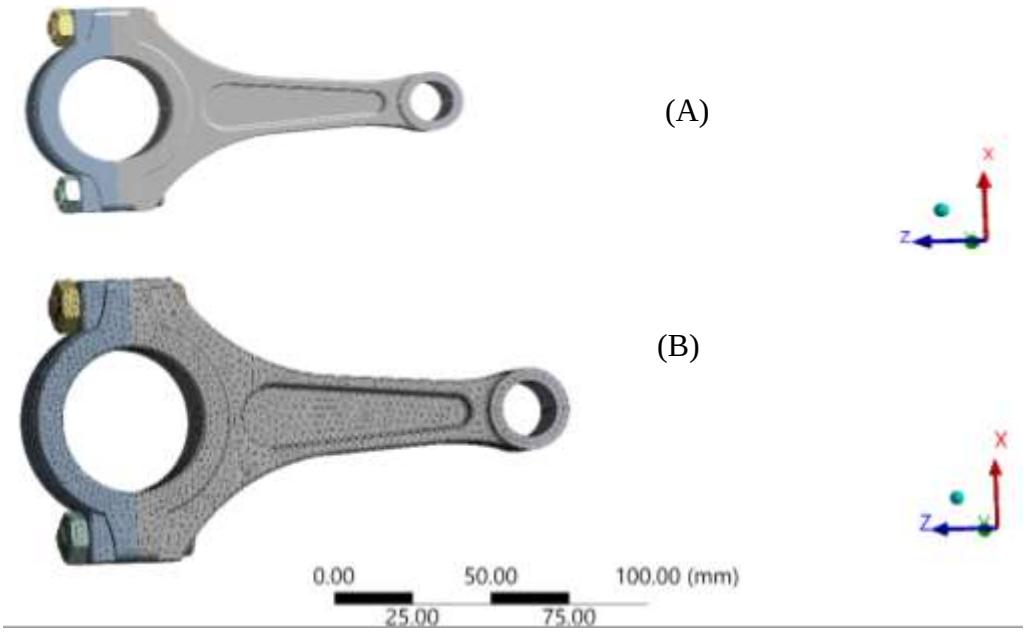

Figure 4.12: Modelled con rod for simulation: A) Model and B) Meshing

4.16. Setting up the contact between the elements of connecting rod

Defining the contact between connecting rod elements is necessary to transfer the loads from the head of a piston onto the crankshaft. The frictional (coulomb's) contact was used in the numerical simulation. The symmetric frictional contacts were established in the contact areas between the upper cap and bolt head, upper cap and bolt shank, upper cap and lower cap, lower cap and bolt shank, lower cap and nut with the value 0.15 [56] to obtain the best-recommended results. The symmetric frictional contact between the bolt thread and the nut thread was prescribed with a coefficient of frictional 0.1. Additionally, table 4.5 illustrates the types of connections in the assembly.

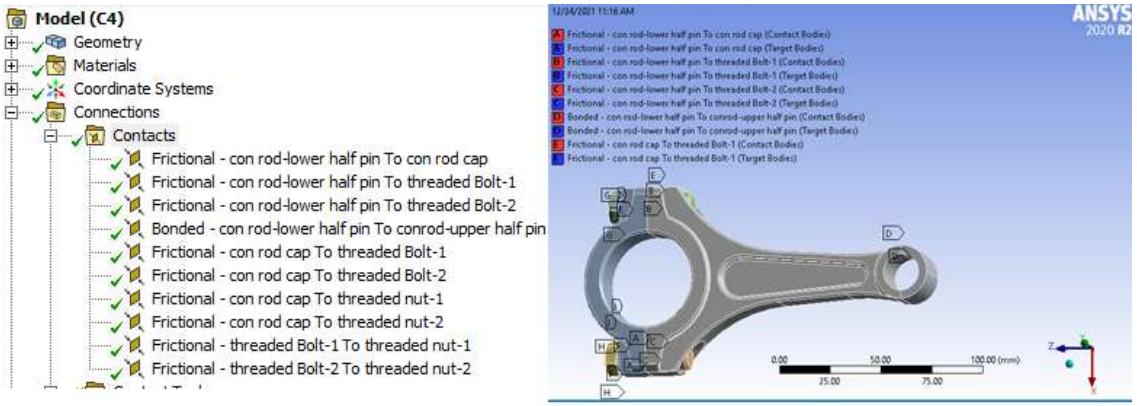

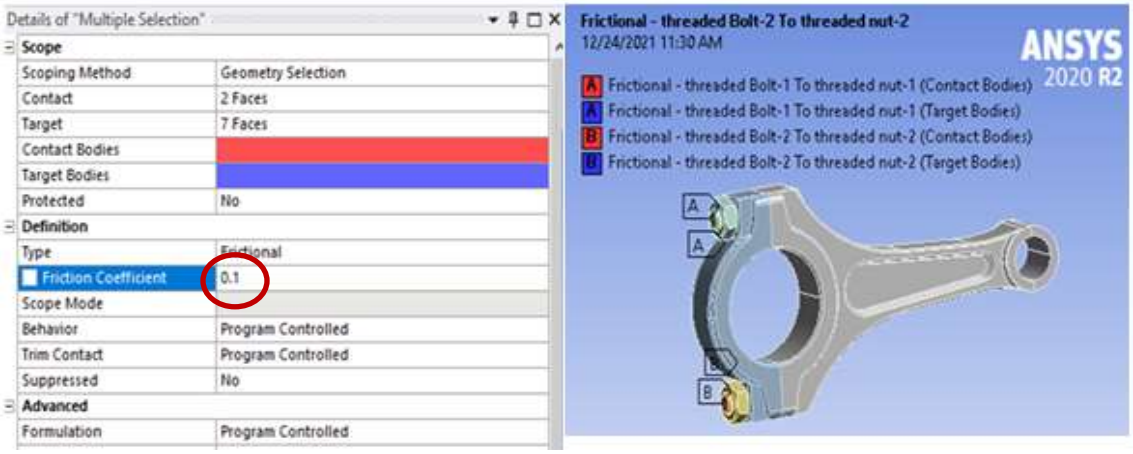

Figure 4.13: Contact between elements of connecting rod bolts

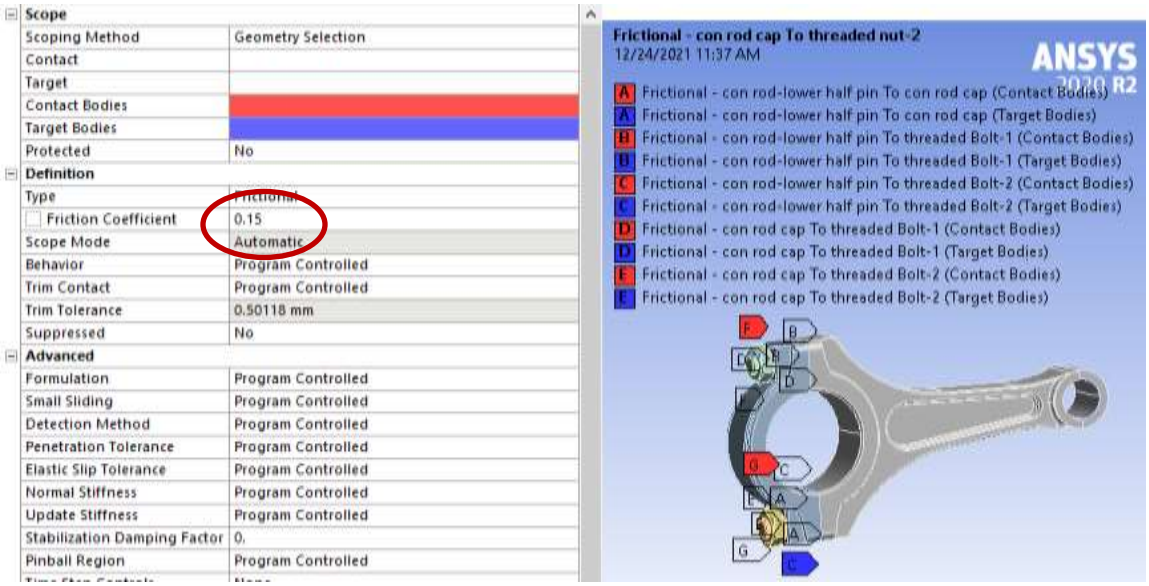

Figure 4.14: Contact between the elements of connecting rod

Table 4.5: Connections in Assemblies

Connections between assemblies			
NO.	Contacts	Frictional	Bonded
1	Conrod to con rod cap	☑	-
2	Conrod to bolt	☑	-
3	Conrod cap to bolt	☑	-
4	Conrod cap to nut	☑	-
5	Bolt to Nut	☑	-

4.17. Bolt pretension values for simulating the model

Two-step loads are considered to estimate the effect of bolt pretension on the total deformation and fatigue life of the connecting rod. At the first step, the two sides bolt and nut are pre-tightened. Then at the second step, the pre-tightened bolt and nut are locked. In the same condition in the second step, the external load that comes from the cylinder head is considered. This simulation part is to get the value of total deformation and to obtain the alternating stress for further simulation of the model (i.e., to use the results as input in the fatigue life simulation of the connecting rod).

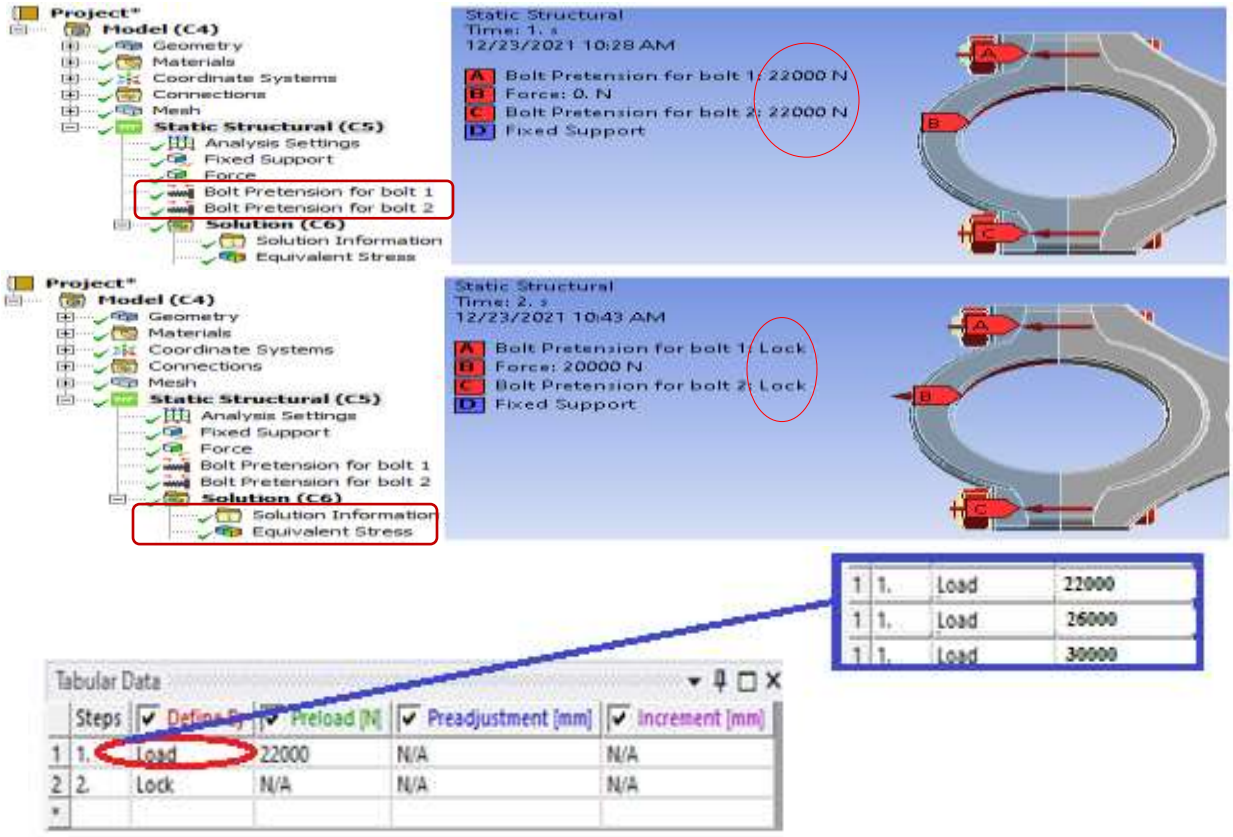

Figure 4.15: Bolt pretension values input for ANSYS

4.18. Connecting rod force as an external loading in ANSYS workbench

Different types of forces generate the stresses in the connecting rod, some because of external loads (including inertia, gas pressure, friction, and weight of connecting rod itself). Assembly (pretension and joint) of parts, the load applied on connecting rod distributed to rod bolts. The stresses occur inside the rod bolts due to tension (alternating stress) that comes from the reciprocating of the connecting rod. So, the axial loads are considered, and analysis is performed

with the help of ANSYS Workbench software. In this analysis, a two-step simulation is considered. At the first step, the bolt pretension is considered, and at the second step, the pressure, inertial, and other loadings like the weight of the connecting rod and frictional force are considered. The pressure and inertial force were applied at the lower cap half end.

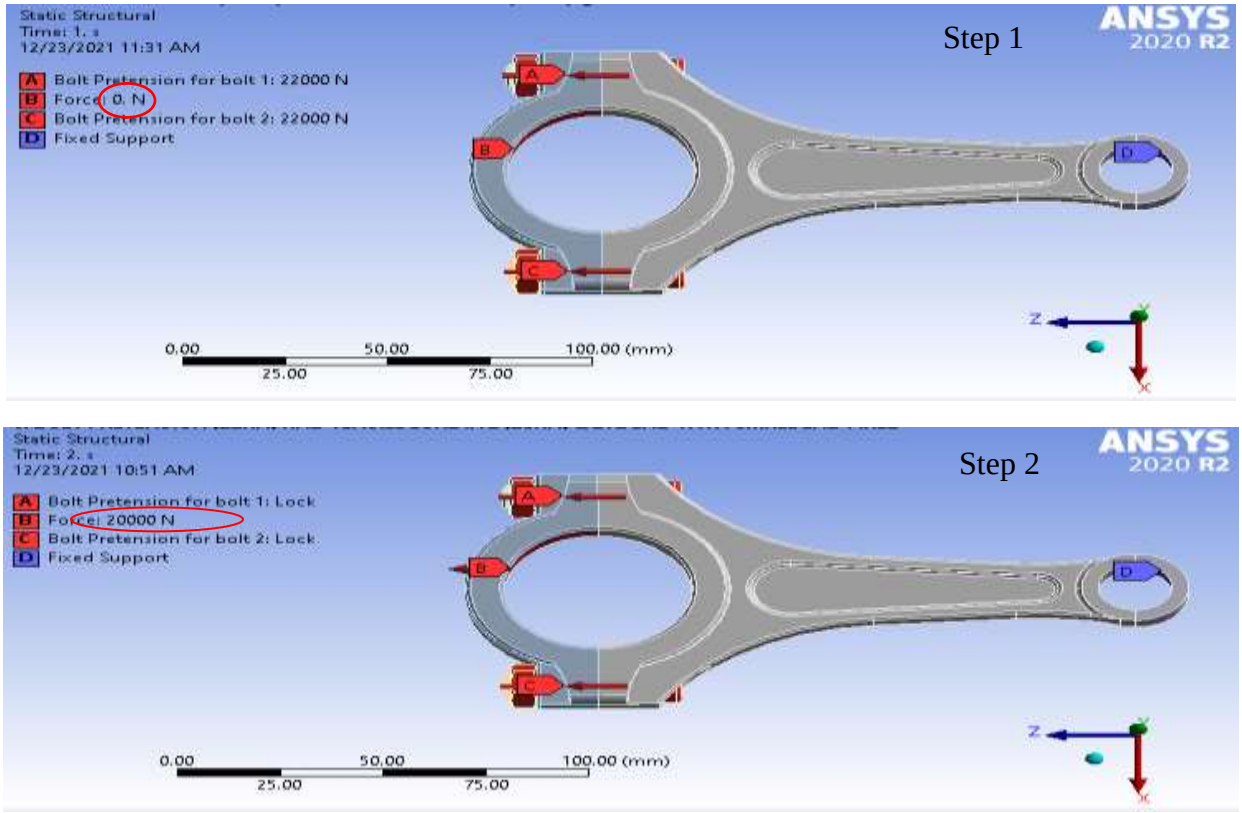

Figure 4.16: Two steps loading in ANSYS workbench

4.19. Force convergence for the model

Convergence is a universal concept in the finite element method. It is a relative method in solving the partial differential equation. Basically, from ANSYS software, if the model contains non-linearity, it cannot be solved directly, so it must be found by iteration. ANSYS used Newton's Raphson method for convergency by default. In this case, the force is converged at the fourth iteration, as shown in figure 4.19.

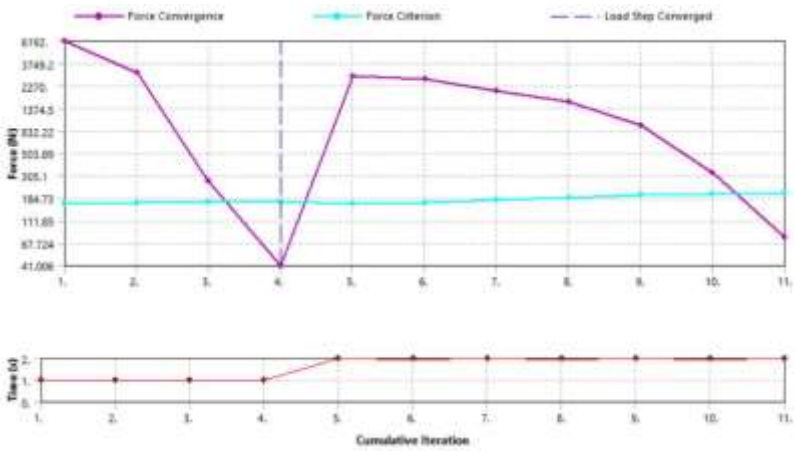

Figure 4.17: Force Convergency

4.20. Fatigue Life prediction procedure

1. Analytical determinations
   - Evaluation of forces acting on connecting rod
     - Gas pressure force
     - Inertia force due to reciprocating mass
     - Frictional force
     - Weight of connecting rod
   - Bolt thread profile determination
   - Bolt pretension (preload) evaluation
2. Simulation using ANSYS workbench
   - Obtaining stress amplitude
3. Determination of the number of cycles using MATLAB
4. Obtaining life and damage using ANSYS workbench 2020 R_2

Steps enclosed in methodology

- Modelling parts of connecting rod using 3D modelling software-Solidworks 2021
  - Parts assembly
  - Saving using **.**step204 format
- Analysis of connecting rod using ANSYS Workbench 2020 R_2
  - Material definition
  - Model import

- Setting up
- Meshing

➲ Finite element analysis of connecting rod bolts

Generally, the engine connecting rod bolt was analyzed by two techniques:

☑ Analytical method

☑ Numerical method using Finite element analysis

4.21. Meshing convergence

Mesh convergence is a critical issue that needs to be fixed. The goal of this analysis is really to create a realistic final solution and to find exact stress and fatigue charts. Mesh convergence analysis is used to understand the relation between input and output values. The analysis is performed for different sizes of an element in ANSYS Workbench based on material properties given in Table 1.2. The output outcomes for various input element sizes, ranging from 8 mm to 2 mm, were investigated (element size). The Von-Mises stresses are recorded at various element sizes and checked for convergence, and stresses values are constant at most areas of conrod and conrod bolts with the element size of 2.5mm.

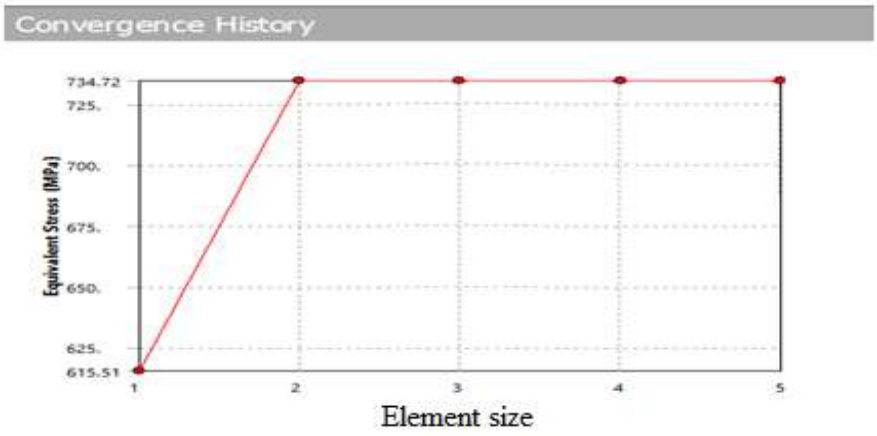

Figure 4.18: Mesh convergency

4.22. Stresses in connecting rod bolts

The rod bolts should be designed with more remarkable performance. It must be able to transmit forces belonging to uniaxial tensile loading due to pulling on the piston. The connecting rods are subjected to mass and gas forces due to the fuel combustion resulting in axial stresses [5]. The

gas force is determined by the speed of rotation, the piston masses, and the oscillating part of the connecting rod consisting of the small end and the shank.

4.23. Diagrammatic representation of the three numerical simulations

In this study, three simulations were conducted. The second simulation used the first simulation as an input to obtain the high cycle fatigue life. All inputs and output (alternating stress) were used as input for the second numerical simulation from the first simulation. Again, for the third simulation, all inputs and output (alternating) were used as input. The technique of the simulations is summarized in figure 4.21.

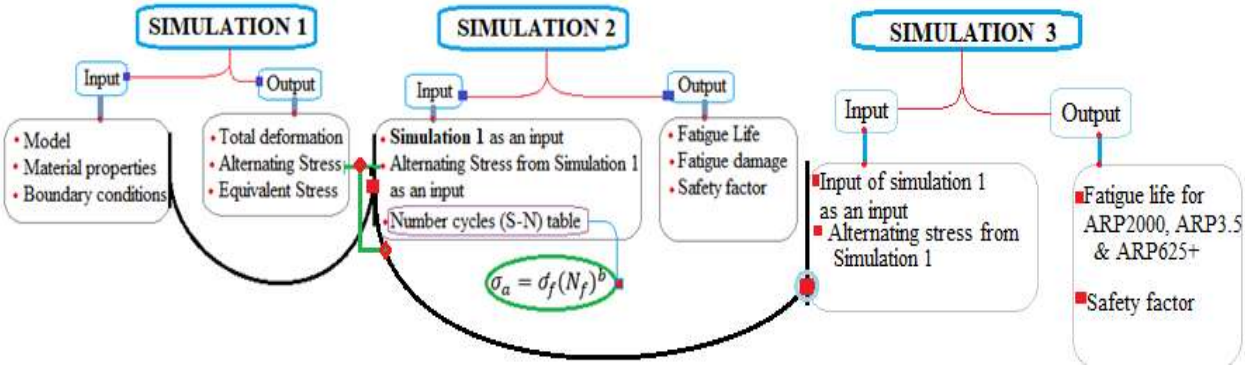

Figure 4.19: Numerical simulations

CHAPTER FIVE
RESULTS AND DISCUSSION

This section presents the results and discussion on the numerical simulation of pre-tightened connecting rod bolts. The discussion about the study is made and is necessary for selecting the best convincing results from all the simulations. The analysis results in this study are concerned with the total deformation and fatigue life prediction of pre-tightened connecting rod bolts and materials and safety factors at different values of bolt pretension at a static point from the operating condition of the connecting rod.

5.1. The effect of bolt pretension on total deformation

The varying values of bolt pretension applied on existing in-use connecting rod bolts to analyze and investigate which factor has a significant effect on rod bolt deformation—taking the different preload values to check for the impact of bolt pretension. From the table of ANSYS results, the graph of bolt pretension versus total deformation was sketched using Origin 6.1 software based on the tabulated result.

5.1.1. Insufficient bolt pretension

From the ANSYS workbench simulation, the insufficient value of bolt preload greatly affected the total deformation of the bolts. The below-tabulated results are the results obtained from ANSYS workbench 2020 R_2 by varying the value of bolt pretension below the appropriate pretension for the real device of a connecting rod.

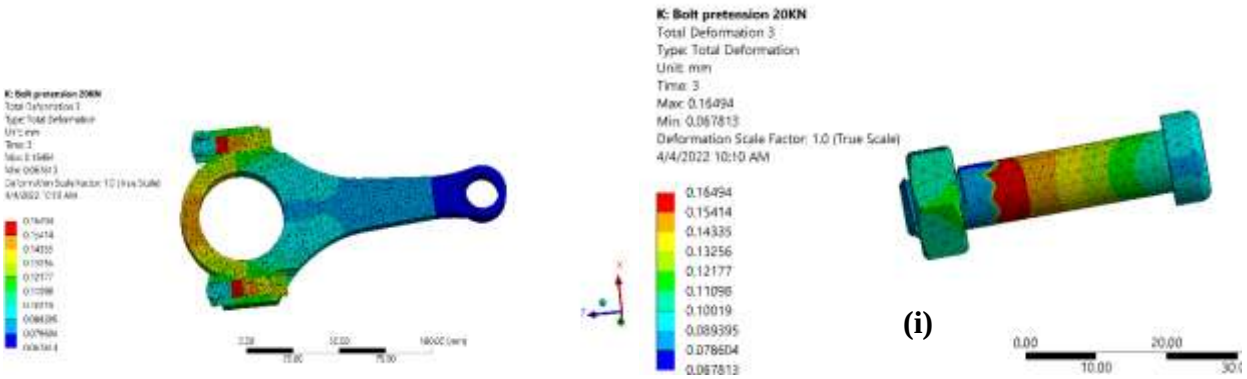

Bolt pretension at 20KN

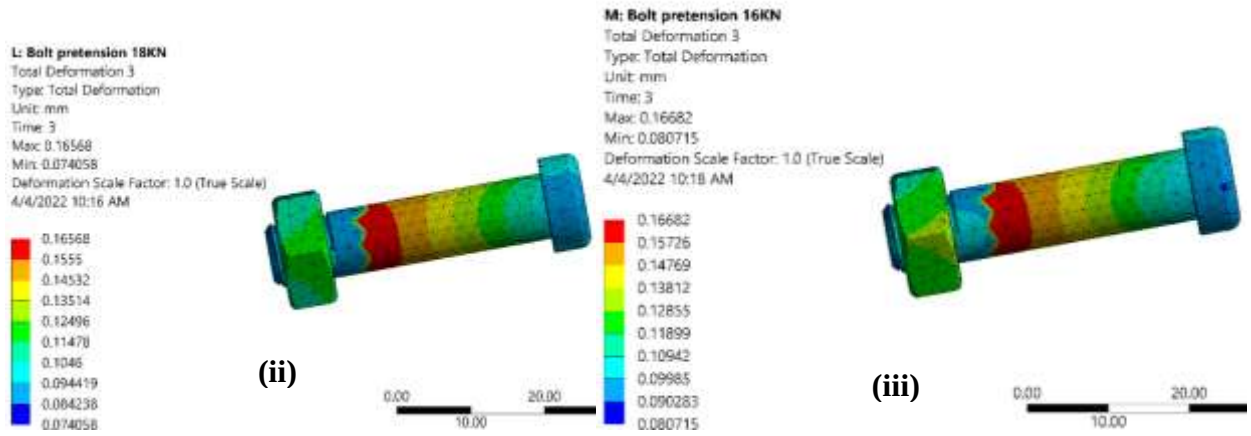

Bolt pretension at 18KN Bolt pretension 16KN

Figure 5.1: Total Deformation at different values of insufficient bolt pretension

Table 5.1: Obtained values at insufficient bolt pretension

Conrod force =20KN (Analytically calculated)	
Bolt Pretension (KN)	**Total deformation (mm)**
0	0.26291
5	0.18357
8	0.17422
10	0.17214
14	0.17031
16	0.16682
17	0.16601
18	0.16568
20	0.16494

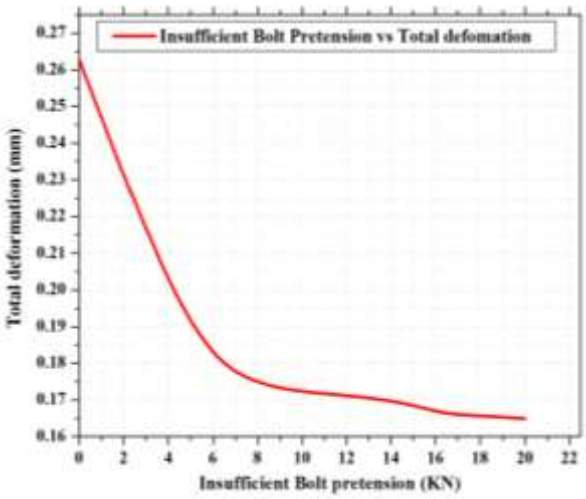

Figure 5.2: Insufficient bolt pretension curve

5.1.2. Appropriate bolt pretension

The appropriate pretension is selected to tighten the bolts based on the total deformation of the ANSYS software's turning point result. That means, according to the ANSYS result, the bolt pretension 22KN is considered a proper bolt pretension when simulating the real geometry of connecting rod bolts. It matched the preload, calculated from the analytical formula depending upon the real device data source.

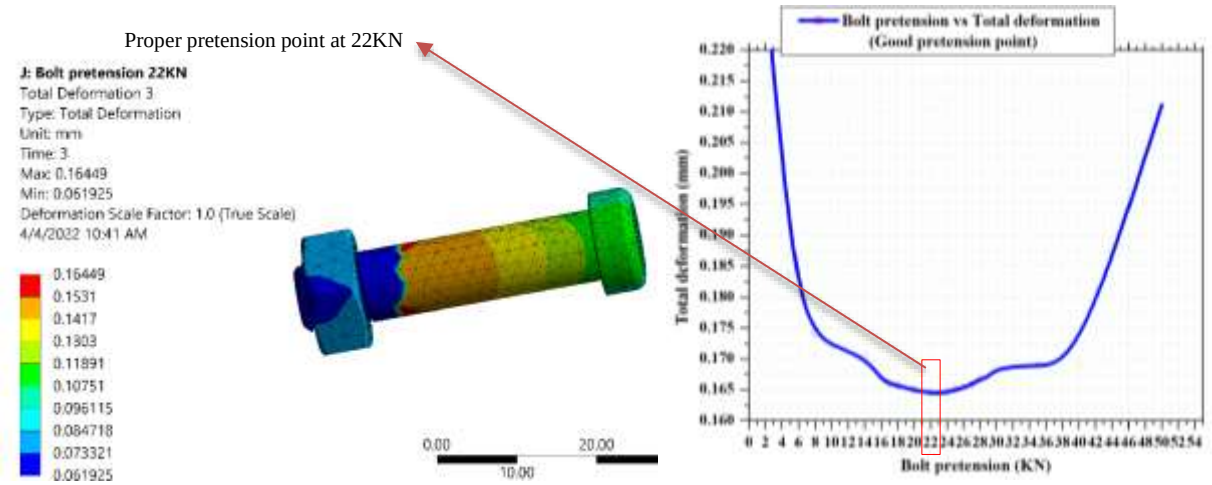

Figure 5.3: Appropriate bolt pretension point (pretension vs. total deformation)

The above graph in figure 5.3 demonstrates that the pretension of bolts dramatically influences the total deformation of connecting rod bolts if an appropriate and tangible tightening force is applied to them. The perfect bolt pretension load should be identified in which the total deformation of the whole assembly is reduced. The graph is plotted based on the results generated from ANSYS Workbench 2020 R_2. It shows that at bolt pretension load equals 22000N, the total deformation for the assembly is decreased so that the appropriate torque for pretension is 32.21N.m.

5.1.3. Excessive bolt pretension

It is also understood that from the ANSYS workbench analysis, the excessive value of bolt preload greatly affects the total deformation of the bolts. The below figures and tabulated results are obtained from varying the value of pretension above the appropriate bolt pretension for the real device of a connecting rod model.

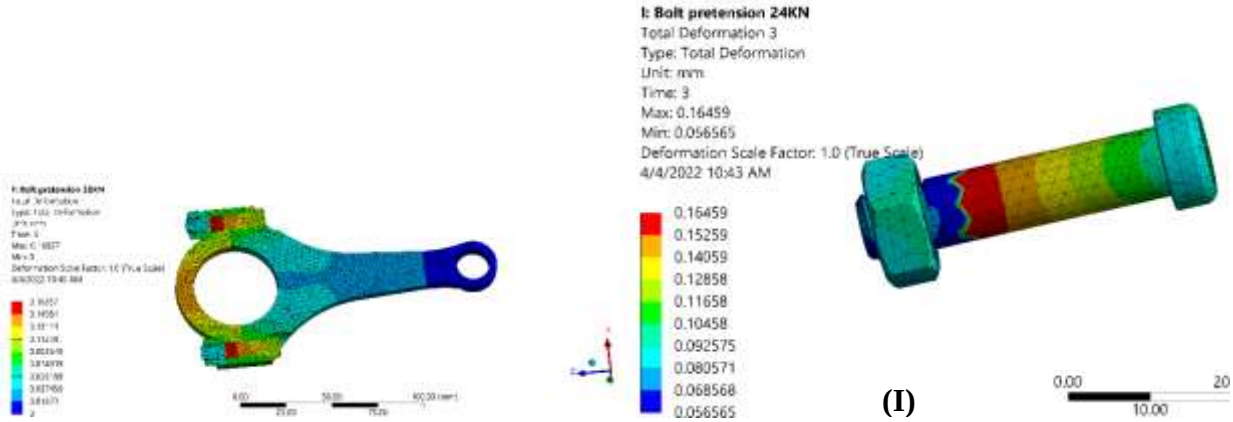

(I)

Bolt pretension 24KN

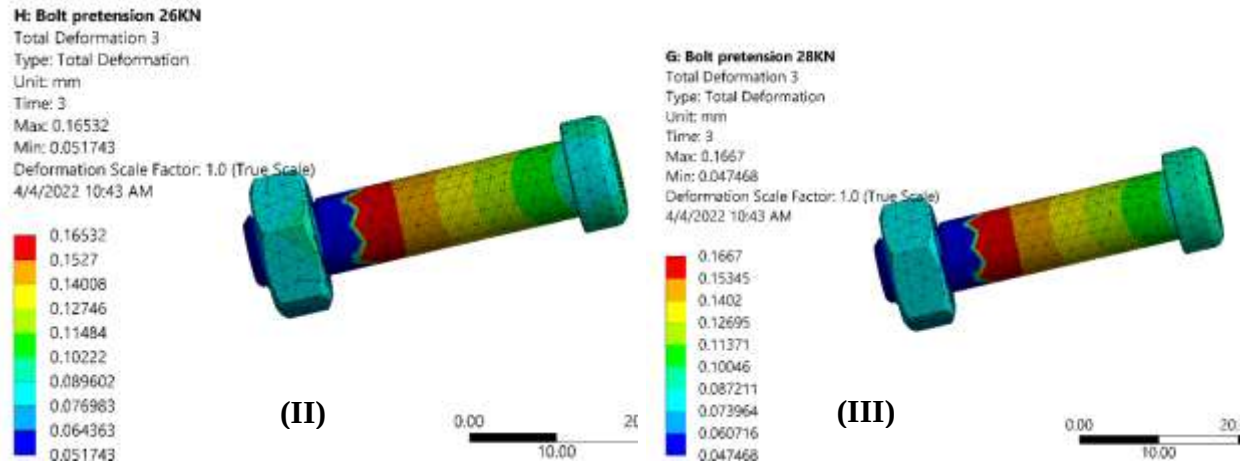

Bolt pretension at 26KN Bolt pretension at 28KN

Figure 5.4: Total Deformation at different values of excessive bolt pretension

Table 5.2: Obtained values at excessive bolt pretension

Conrod force =20KN	
Bolt Pretension (KN)	**Total deformation (mm)**
22	0.16449
23	0.16451
24	0.16459
25	0.16499
26	0.16532
27	0.16587
28	0.1667
29	0.1670
30	0.16857
35	0.16897
40	0.16911
50	0.21111

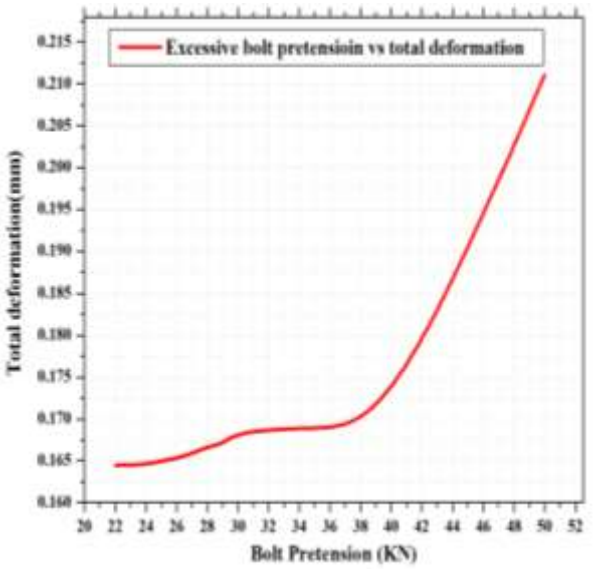

Figure 5.5: Excessive bolt pretension curve

From figures 5.4 and 5.5 and Table 5.2, it can be said that the simulated excessive bolt pretension increased the total deformation of the connecting rod bolts.

5.2. The impact of bolt pretension on equivalent and alternating stresses

Like the above simulations, the effect of bolt pretension on the number of stresses produced in the connecting rod bolts is also simulated and summarized in table 5.3 below. It is confirmed that the bolt pretension value influences the equivalent stresses produced by the geometry due to two-step

loads from bolt pretension and connecting rod forces. Table 5.3 presented the results simulated at different values of bolt pretension. As the value of bolt pretension increases, the equivalent and total equivalent stresses also increase in the both steps. The alternating stress also behaves the same as equivalent stress, as shown in the same table 5.3 below.

Table 5.3: Bolt pretension effect on conrod bolts equivalent stress and alternating stress

Conrod force for TOYOTA D4D Dolphin 20KN				
Pretension (KN)	**Equivalent stress (MPa)**		**Alternating stress (MPa)**	
	Step 1	**Step 2**	**Step 1**	**Step 2**
0	79.1	898.9	39.25	449.1
5	336	967.3	167.55	483
8	401.9	1250	200.5	624
10	552.7	1316.4	276.05	657.1
14	831.9	1627.6	415.5	813
16	1099.6	1714.2	547.85	854.85
18	1238.9	1792	617.23	893.62
19	1290.5	1844.2	645	921.75
20	1377.9	1874.3	686.45	934.63
22	1515.1	1959.1	754.76	976.87
24	1653.2	2049.6	823.51	1021.93
25	1688.1	2099.3	642.638	731.296
26	1794.6	2145	893.94	1069.42
28	1932.9	2245.4	962.86	1119.38
30	2073.3	2349.1	1032.95	1170.97
35	2290.7	2451.1	1145	1225
40	2488.1	2655.6	1243.9	1327.25
50	2644.4	2822.9	1321.85	1411

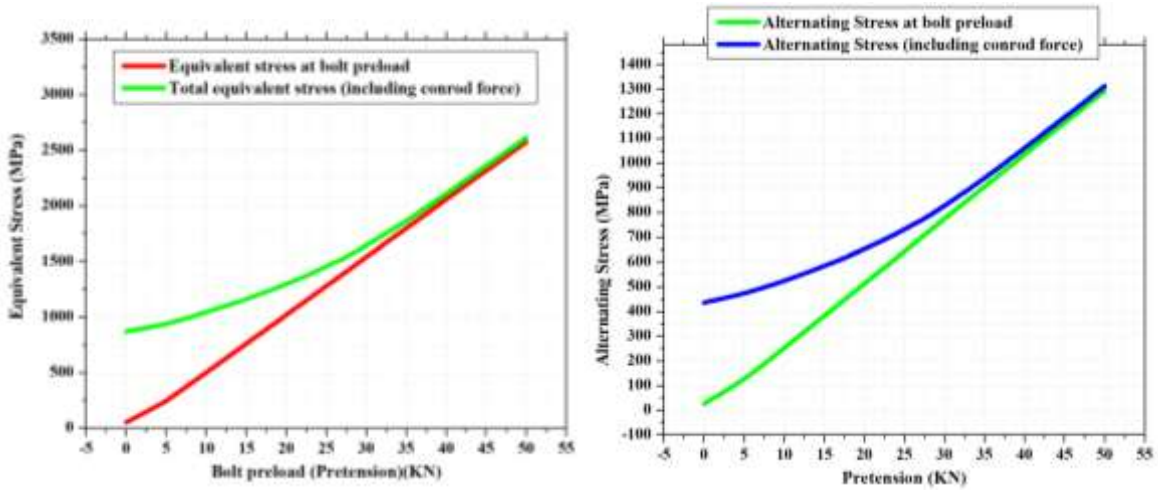

Figure 5.6: Bolt Pretension versus equivalent and alternating stresses

5.3. Fatigue life prediction for existing material-ARP2000

- ☑ The mean Stress at Pretension: step 1 (time 1): $\sigma_{max} = 1515.1MPa, and\ \sigma_{min} = 5.5798MPa$. Mean stress, $\sigma_m = \frac{\sigma_{max}+\sigma_{min}}{2}$
- ☑ The mean stress at Pretension + Connecting rod force: step 2 (time 2):$\sigma_{max} = 1959.1MPa, and\ \sigma_{min} = 5.365MPa$. Mean stress, $\sigma_a = \frac{\sigma_{max}+\sigma_{min}}{2}$

Alternating Stresses: The stresses amplitude taken from the ANSYS result is specifically the selected result for the bolts only to reduce the effects of other assembled parts of connecting rod. The stress is obtained using the details of the Equivalent stress dialogue box, selecting and changing "All bodies" into "2 bodies".

At Pretension: STEP 1:$\sigma_{max} = 1515.1MPa$, and $\sigma_{min} = 5.5798MPa$

Alternating stress, $\sigma_a = \frac{\sigma_{max}-\sigma_{min}}{2} = 754.76MPa$

At Pretension + connecting rod force: STEP 2: $\sigma_{max} = 1959.1MPa$ and $\sigma_{min} = 5.365MPa$

Alternating stress, $\sigma_a = \frac{\sigma_{max}-\sigma_{min}}{2} = 976.87MPa$

Alternating stress range: $754.76MPa \leq \sigma_a \leq 976.87MPa$

The S-N curve graph was plotted using MATLAB code by dividing the gap into nine or incrementing $24.679x10^6$ (i.e., $\frac{976.87*10^6-754.76*10^6}{9}=24.679x10^6$). The MATLAB code is written to estimate the fatigue life of connecting rod shown in Appendices. The fatigue life was obtained by conducting FEA with the action of loads including; bolt tightening load, piston pin interference load, uniaxial tensile load to get the alternating stresses. To simulate the life and damage, S-N curves tabular data is necessary as an input in ANSYS workbench 2020 R_2. By inputting the stress

life relation formula into the MATLAB software, it was abled to generate the tabulated data results at some of the points between the obtained alternating stress range. So, fatigue life at each alternative stress is calculated based on the formula in equation 3.14. The Stress-Life (S-N) curve data was obtained at first from the modelled actual device using ANSYS workbench 2020 R_2 and MATLAB. The alternating stress is used as an input for the analysis and simulation of fatigue life and fatigue damage on simulation two.

5.3.1. Number of Cycles at different bolt pretension

The alternating stresses that are simulated using ANSYS workbench 2020 R_2 at proper pretension and above proper pretension (i.e., 22KN, 26KN, and 30KN bolt pretensions) are taken to MATLAB software to get the tabulated number of cycles for the alternating results obtained that range from 754.76MPa to 976.87MPa (at proper pretension), 893.94MPa to 1069.42Mpa and 1032.95MPa to 1171MPa (above proper pretension). The value of connecting rod force has remained the same, 20KN. The results are tabulated as follows:

Table 5.4: Number of cycles at different values of bolt pretension

[Fconrod=20KN], [bolt pretension=22KN]		**[Fconrod=20KN], [bolt pretension=26KN]**		**[Fconrod=20KN], [bolt pretension=30KN]**	
Alternating Stress (MPa)	Number of Cycles (10^6)	Alternating Stress (MPa)	Number of Cycles (10^6)	Alternating Stress (MPa)	Number of Cycles (10^6)
754.76	498.93	893.94	493.62	1033	489.13
779.439	497.92	913.438	492.95	1048.3	488.68
804.118	496.94	932.936	492.29	1063.6	488.23
828.797	495.99	952.434	491.65	1079	487.79
853.476	495.07	971.932	491.02	1094.3	487.35
878.155	494.18	991.43	490.4	1109.6	486.92
902.834	493.31	1010.9	489.8	1125	486.5
927.513	492.47	1030.4	489.21	1140.3	486.08
952.192	491.65	1049.9	488.63	1155.7	485.67
976.87	490.7	1069.42	487.98	1171	485.21

As shown in table 5.4, the simulation showed that the bolt pretension at 22KN has more cycles to failure than other values of bolt pretension encircled using red colour.

5.3.2. The effect of bolt pretension on fatigue life of conrod bolts using MATLAB

In this graphical representation of the results, MATLAB program code is used to compare bolt pretension at different values to identify the effect of bolt pretension on the component's life cycle. The written MATLAB program code is shown in Appendix III. The program results are shown in the figures below.

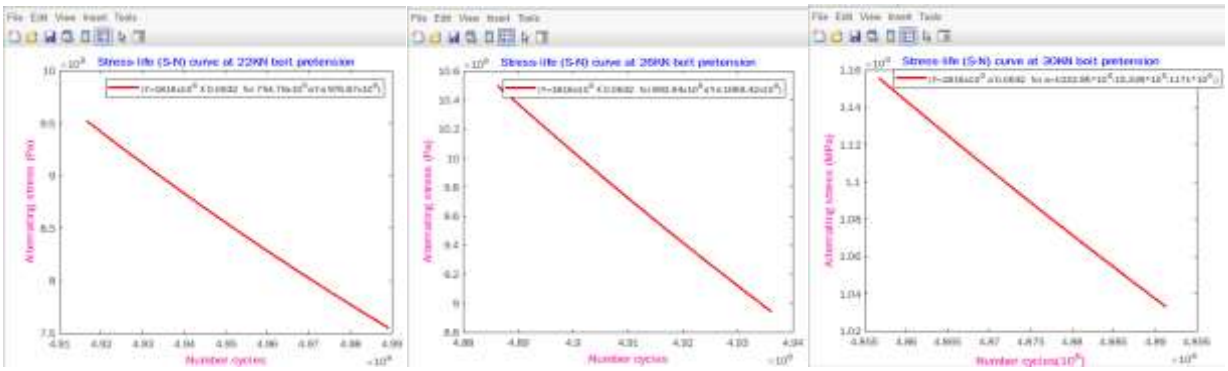

Figure 5.7: S-N curves for ARP2000 at different values of bolt pretension

The combined program code is shown in Appendix IV, which identified which bolt pretension is proper and recommended to tighten connecting rod with the cap for a good life span of the engine connecting rod, as shown in figure 5.8.

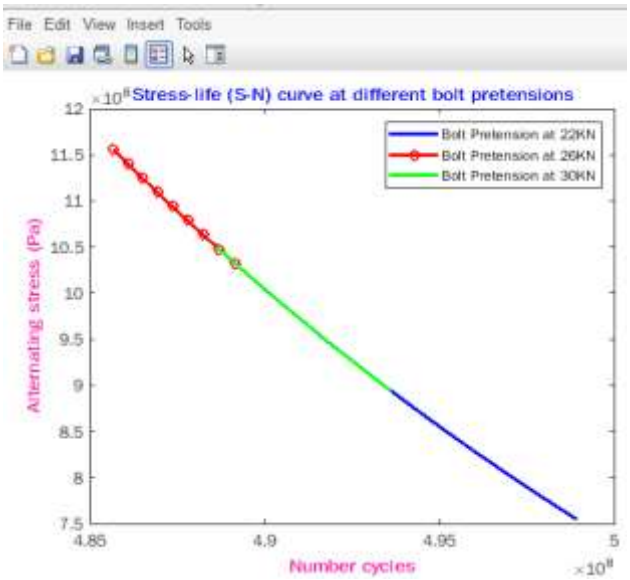

Figure 5.8: Comparison for ARP2000 fatigue life curve at different bolt pretension

From the comparison, the bolt pretension at 22KN has a better number of cycles than 26KN and 30KN bolt pretensions. From the MATLAB code program, one can say that the appropriate bolt pretension for the entire connecting rod bolt is 22KN.

5.3.3. The effect of bolt pretension on fatigue parameters using ANSYS

As from the beginning, the tightening torque value significantly affects the fatigue life and fatigue damage of the component-connecting rod bolts, as understood from the different simulations from the ANSYS workbench. The results are shown in the figures below.

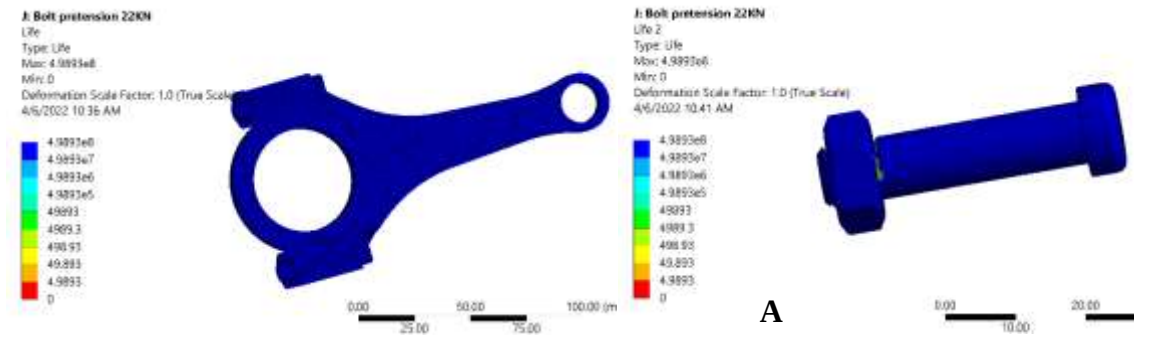

Bolt pretension at 22KN

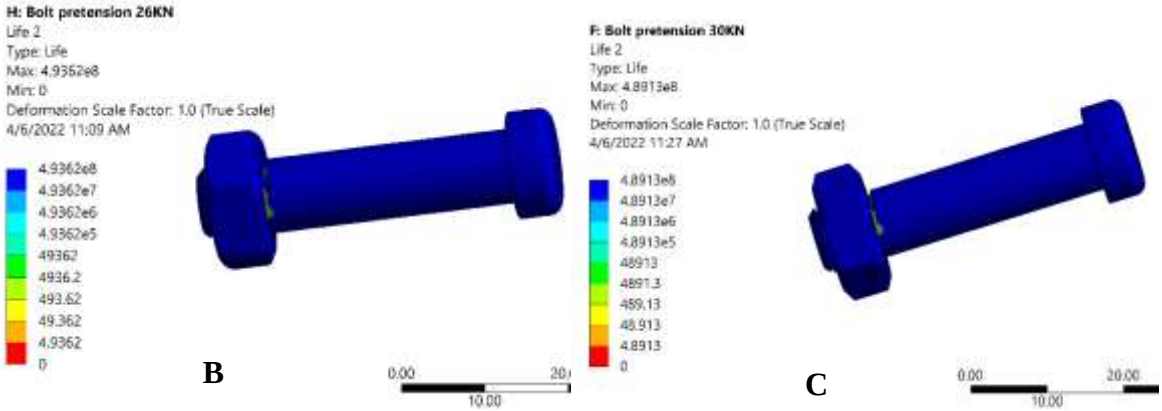

Bolt pretension at 26KN Bolt pretension at 30KN

Figure 5.9: Fatigue Life at different values of bolt pretension

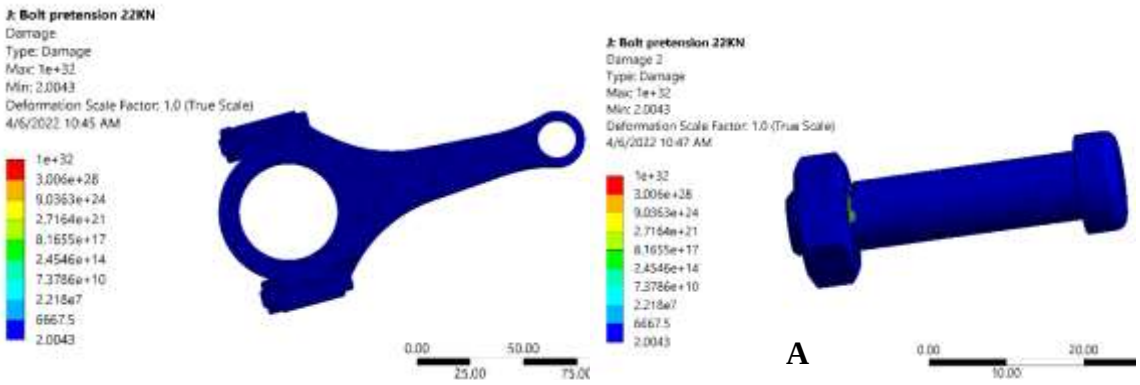

Bolt pretension at 22KN

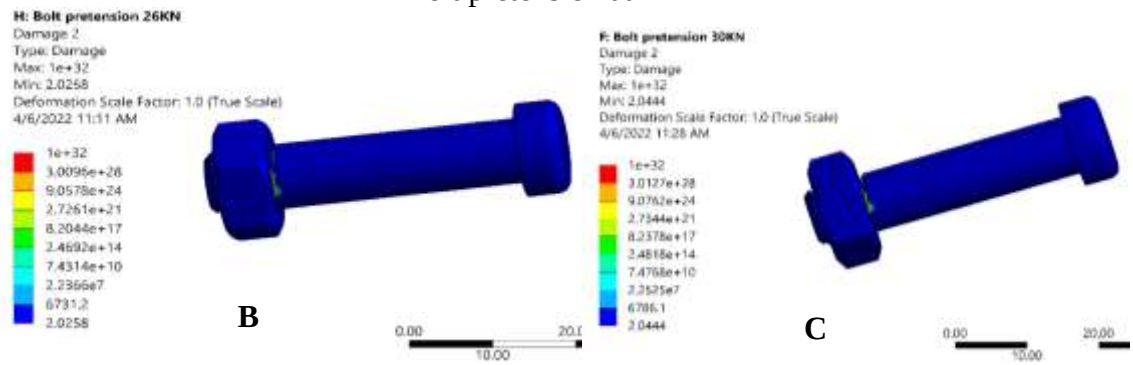

Bolt pretension at 26KN Bolt pretension at 30KN

Figure 5.10: Fatigue Damage at different values of bolt pretension

5.4. Fatigue life prediction for interchangeably used materials

As shown in detail in chapter three, the alternating stress-life relationship equation for the replacement materials is analytically obtained. The fatigue strength ($\acute{\sigma_f}$) and fatigue strength exponent (b) is analytically calculated, and the alternating stresses are obtained from the simulation in the ANSYS workbench by varying the bolt pretension. As mentioned, the materials are ARP 3.5 and ARP 625+. The number of life of connecting rod bolts was obtained at different alternating stresses depending on the value of bolt pretension using the MATLAB code program. Both the values and the stress-life curve are obtained using MATLAB code. The number of life is obtained based on equation [3.16].

5.4.1. Fatigue life prediction for ARP 3.5

The MATLAB code for this material is written in Appendix V, VI, and VII.

Table 5.5: Fatigue life for ARP 3.5

[F_{conrod}=20KN], [bolt pretension=22KN]		**[F_{conrod}=20KN], [bolt pretension=26KN]**		**[F_{conrod}=20KN], [bolt pretension=30KN]**	
Alternating Stress (MPa)	Number of Cycles (10^6)	Alternating Stress (MPa)	Number of Cycles (10^6)	Alternating Stress (MPa)	Number of Cycles (10^6)
754.76	407.59	893.94	402	1033	397.29
779.439	406.52	913.438	401.29	1048.3	396.81
804.118	405.49	932.936	400.6	1063.6	396.34
828.797	404.49	952.434	399.93	1079	395.88
853.476	403.52	971.932	399.27	1094.3	395.42
878.155	402.59	991.43	398.62	1109.6	394.97
902.834	401.68	1010.9	397.99	1125	394.53
927.513	400.79	1030.4	397.37	1140.3	394.1
952.192	399.94	1049.9	396.76	1155.7	393.67
976.87	398.90	1069.42	396.01	1171	393.34

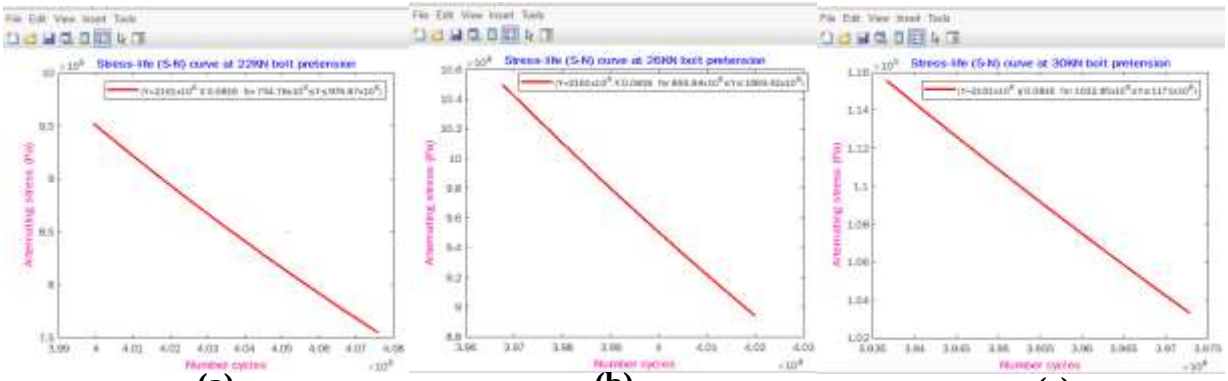

(a) **(b)** **(c)**

Figure 5.11: Fatigue life estimation for ARP 3.5 at different bolt pretension values

5.4.2. Fatigue life prediction for ARP 625+

The MATLAB code for this material is written in Appendix VIII, IX, and X.

Table 5.6: Fatigue life for ARP625+

[F_{conrod}=20KN], [bolt pretension=22KN]		**[F_{conrod}=20KN], [bolt pretension=26KN]**		**[F_{conrod}=20KN], [bolt pretension=30KN]**	
Alternating Stress (MPa)	Number of Cycles (10^6)	Alternating Stress (MPa)	Number of Cycles (10^6)	Alternating Stress (MPa)	Number of Cycles (10^6)
754.76	409.71	893.94	404.15	1033	399.4
779.439	408.65	913.438	403.44	1048.3	398.98
804.118	407.62	932.936	402.75	1063.6	398.51
828.797	406.62	952.434	402.08	1079	398.05
853.476	405.66	971.932	401.42	1094.3	397.6
878.155	404.73	991.43	400.78	1109.6	397.15
902.834	403.82	1010.9	400.15	1125	396.71
927.513	402.94	1030.4	399.53	1140.3	396.27
952.192	402.09	1049.9	398.93	1155.7	395.85
976.87	401.42	1069.42	398.12	1171	395.31

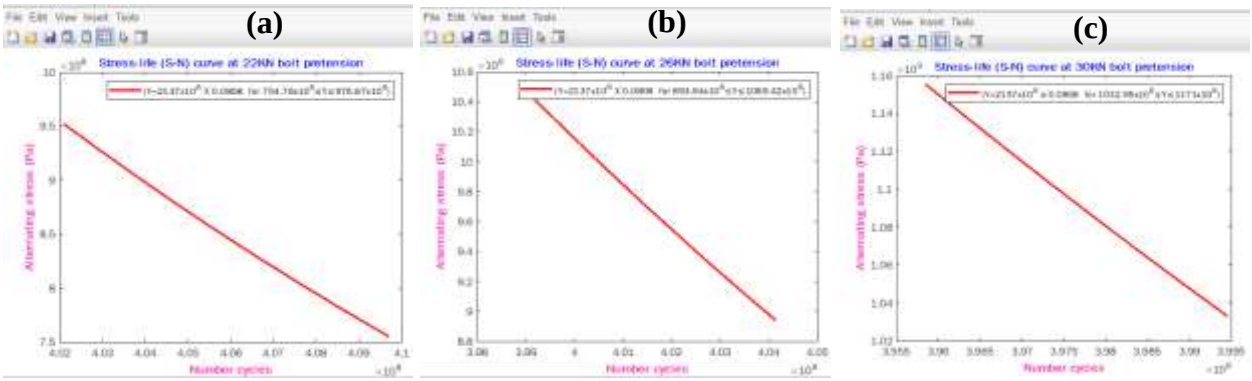

Figure 5.12: Fatigue life estimation for ARP625+ at different bolt pretension values

5.5. Comparison for the materials at different values of bolt pretension

Table 5.7: Comparison of materials at 22KN bolt pretension

[F_{conrod}=20KN], [bolt pretension=22KN]			
Alternating Stress (MPa)	**Alternating Stress (MPa)**		
	ARP2000	**ARP625+**	**ARP3.5**
754.76	498.93	409.71	407.59
779.439	497.92	408.65	406.52
804.118	496.94	407.62	405.49
828.797	495.99	406.62	404.49
853.476	495.07	405.66	403.52
878.155	494.18	404.73	402.59
902.834	493.31	403.82	401.68
927.513	492.47	402.94	400.79
952.192	491.65	402.09	399.94
976.87	490.7	401.42	398.90

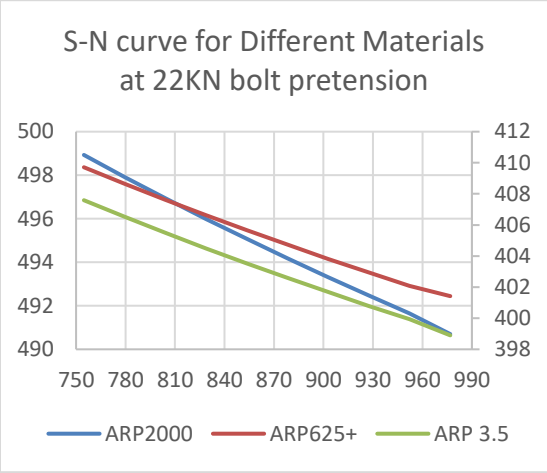

Figure 5.13:S-N curve for different materials at 22KN bolt pretension

Table 5.8: Comparison of materials at 26KN bolt pretension

[F_{conrod}=20KN], [bolt pretension=26KN]			
Alternating Stress (MPa)	**Alternating Stress (MPa)**		
	ARP2000	**ARP625+**	**ARP3.5**
893.94	493.62	404.15	402
913.438	492.95	403.44	401.29
932.936	492.29	402.75	400.6
952.434	491.65	402.08	399.93
971.932	491.02	401.42	399.27
991.43	490.4	400.78	398.62
1010.9	489.8	400.15	397.99
1030.4	489.21	399.53	397.37
1049.9	488.63	398.93	396.76
1069.42	487.98	398.12	396.01

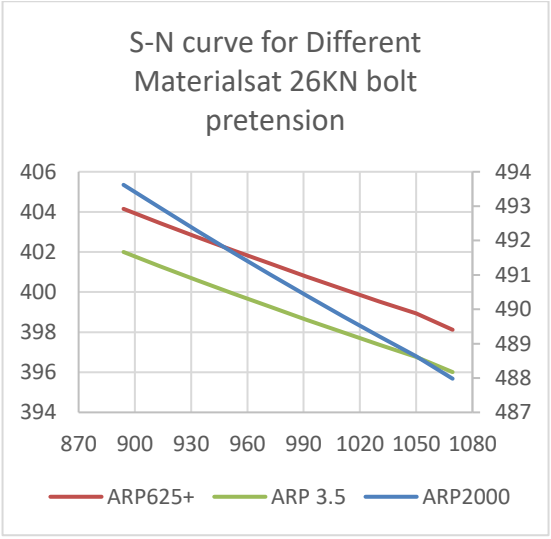

Figure 5.14: S-N curve for different materials at 26KN bolt pretension

Table 5.9: Comparison of materials at 30KN bolt pretension

[F_{conrod}=20KN], [bolt pretension=30KN]			
Alternating Stress (MPa)	Alternating Stress (MPa)		
	ARP2000	ARP625+	ARP3.5
1033	489.13	399.4	397.29
1048.3	488.68	398.98	396.81
1063.6	488.23	398.51	396.34
1079	487.79	398.05	395.88
1094.3	487.35	397.6	395.42
1109.6	486.92	397.15	394.97
1125	486.5	396.71	394.53
1140.3	486.08	396.27	394.1
1155.7	485.67	395.85	393.67
1171	485.21	395.31	393.34

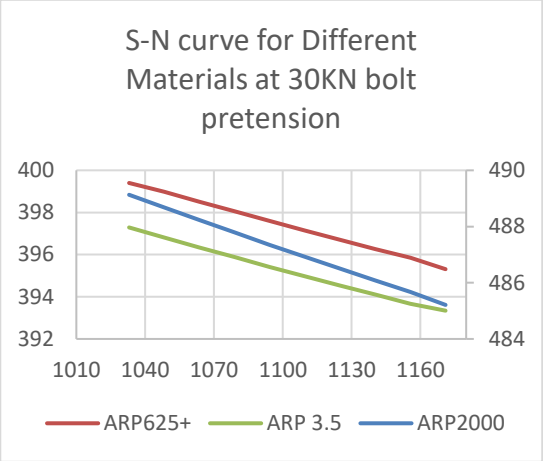

Figure 5.15: S-N curve for different materials at 30KN bolt pretension

From the above tables and graphs, it can be concluded that the simulation for ARP2000, ARP 625+, and ARP 3.5 at different values of bolt pretension identified which material has a better life. ARP2000 material has an acceptable and better fatigue life at high cycle than ARP 625+ and ARP 3.5 at all simulated values of bolt pretension with common connecting rod force.

5.6. Comparison of Safety factor for existing material with replacement materials

The two materials used as a replacement were compared with the existing material to identify the materials safety factor. The simulations have been conducted on the common boundary condition and tensile loading with varying the values of the connecting rod bolts pretension. The final second step simulated results are taken shown in table 5.10.

Table 5.10: Safety factor for existing and replacement materials

Bolt pretension (KN)	Safety factor		
	ARP2000	ARP 625+	ARP 3.5
22	1.74	1.61	1.59
26	1.54	1.32	1.28
30	1.26	1.15	1.11

When the bolt pretension value increased from 22KN to 50KN, the safety factor for all materials (ARP2000, ARP625+ and ARP 3.5) oppositely decreased, as shown in figure 5.16. From these results, one can understand that excessive bolt pretension reduces the materials' safety factor.

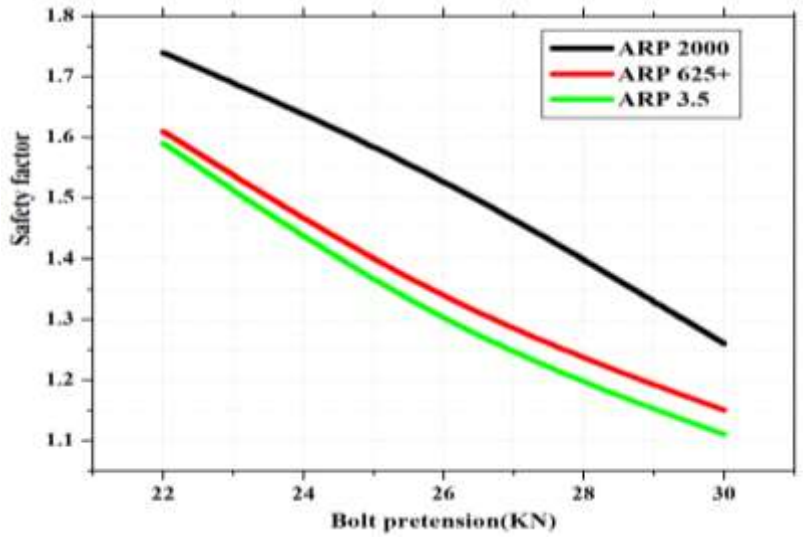

Figure 5.16: Bolt Pretension versus safety factor for different materials

5.7. Validation of the results

To justify the analyzed results obtained from ANSYS Workbench 2020 R_2 and MATLAB, the study put the other works of paper and compared the common graph trend for high cycle fatigue life of the different components. The conducted results graph trend is drawn in figure 5.17 and 5.18 with the common and previous graph of high cycle fatigue life.

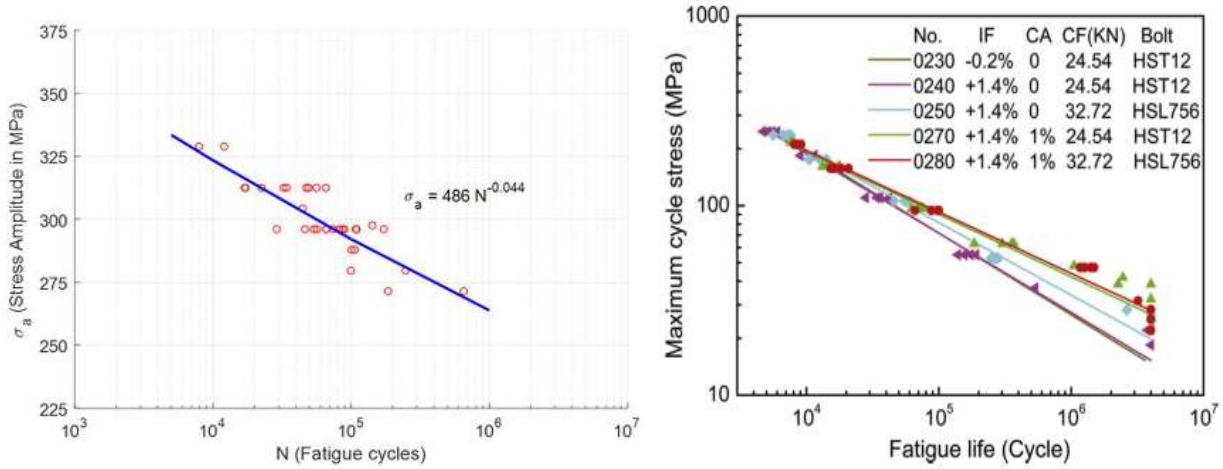

Figure 5.17: Experimental S-N curve for high cycle AISI 4130 tensile specimen [9] [15]

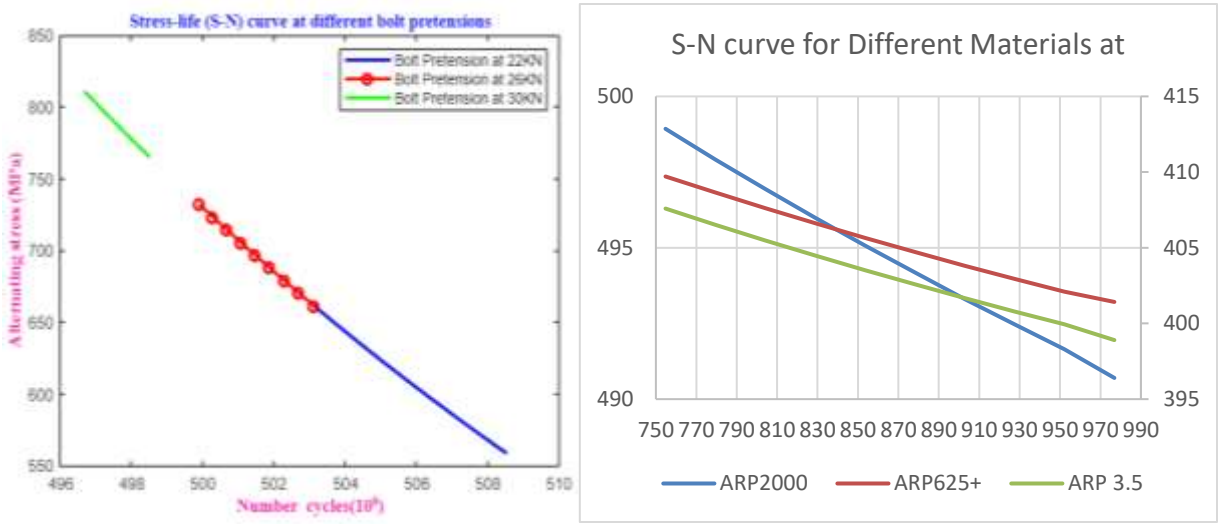

Figure 5.18: S-N curve obtained using Finite Element Modeling in this study

5.8. Finite Element Analysis (ANSYS Workbench 2020 R2) results against the practically deformed connecting rod bolts

When the simulations are cross-checked and compared with the practically deformed component image (observation) taken from Henok Tsige Garage Center, the simulations are correct and optimum to the real on duty failed component.

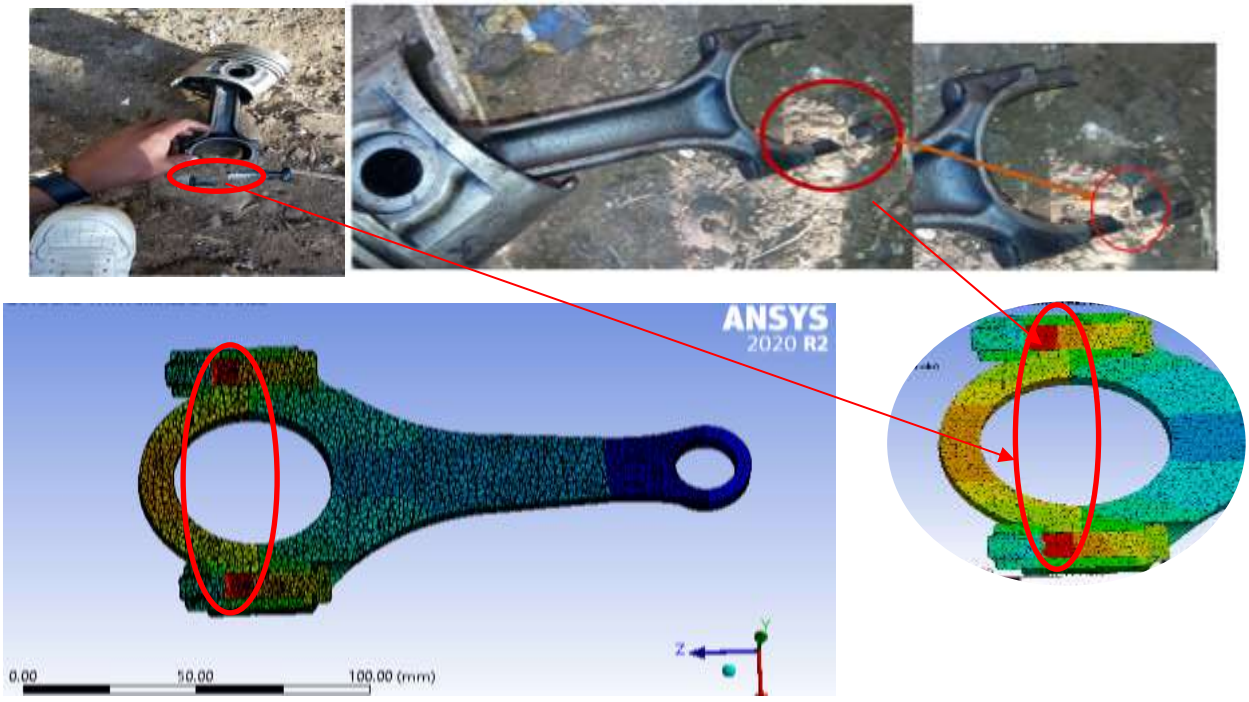

Figure 5.19: Comparison with the practically deformed connecting rod bolts

CHAPTER SIX
CONCLUSION, RECOMMENDATION AND FUTURE WORK

6.1. Conclusion

In this thesis, the main objective is to analyze the high cycle fatigue life prediction of pre-tightened four-wheel connecting rod bolts for the particular problem identified for the 2006 Model TOYOTA D4D Dolphin. It is essential to determine and select the best fit or appropriate bolt pretension for connecting rod bolts to improve fatigue life, fatigue damage, deformation, and the material strength. Initially, from the data collected at Henok Tsige Garage Center, the practical connecting rod forces and their bolts preload were determined. The design and model have been prepared using Solidworks 2021 and imported to ANSYS Workbench 2020 R_2. The modelled geometry has been categorized into three different general simulations. Simulation one was run to obtain the total deformation and alternating stress at different values of bolt pretension. Simulation two used the alternating stresses as an input to obtain number cycles using MATLAB and inputting into ANSYS to get and determine the effect of bolt pretension on fatigue life and fatigue damage. The third simulation was on the material used for connecting rod bolts interchangeably and their safety factor in changing the values of bolt pretension. From the results obtained, the study conclusions are summarized as follows.

- ✧ The predicted high cycle fatigue life is smartly matched the common trends for the S-N curve in comparison with different experimental works of literature [9] [23]
- ✧ The total deformation increased with insufficient (<22KN) and excessive (>22KN) bolt pretensions. It decreased at the appropriate bolt pretension of 22KN, as was shown by the graphical and tabular form in chapter five.
- ✧ The location of the deformed bolt correctly shows the same with the device deformed in real.
- ✧ The effect of bolt pretension on the high cycle fatigue life and damage at different values of torque was determined. The fatigue life of connecting rod bolts increased from $489.13*10^6$ to $498.93*10^6$ number of the cycle when the bolt pretension decreased from 30KN to 22KN as tabulated in Table 5.5.

- ✧ When the bolt pretension values increase, the alternating and equivalent stresses increase. This, in turn, decreases the number of cycles of connecting rod bolts.
- ✧ High cycle fatigue life for different materials used for TOYOTA D4D Dolphin connecting rod bolts has been estimated and compared. For ARP2000, when the bolt pretension increased from 22KN to 30KN, the number of cycles decreased from $498.93*10^6$ to $489.13*10^6$; for ARP625+, $409.71*10^6$ to $399.4*10^6$, and for ARP 3.5, $407.59*10^6$ to $397.29*10^6$.From these results, the material ARP2000 has more cycles. Therefore, the existing material for the TOYOTA D4D Dolphin connecting rod bolts is better than those used as a replacement.
- ✧ The torque specification manual for TOYOTA D4D Dolphin connecting rod bolt pretension recommends 32N.m to 43N.m (i.e., 21.471KN to 32.74KN), which is not specific. But, in this study, the recommended bolt pretension should be 22KN.
- ✧ The failure problem observed at Henok Garage Center regarding the TOYOTA D4D Dolphin engine was due to improper bolt pretension and material used for replacement.

6.2. Recommendation and Future work

As it is understandable in this research, the appropriate bolt pretension is recommended and applied to the connecting rod bolts to reduce the high cycle fatigue failure and deformation. This study recommend Henok Garage Center to use the proper bolt pretension value as it is observed that the mechanics are using the non-recommended clamping force to tighten the bolts by simply turning the nuts until it will beyond their applied force. Additionally, it is suggested to use the existing in-use material for replacement rather than using ARP625+ and ARP3.5. The TOYOTA company should also use the specific torque recommendation for D4D Dolphin rather than recommending the torque value range. The dynamic analysis of connecting rod bolts did not cover in this study. So, I recommend further work on the dynamic numerical simulation and examining other connecting rod bolts at different crank angles with varying bolt pretension values since the connecting rod position in this study is at the top dead center. Further research can also be done on other materials like composite materials in comparison with traditional materials to examine the thermal fatigue of connecting rod bolts.

REFERENCES

[1] B. Babu, T. Florence, M. Punithavalli, and B. R. Rohit, "ISSN 2349-316X Wisdom Interdisciplinary Society of Engineers Design And Experimental Analysis Of Optimization Technique Used In Connecting Rod ISSN 2349-316X Wisdom Interdisciplinary Society of Engineers," vol. 2, no. 10, pp. 1–9, 2015.

[2] C. Carter, "Low Cycle Fatigue Life Improvements Realized By Reduced," 2011.

[3] A. Gots and A. N. Gots, "The method of determining the efforts of the pre-tightening of bolts to a bearing of the crankshaft, automobile and tractor engines," *Izv. MGTU MAMI*, vol. 0, no. 3, pp. 15–20, Sep. 2018, Accessed: Oct. 25, 2021. [Online]. Available: https://journals.eco-vector.com/2074-0530/article/view/66816.

[4] K. Bari, A. Rolfe, A. Christofi, C. Mazzuca, and K. V. Sudhakar, "Forensic investigation of a failed connecting rod from a motorcycle engine," *Case Stud. Eng. Fail. Anal.*, vol. 9, pp. 9–16, Oct. 2017, doi: 10.1016/J.CSEFA.2017.05.002.

[5] M. Kumar and S. N. Prajapati, "Design, Buckling and Fatigue Failure Analysis of Connecting Rod: A Review," *Int. J. Adv. Eng. Res. Sci.*, vol. 4, no. 7, pp. 39–44, 2017, doi: 10.22161/ijaers.4.7.7.

[6] H. T. G. Center, "The data collected for connecting rod problem and geometry."

[7] A. Romeo, "ZRP Applications !"

[8] "Connecting Rod Bolt Installation Instructions," p. 61.

[9] "Fatigue-life curve-4130 Steel - EVOCD." https://icme.hpc.msstate.edu/mediawiki/index.php/Fatigue-life_curve-4130_Steel.html#cite_note-ref7-6 (accessed Jan. 13, 2022).

[10] D. QQ, P. JC, Z. P, L. SX, and Z. ZF, "Quantitative Relations between S-N Curve Parameters andTensile Strength for Two Steels: AISI 4340 and SCM 435," *Res. Rev. J. Mater. Sci.*, vol. 6, no. 1, pp. 1–16, Feb. 2018, doi: 10.4172/2321-6212.1000207.

[11] "What is Fatigue Life – S-N Curve - Woehler Curve - Definition | Material Properties." https://material-properties.org/what-is-fatigue-life-s-n-curve-woehler-curve-definition/ (accessed Jan. 13, 2022).

[12] W. González-Viñas and H. L. Mancini, "An introduction to materials science," p. 180, 2004.

[13] W. D. Callister and D. G. Rethwisch, "Materials science and engineering : an introduction," p. 960.

[14] K. Singh, F. Sadeghi, M. Correns, and T. Blass, "A microstructure based approach to model effects of surface roughness on tensile fatigue," *Int. J. Fatigue*, vol. 129, p. 105229, Dec. 2019, doi: 10.1016/J.IJFATIGUE.2019.105229.

[15] X. Liu, H. Cui, S. Zhang, H. Liu, G. Liu, and S. Li, "Experimental and numerical investigations on fatigue behavior of aluminum alloy 7050-T7451 single lap four-bolted joints," *J. Mater. Sci. Technol.*, vol. 34, no. 7, pp. 1205–1213, 2018, doi: 10.1016/j.jmst.2017.09.020.

[16] "Causes of Bolt and Bolted Joint Failures | Strategies for Prevention." https://www.htlgroup.com/general/failure-modes-of-bolt-and-bolted-joints/ (accessed Mar. 15, 2022).

[17] D. S. Oh, J. H. Kim, and S. H. Seo, "Failure Analysis by Fracture Study of Connecting Rod Bolts in Diesel Engine for Military Tracked Vehicles," *J. Korea Acad. Coop. Soc.*, vol. 21, no. 7, pp. 191–200, 2020, doi: 10.5762/KAIS.2020.21.7.191.

[18] X. Zhu, J. Xu, Y. Liu, B. Cen, X. Lu, and Z. Zeng, "Failure analysis of a failed connecting rod cap and connecting bolts of a reciprocating compressor," *Eng. Fail. Anal.*, vol. 74, pp. 218–227, 2017, doi: 10.1016/j.engfailanal.2017.01.016.

[19] Q. Yu, H. Zhou, X. Yu, and X. Yang, "High-temperature low cycle fatigue life prediction and experimental research of pre-tightened bolts," *Metals (Basel).*, vol. 8, no. 10, 2018, doi: 10.3390/met8100828.

[20] N. Habibi and M. Amoorezayi, "A 3D Simulation of Bolted Joint and Fatigue Life

Estimation Using Critical A 3D Simulation of Bolted Joint and Fatigue Life Estimation Using Critical Distance Technique," vol. 4, no. October, pp. 2588–2597, 2019.

[21] Q. M. Yu, X. J. Yang, and H. L. Zhou, "An experimental study on the relationship between torque and preload of threaded connections," *Adv. Mech. Eng.*, vol. 10, no. 8, pp. 1–10, 2018, doi: 10.1177/1687814018797033.

[22] T. Seifert, "Computational methods for fatigue life prediction of high temperature components in combustion engines and exhaust systems," no. July, 2008.

[23] M. Saranik, L. Jézéquel, and D. Lenoir, "Experimental and numerical study for fatigue life prediction of bolted connection," *Procedia Eng.*, vol. 66, pp. 354–368, 2013, doi: 10.1016/j.proeng.2013.12.090.

[24] M. Sapieta and P. Sulka, "Life analysis of the bolted joint," *MATEC Web Conf.*, vol. 254, p. 02004, 2019, doi: 10.1051/matecconf/201925402004.

[25] I. O. P. C. Series and M. Science, "Experimental study on the effect of shape of bolt and nut on fatigue strength for bolted joint Experimental study on the effect of shape of bolt and nut on fatigue strength for bolted joint," 2018, doi: 10.1088/1757-899X/372/1/012016.

[26] B. Zheng, Y. Liu, and R. Liu, "Stress and Fatigue of Connecting Rod in Light Vehicle Engine," pp. 14–17, 2013.

[27] "List of Toyota Engines - Specifications, Problems, Maintenance Info on MotorReviewer.com." https://www.motorreviewer.com/make.php?make_id=25 (accessed Jan. 12, 2022).

[28] "Toyota 3RZ-FE 2.7L Engine Specs, Problems, Reliability, oil - In-Depth Review." https://www.motorreviewer.com/engine.php?engine_id=153 (accessed Jan. 12, 2022).

[29] "AutoSpeed - Bolt Materials and Terms." https://www.autospeed.com/cms/a_113138/article (accessed Jan. 22, 2022).

[30] P. Catalogue, "Motorsport is not just business …," 2017.

[31] F. Metal *et al.*, "AISI 4340 Steel , oil quenched 855 ° C (1570 ° F), 230 ° C (450 ° F) temper for 4 hrs . MatWeb , Your Source for Materials Information - WWW . MATWEB . COM / MatWeb , Your Source for Materials Information - WWW . MATWEB . COM /," pp. 1–2.

[32] G. Shanmugasundar, M. Dharanidharan, D. Vishwa, and A. P. Sanjeev Kumar, "Design, analysis and topology optimization of connecting rod," *Mater. Today Proc.*, vol. 46, pp. 3430–3438, 2020, doi: 10.1016/j.matpr.2020.11.778.

[33] J. Ramani, S. Shukla, P. S.-J. of E. Research, and undefined 2014, "FE-Analysis of Connecting Rod of IC Engine by Using Ansys for Material Optimization," *core.ac.uk*, vol. 4, no. 3, pp. 216–220, 2014, Accessed: Oct. 25, 2021. Available: https://core.ac.uk/download/pdf/25918428.pdf.

[34] M. Kumar, "International Journal of Advance Engineering and Research Fatigue Failure Analysis of Connecting Rod of Different Cross-Sections," pp. 7–14, 2017.

[35] "Engine specifications," Available: https://www.engine-specs.net/toyota/5e-fe.html.

[36] B. S. N. Murthy, K. A. Kumar, M. A. Shafeeq, and S. S. S. Praveen, "Design and Analysis of Connecting Rod for Weight and Stress Reduction," vol. 7, no. 03, pp. 1–5, 2019.

[37] K. S. More, "Design and Analysis of Connecting Rod for High- Speed Application in I . C Engine," vol. 5, no. 05, pp. 116–120, 2016.

[38] L. Motion, "Theory of Machines," *Students Q. J.*, vol. 34, no. 133, p. 61, 1963, doi: 10.1049/sqj.1963.0048.

[39] P. Singh, D. Pramanik, and R. V. Singh, "Fatigue and Structural Analysis o f Connecting Rod ' s Material Due to (C . I) Using FEA," 2015.

[40] S. T. de M. Ferreira *et al.*, "Mechanical Characterization and Micro-Wear of FeB-Fe2B Layers on Boriding AISI D2 and AISI 4340 Steels," *Mater. Sci. Appl.*, vol. 12, no. 7, pp. 330–344, Jul. 2021, doi: 10.4236/MSA.2021.127022.

[41] N. S. Ottosen, R. Stenström, and M. Ristinmaa, "Continuum approach to high-cycle fatigue modeling," *Int. J. Fatigue*, vol. 30, no. 6, pp. 996–1006, 2008, doi: 10.1016/j.ijfatigue.2007.08.009.

[42] "Fluctuating Stresses – Vijay K Jadon." https://vijayonline.in/2020/07/25/fluctuating-stresses/ (accessed Dec. 04, 2021).

[43] H. Fu and Y. Liang, "Study of the surface integrity and high cycle fatigue performance of AISI 4340 steel after composite surface modification," *Metals (Basel).*, vol. 9, no. 8, 2019, doi: 10.3390/met9080856.

[44] Q. Yu, H. Zhou, and L. Wang, "Finite element analysis of relationship between tightening torque and initial load of bolted connections," *Res. Artic. Adv. Mech. Eng.*, vol. 7, no. 5, pp. 1–8, 2015, doi: 10.1177/1687814015588477.

[45] "Metric Fine Thread Data - Newman Tools." https://www.newmantools.com/tech/threadmf.htm (accessed Jan. 24, 2022).

[46] "threadmf @ www.newmantools.com." Available: https://www.newmantools.com/tech/threadmf.htm.

[47] D. I. N. Iso, "07170 Hexagon head bolts DIN 931 / DIN EN ISO 4014 / DIN EN 24014 07170 Hexagon head bolts DIN 931 / DIN EN ISO 4014 / DIN EN 24014," no. A 2, pp. 1–6.

[48] "Metrics in Engineering - ISO Metric Threads and Tapping Sizes." http://www.metrication.com/engineering/threads.html (accessed Jan. 24, 2022).

[49] A. R. T. Code, "Din 934 (07/1982) *," vol. 934, pp. 298–307, 2001.

[50] "AISI 4340 Steel, oil quenched 855°C (1570°F), 230°C (450°F) temper for 4 hrs." http://www.matweb.com/search/DataSheet.aspx?MatGUID=b5fe87c8cdde4431b62ad990d4f2042c&ckck=1 (accessed Nov. 25, 2021).

[51] E. Ilia, P. Plamondon, J. P. Masse, and G. L'Espérance, "Copper precipitation at engine

operating temperatures in powder-forged connecting rods manufactured with Fe–Cu–C alloys," *Mater. Sci. Eng. A*, vol. 767, no. September, p. 138383, 2019, doi: 10.1016/j.msea.2019.138383.

[52] "Creep of aerospace materials," *Introd. to Aerosp. Mater.*, pp. 521–533, 2012, doi: 10.1533/9780857095152.521.

[53] H. J. Frost and M. F. Ashby, "Deformation-mechanism maps : the plasticity and creep of metals and ceramics," p. 166, 1982.

[54] "AISI/SAE 4340 Alloy Steel- 4340 Steel Properties | All Metals & Forge Group." https://steelforge.com/alloy-steel-4340/ (accessed Mar. 29, 2022).

[55] "AISI 4340 Alloy Steel (UNS G43400)." https://www.azom.com/article.aspx?ArticleID=6772 (accessed Mar. 29, 2022).

[56] L. Witek, P. Z.-E. F. Analysis, and undefined 2019, "Stress and failure analysis of the connecting rod of diesel engine," *Elsevier*, Accessed: Oct. 25, 2021. [Online]. Available: https://www.sciencedirect.com/science/article/pii/S1350630718312378.

APPENDICES

8.1. Appendix I

DATA COLLECTED FROM HENOK TSIGE GARGE CENTER FOR 2006 MODEL-TOYOTA D4D Dolphin

A Photo of red 2006 Model TOYOTA D4D Dolphin with the problem of deformed connecting rod bolts

A photo of another car with the same model and with the same problem

Data collected	2006 Model-TOYOTA D4D Dolphin
Category	Connecting Rods
Engine make	TOYOTA
Model	3RZ-FE 2.7L
Shape	I-Beam
Length (mm)	130.5
Pin Diam.	18
Housing Bore	46
B.E width	20.85
Weight (g)	426
Bolt size	8=5/16''
Material	ARP2000/ARP625+/ARP 3.5
Bolt Pretension minimum torque (N.m)	32 N.m
Bolt Pretension maximum torque (N.m)	43N.m
Bolt Pretension minimum Preload (N)	21471
Bolt Pretension maximum Preload (N)	32740

TOYOTA 3RZ-FE 2.7L model Engine Specifications

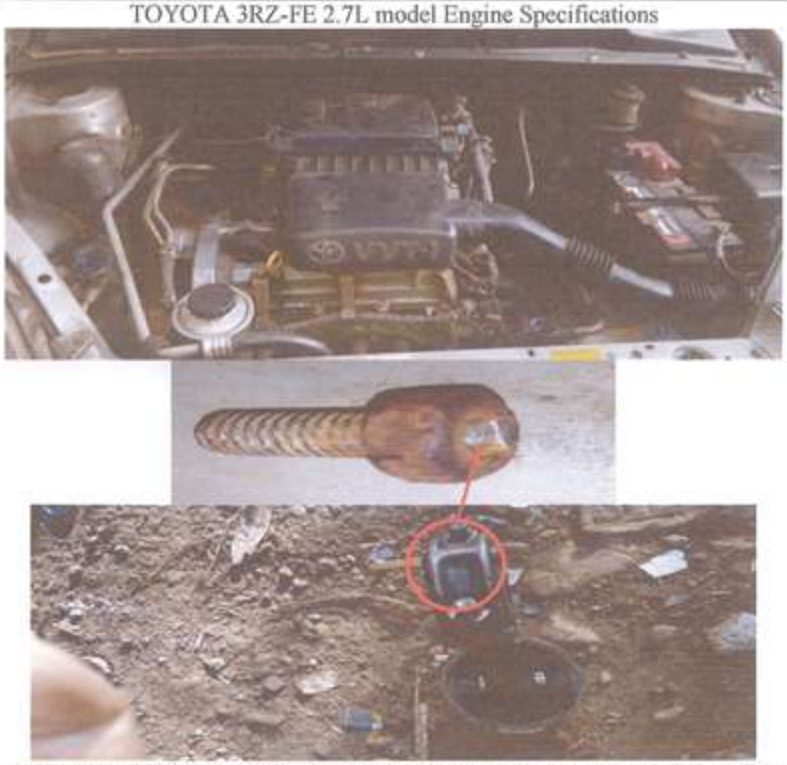

DEFORMED CONNECTING ROD BOLT-Photo taken from Henok Tsige Center

Properties List	Specifications
Fuel type	Gasoline
Fuel system	Multi-point fuel injection
Configuration	Inline
Number of cylinders	4
Valves per cylinder	4
Valve train layout	DOHC
Bore (mm)	95
Stroke (mm)	95
Displacement (cc)	2693
Type of IC engine	Four strokes, naturally aspirated
Compression ratio	9.5: 1
Power (hp)	150hp/4800rpm
Torque (N.m)	240/4000rpm
Torque (τ)	240Nm/4000 rpm
Connecting rod length (ℓ)	141mm
Cylinder Diameter (d)	74mm
Maximum Speed	4800rpm
Engine weight	173kg
Firing order	1-3-4-2
Engine oil weight	SAE 5W-30

Applications

- Toyota Tacoma
- Toyota 4Runner
- Toyota T100
- Toyota Granvia
- Toyota Hilux
- **Toyota HiAce (Toyota D4D Dolphin)**
- Toyota HiAce Regius
- Toyota Land Cruiser Prado
- Toyota Touring HiAce

8.2. Appendix II

M8x1 bolt model using Solidworks software

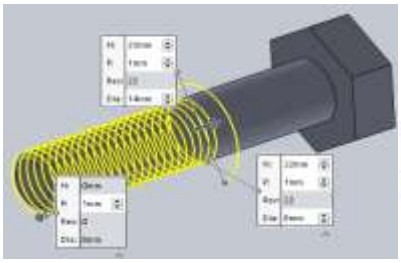

Height and Pitch of thread profile

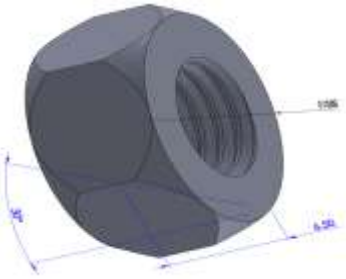

Nut thread using combining method

Exploded view of the connecting rod modelled using SOLIDWORKS 2021

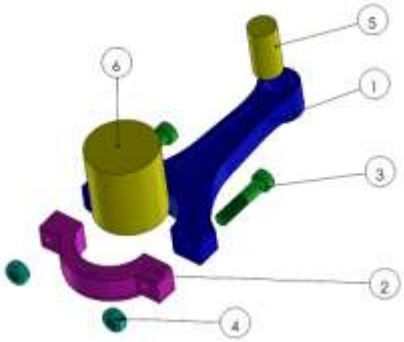

ITEM NO.	PART NUMBER	DESCRIPTION	QTY.
1	CON ROD	CONNECTING ROD	1
2	CON ROD CAP	LOWER CONNECTING ROD CAP/ BIG END	1
3	THREADED BOLT	M8X1 BOLTS	2
4	THREADED NUT	CONNECTING ROD NUT	2
5	UPPER PIN	CYLINDER HEAD AND UPPER ROD CONNECTOR	1
6	CRANK SHAFT	ASSEMBLY PART WITH BIG END	1

Connecting rod model

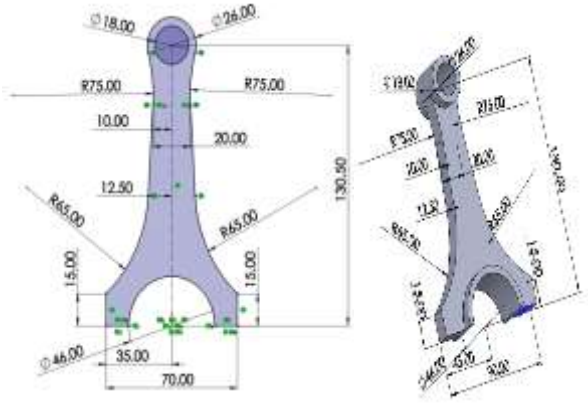

Upper cap connecting rod

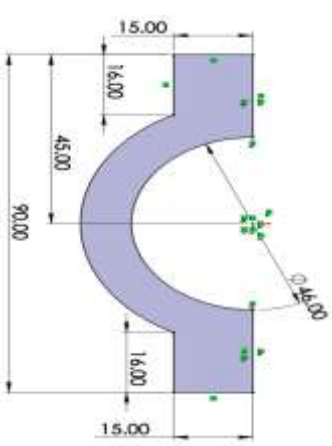

Lower cap connecting rod

Assembly of the model

8.3. Appendix III

```
                    %BOLT PRETENSION AT 22KN
% By BIKILA DEBELA graph of Stress-life curve
% Alternating stress versus number of cycles
%CREATEFIGURE(X1, Y1, X2, Y2, X3, Y3)
%  a:  vector of the number of cycles at 22kN bolt pretension data
%  X:  vector of alternating stress at 22KN bolt pretension data
% Create figure
figure1 = figure('NumberTitle','off','Name','S-N curve at 22kN pretension');
a=754.76*10^6:24.679*10^6:976.87*10^6; %from minimum alternating stress to
maximum alternating stress with the increment of 24.679*10^6
X=(a.^-0.0632)*(1816*10^6);%Y represents Alternating stress, and X represents the
number of cycles
% Create plot
plot(X,a,'-r','DisplayName','Bolt Pretension at 22KN',...
    'LineWidth',2);
% Create legend
legend('(Y=1816x10^6 X^-0.0632  for 754.76x10^6≤Y≤976.87x10^6)')
% Create title
title('Stress-life (S-N) curve at 22KN bolt pretension',...
    'HorizontalAlignment','center',...
    'FontWeight','bold',...
    'FontName','Times',...
    'Color',[0 0 1]);
% Create xlabel
xlabel('Number cycles(10^6)','FontWeight','bold','FontName','Times',...
    'Color',[1 0.0745098039215686 0.650980392156863]);
% Create ylabel
ylabel('Alternating stress (MPa)','FontWeight','bold','FontName','Times',...
    'Color',[1 0.0745098039215686 0.650980392156863]);
```

```
                                %BOLT PRETENSION AT 26KN
% By BIKILA DEBELA graph of Stress-life curve
% Alternating stress versus number of cycles
%CREATEFIGURE(X1, Y1, X2, Y2, X3, Y3)
%  a:  vector of number of cycles at 26kN bolt pretension data
%  X:  vector of alternating stress at 26KN bolt pretension data
% Create figure
figure1 = figure('NumberTitle','off','Name','S-N curve at 26KN pretension');
a=893.94*10^6:19.498*10^6:1069.42*10^6; %from minimum alternating stress to
maximum alternating stress with the increment of 19.498*10^6
X=(a.^-0.0632)*(1816*10^6);%Y represents Alternating stress and X represents
number of cycles
% Create plot
plot(X,a,'-r','DisplayName','Bolt Pretension at 26KN',...
    'LineWidth',2);
% Create legend
legend('(Y=1816x10^6 X^-0.0632  for 893.94x10^6≤Y≤1069.42x10^6)')
% Create title
title('Stress-life (S-N) curve at 26KN bolt pretension',...
    'HorizontalAlignment','center',...
    'FontWeight','bold',...
    'FontName','Times',...
    'Color',[0 0 1]);
% Create xlabel
xlabel('Number cycles','FontWeight','bold','FontName','Times',...
    'Color',[1 0.0745098039215686 0.650980392156863]);
% Create ylabel
ylabel('Alternating stress (Pa)','FontWeight','bold','FontName','Times',...
    'Color',[1 0.0745098039215686 0.650980392156863]);
                                %BOLT PRETENSION AT 30KN
% By BIKILA DEBELA graph of Stress-life curve
% Alternating stress versus number of cycles
%CREATEFIGURE(A, B, C, D, E, F)
%  a:  vector of number of cycles at 30kN bolt pretension data
%  X:  vector of alternating stress at 30KN bolt pretension data
% Create figure
figure1 = figure('NumberTitle','off','Name','S-N curve at 30kN pretension');
a=1032.95*10^6:15.339*10^6:1171*10^6; %from minimum alternating stress to maximum
alternating stress with the increment of 15.339*10^6
X=(a.^-0.0632)*(1816*10.^6);%Y represents Alternating stress and X represents
number of cycles
% Create plot
plot(X,a,'-r','DisplayName','Bolt Pretension at 30KN',...
    'LineWidth',2);
% Create legend
legend('(Y=1816x10^6 a^-0.0632  for 1032.95x10^6≤Y≤1171x10^6)')
% Create title
title('Stress-life (S-N) curve at 30KN bolt pretension',...
```

```
    'HorizontalAlignment','center',...
    'FontWeight','bold',...
    'FontName','Times',...
    'Color',[0 0 1]);
% Create xlabel
xlabel('Number cycles(10^6)','FontWeight','bold','FontName','Times',...
    'Color',[1 0.0745098039215686 0.650980392156863]);
% Create ylabel
ylabel('Alternating stress (MPa)','FontWeight','bold','FontName','Times',...
    'Color',[1 0.0745098039215686 0.650980392156863]);
```

8.4. Appendix IV

```
                %COMPARISON AT 22KN, 26KN, AND 30KN BOLT PRETENSION
% By BIKILA DEBELA graph of Stress-life curve
% Alternating stress versus number of cycles
%CREATEFIGURE(X1, Y1, X2, Y2, X3, Y3)
% A:  vector of number of cycles at 22kN bolt pretension data
% B:  vector of alternating stress at 22KN bolt pretension data
% C:  vector of number of cycles at 26kN bolt pretension data
% D:  vector of alternating stress at 26KN bolt pretension data
% E:  vector of number of cycles at 30kN bolt pretension data
% F:  vector of alternating stress at 30KN bolt pretension data
% Create figure
figure1 = figure('NumberTitle','off','Name','S-N curve at 22kN,26KN and 30KN
pretension');
A=[508.52,507.79,507.08,506.38,505.70,505.03,504.38,503.74,503.12];
B=[558.394,571.248,584.102,596.956,609.810,622.664,635.518,648.372,661.226];
C=[503.12,502.69,502.28,501.87,501.46,501.06,500.67,500.28,499.89];
D=[661.266,670.115,678.964,687.813,696.662,705.511,714.360,723.209,732.058];
E=[498.51,498.28,498.04,497.81,497.58,497.35,497.12,496.90,496.67];
F=[764.744,770.506,776.268,782.030,787.792,793.554,799.316,805.078,810.84];
% Create plot
plot(A,B,'-b',C,D,'-ro',E,F,'-g','DisplayName','Bolt Pretension at 22KN',...
    'LineWidth',2);
% Create legend
legend('Bolt Pretension at 22KN','Bolt Pretension at 26KN','Bolt Pretension at
30KN')
% Create title
title('Stress-life (S-N) curve at different bolt pretensions',...
    'HorizontalAlignment','center',...
    'FontWeight','bold',...
    'FontName','Times',...
    'Color',[0 0 1]);
% Create xlabel
xlabel('Number cycles(10^6)','FontWeight','bold','FontName','Times',...
    'Color',[1 0.0745098039215686 0.650980392156863]);
% Create ylabel
```

```
ylabel('Alternating stress (MPa)','FontWeight','bold','FontName','Times',...
    'Color',[1 0.0745098039215686 0.650980392156863]);
```

8.5. Appendix V

```
% By BIKILA DEBELA graph of Stress-life curve
% Alternating stress versus number of cycles
%CREATEFIGURE(X1, Y1, X2, Y2, X3, Y3)
%  a:  vector of number of cycles at 22kN bolt pretension data
%  X:  vector of alternating stress at 22KN bolt pretension data
% Create figure
figure1 = figure('NumberTitle','off','Name','S-N curve at 22kN pretension');
a=754.76*10^6:24.679*10^6:976.87*10^6; %from minimum alternating stress to
maximum alternating stress with the increment of 24.679*10^6
X=(a.^-0.0816)*(2161*10^6);%Y represents Alternating stress and X represents
number of cycles
% Create plot
plot(X,a,'-r','DisplayName','Bolt Pretension at 22KN',...
    'LineWidth',2);
% Create legend
legend('(Y=2161x10^6 X^-0.0816  for 754.76x10^6≤Y≤976.87x10^6)')
% Create title
title('Stress-life (S-N) curve at 22KN bolt pretension',...
    'HorizontalAlignment','center',...
    'FontWeight','bold',...
    'FontName','Times',...
    'Color',[0 0 1]);
% Create xlabel
xlabel('Number cycles','FontWeight','bold','FontName','Times',...
    'Color',[1 0.0745098039215686 0.650980392156863]);
% Create ylabel
ylabel('Alternating stress (Pa)','FontWeight','bold','FontName','Times',...
    'Color',[1 0.0745098039215686 0.650980392156863]);
```

8.6. Appendix VI

```
% By BIKILA DEBELA graph of Stress-life curve
% Alternating stress versus number of cycles
%CREATEFIGURE(X1, Y1, X2, Y2, X3, Y3)
%  a:  vector of number of cycles at 26kN bolt pretension data
%  X:  vector of alternating stress at 26KN bolt pretension data
% Create figure
figure1 = figure('NumberTitle','off','Name','S-N curve at 26KN pretension');
a=893.94*10^6:19.498*10^6:1069.42*10^6; %from minimum alternating stress to
maximum alternating stress with the increment of 19.498*10^6
X=(a.^-0.0816)*(2161*10^6);%Y represents Alternating stress and X represents
number of cycles
% Create plot
```

```
plot(X,a,'-r','DisplayName','Bolt Pretension at 26KN',...
    'LineWidth',2);
% Create legend
legend('(Y=2161x10^6 X^-0.0816  for 893.94x10^6≤Y≤1069.42x10^6)')
% Create title
title('Stress-life (S-N) curve at 26KN bolt pretension',...
    'HorizontalAlignment','center',...
    'FontWeight','bold',...
    'FontName','Times',...
    'Color',[0 0 1]);
% Create xlabel
xlabel('Number cycles','FontWeight','bold','FontName','Times',...
    'Color',[1 0.0745098039215686 0.650980392156863]);
% Create ylabel
ylabel('Alternating stress (Pa)','FontWeight','bold','FontName','Times',...
    'Color',[1 0.0745098039215686 0.650980392156863]);
```

8.7. Appendix VII

```
% By BIKILA DEBELA graph of Stress-life curve
% Alternating stress versus number of cycles
%CREATEFIGURE(A, B, C, D, E, F)
%  a:  vector of number of cycles at 30kN bolt pretension data
%  X:  vector of alternating stress at 30KN bolt pretension data
% Create figure
figure1 = figure('NumberTitle','off','Name','S-N curve at 30kN pretension');
a=1032.95*10^6:15.339*10^6:1171*10^6; %from minimum alternating stress to maximum
alternating stress with the increment of 15.339*10^6
X=(a.^-0.0816)*(2161*10.^6);%Y represents Alternating stress and X represents
number of cycles
% Create plot
plot(X,a,'-r','DisplayName','Bolt Pretension at 30KN',...
    'LineWidth',2);
% Create legend
legend('(Y=2161x10^6 a^-0.0816  for 1032.95x10^6≤Y≤1171x10^6)')
% Create title
title('Stress-life (S-N) curve at 30KN bolt pretension',...
    'HorizontalAlignment','center',...
    'FontWeight','bold',...
    'FontName','Times',...
    'Color',[0 0 1]);
% Create xlabel
xlabel('Number cycles','FontWeight','bold','FontName','Times',...
    'Color',[1 0.0745098039215686 0.650980392156863]);
% Create ylabel
ylabel('Alternating stress (Pa)','FontWeight','bold','FontName','Times',...
    'Color',[1 0.0745098039215686 0.650980392156863]);
```

8.8. Appendix VIII

```
% By BIKILA DEBELA graph of Stress-life curve
% Alternating stress versus number of cycles
%CREATEFIGURE(X1, Y1, X2, Y2, X3, Y3)
%  a:  vector of number of cycles at 22kN bolt pretension data
%  X:  vector of alternating stress at 22KN bolt pretension data
% Create figure
figure1 = figure('NumberTitle','off','Name','S-N curve at 22kN pretension');
a=754.76*10^6:24.679*10^6:976.87*10^6; %from minimum alternating stress to
maximum alternating stress with the increment of 24.679*10^6
X=(a.^-0.0808)*(2137*10^6);%Y represents Alternating stress and X represents
number of cycles
% Create plot
plot(X,a,'-r','DisplayName','Bolt Pretension at 22KN',...
    'LineWidth',2);
% Create legend
legend('(Y=2137x10^6 X^-0.0808  for 754.76x10^6≤Y≤976.87x10^6)')
% Create title
title('Stress-life (S-N) curve at 22KN bolt pretension',...
    'HorizontalAlignment','center',...
    'FontWeight','bold',...
    'FontName','Times',...
    'Color',[0 0 1]);
% Create xlabel
xlabel('Number cycles','FontWeight','bold','FontName','Times',...
    'Color',[1 0.0745098039215686 0.650980392156863]);
% Create ylabel
ylabel('Alternating stress (Pa)','FontWeight','bold','FontName','Times',...
    'Color',[1 0.0745098039215686 0.650980392156863]);
```

8.9. Appendix IX

```
% By BIKILA DEBELA graph of Stress-life curve
% Alternating stress versus number of cycles
%CREATEFIGURE(X1, Y1, X2, Y2, X3, Y3)
%  a:  vector of number of cycles at 26kN bolt pretension data
%  X:  vector of alternating stress at 26KN bolt pretension data
% Create figure
figure1 = figure('NumberTitle','off','Name','S-N curve at 26KN pretension');
a=893.94*10^6:19.498*10^6:1069.42*10^6; %from minimum alternating stress to
maximum alternating stress with the increment of 19.498*10^6
X=(a.^-0.0808)*(2137*10^6);%Y represents Alternating stress and X represents
number of cycles
% Create plot
plot(X,a,'-r','DisplayName','Bolt Pretension at 26KN',...
    'LineWidth',2);
% Create legend
```

```
legend('(Y=2137x10^6 X^-0.0808  for 893.94x10^6≤Y≤1069.42x10^6)')
% Create title
title('Stress-life (S-N) curve at 26KN bolt pretension',...
    'HorizontalAlignment','center',...
    'FontWeight','bold',...
    'FontName','Times',...
    'Color',[0 0 1]);
% Create xlabel
xlabel('Number cycles','FontWeight','bold','FontName','Times',...
    'Color',[1 0.0745098039215686 0.650980392156863]);
% Create ylabel
ylabel('Alternating stress (Pa)','FontWeight','bold','FontName','Times',...
    'Color',[1 0.0745098039215686 0.650980392156863]);
```

8.10. Appendix X

```
% By BIKILA DEBELA graph of Stress-life curve
% Alternating stress versus number of cycles
%CREATEFIGURE(A, B, C, D, E, F)
%  a:  vector of number of cycles at 30kN bolt pretension data
%  X:  vector of alternating stress at 30KN bolt pretension data
% Create figure
figure1 = figure('NumberTitle','off','Name','S-N curve at 30kN pretension');
a=1032.95*10^6:15.339*10^6:1171*10^6; %from minimum alternating stress to maximum
alternating stress with the increment of 15.339*10^6
X=(a.^-0.0808)*(2137*10.^6);%Y represents Alternating stress and X represents
number of cycles
% Create plot
plot(X,a,'-r','DisplayName','Bolt Pretension at 30KN',...
    'LineWidth',2);
% Create legend
legend('(Y=2137x10^6 a^-0.0808  for 1032.95x10^6≤Y≤1171x10^6)')
% Create title
title('Stress-life (S-N) curve at 30KN bolt pretension',...
    'HorizontalAlignment','center',...
    'FontWeight','bold',...
    'FontName','Times',...
    'Color',[0 0 1]);
% Create xlabel
xlabel('Number cycles','FontWeight','bold','FontName','Times',...
    'Color',[1 0.0745098039215686 0.650980392156863]);
% Create ylabel
ylabel('Alternating stress (Pa)','FontWeight','bold','FontName','Times',...
    'Color',[1 0.0745098039215686 0.650980392156863]);
```